SYNTHESIS, CHARACTERIZATION, AND REACTIVITY OF CROSS-CONJUGATED FRAMEWORKS

by

Victoria Leigh Hamilton

A thesis submitted to the faculty of
The University of North Carolina at Charlotte
in partial fulfillment of the requirements
for the degree of Master of Science in
Chemistry

Charlotte

2018

Approved by:

_____
Markus Etzkorn

_____
Craig Ogle

_____
Christopher Bejger

_____
Douglas Shafer

ABSTRACT

VICTORIA LEIGH HAMILTON. Synthesis, Characterization, and Reactivity of Cross-Conjugated Frameworks. (Under the direction of DR. MARKUS ETZKORN)

Molecules with cross-conjugated π-systems possess unique structures and reactivity due to their distinctive form of conjugation that fundamentally differs from the isomeric through conjugated systems by atom connectivity. Many of the organic compounds that played a vital role in the development of industrial organic chemistry are cross-conjugated systems or were transformed to cross-conjugated organic salts (*e.g.*, dyes such as indigo). Our larger goal to synthesize novel cross-conjugated frameworks with potential for biological or materials applications, depended on a preparative scale synthesis of necessary precursors.

We prepared a small library of arene-substituted isoindanone derivatives that necessitated optimization of synthetic routes according to electronic demands of the individual systems. Reproducible routes were actualized to afford multigram quantities of these compounds as the necessary precursors to the polycyclic scaffolds targeted herein.

Through this project we have established reliable protocols to novel isoindenone dimers that are synthetically intriguing substrates, which may be utilized to further investigate the electronic structure of their fleeting-intermediate monomers. Other intermediates, *i.e.* dibenzo[b,e]fulvalenes, have provided access to novel bimetallic complexes through ligand association reactions with appropriate transition metal carbonyl moieties. The introduction of arene substituents that are electron-donating or electron-withdrawing provided electronic contrast between these structures.

TABLE OF CONTENTS

LIST OF TABLES

LIST OF FIGURES

LIST OF ABBREVIATIONS

Å	Angstrom
DFT	Density Functional Theory
DMSO	Dimethyl Sulfoxide
DTDA	Diene-Transmissive Diels-Alder
GCMS	Gas Chromatography Mass Spectrometry
HOMO	Highest Occupied Molecular Orbital
IR	Infrared Spectroscopy
LUMO	Lowest Unoccupied Molecular Orbital
η	Hapticity
NBS	N-Bromosuccinimide
NMR	Nuclear Magnetic Resonance
PTSA	*para*-Toluenesulfonic Acid
RBF	Round Bottom Flask
THF	Tetrahydrofuran
TLC	Thin Layer Chromatography
UV/Vis	Ultraviolet/Visible Spectroscopy
vdW	Van der Waals

CHAPTER 1: BACKGROUND

1.1. Cross-Conjugation

Cross-conjugated molecules possess unique structures and reactivity patterns due to their distinctive form of conjugation. The fundamental difference between through and cross-conjugated systems is the atom connectivity. For example, in acyclic polyenes through conjugated π-systems have vicinally connected olefinic units, whereas cross-conjugated π-systems are geminally connected (**Figure 1**). This geminal

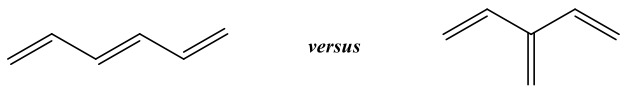

1 **2**

Figure 1. Depiction of simple through conjugated (**1**) and cross-conjugated (**2**) molecules to illustrate inherent connectivity differences.

connectivity mandates a bifurcation point and results in branching, a defining property of cross-conjugated systems. These bifurcation points disrupt the conjugation pathway in a classical sense that has been described as: a system possessing three unsaturated groups, two of which although conjugated to a third unsaturated center are not conjugated to each other.[1] Consequently, cross-conjugation leads to structural, physical, and electronic properties that differ greatly from through conjugated molecules. There are three fundamental classes of oligo-olefins that exhibit cross-conjugation: the dendralenes, the radialenes, and the fulvenes; the latter represents a hybrid system that contains both through and cross-conjugation (**Figure 2**).

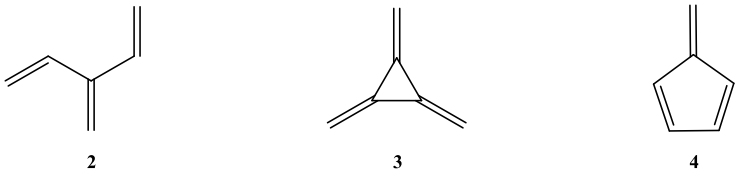

2 3 4

Figure 2. Representative compounds from the fundamental classes that exhibit cross-conjugation: [3]dendralene (**2**), [3]radialene (**3**), and fulvene (**4**).

1.1.1. Structural Consequences of Cross-Conjugation

The characteristic branching inherent to cross-conjugated molecules makes the steric strain between the branches in cross-conjugated systems much more common than in the through conjugated isomers. Given the ease of rotation about the single bonds at the bifurcation points, this strain often leads to structural distortion that deviates from planarity for the conjugated π-system. Dendralenes have been experimentally determined to have non-planar conformations.[2] Radialenes often adopt puckered ring conformations,[3,4] with [6]radialenes existing in both chair and twist-boat conformations.[5-7]

1.1.2. Electronic Properties of Cross-Conjugated Molecules

With disruption to the classical conjugation pathways in cross-conjugated compounds due to bifurcation points, there is often competition observed between the cross-conjugated pathways. This disruption weakens the overall electronic delocalization in the molecule that results in interesting and potentially tunable electronic properties that differ from the through conjugated analogs. Electronic transitions of cross-conjugated compounds have been studied via UV/Vis spectroscopy, often observing a decreased λ_{max} than would be predicted for a through conjugated analog. As the conjugation of a molecule increases the λ_{max} increases because as conjugation increases the energy required for an electron to transition from the HOMO to the LUMO decreases, therefore, the wavelength of maximum absorption increases. With a decrease in the classical conjugation of these

molecules, a decrease in λ_{max} can be reasoned. Another difficulty in quantifying electronic properties of cross-conjugated molecules is that they depend on the preferred conjugation pathway of the molecule, which can change based on environment.

Van Walree *et al.* performed absorption and fluorescence studies on 1,1-diphenylethene (**5**) and 2,3-diphenylbutadiene (DPB) (**6**) that showed in both compounds there is substantial charge transfer (**Figure 3**). However, with the introduction of a second branching site in DPB the corresponding charge transfer band is observed with reduced intensity.[8]

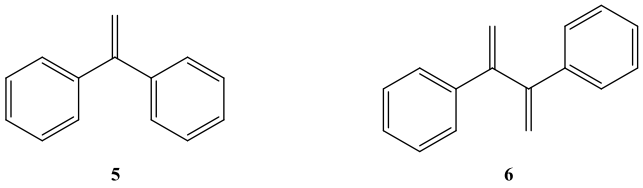

5 **6**

Figure 3. Compounds **5** and **6** that were investigated for differences in electronic properties due to varying degrees of branching.

1.1.3. Reactivity of Cross-Conjugated Systems

Cross-conjugated compounds exhibit reactivities that are equally unique as the compounds themselves. Dendralenes commonly undergo Diene-Transmissive Diels-Alder (DTDA) reactions to deliver polycyclic scaffolds that significantly increase structural complexity. However, when one or more carbon atoms in the framework of parent dendralenes are replaced by heteroatoms, the resulting heterodendralenes are rarely reported to undergo the same DTDA reactions.[9-12] Reactivity studies on radialenes are predominantly absent from the experimental literature, these compounds have often been prepared as the ultimate synthetic target and have rarely been utilized for subsequent synthetic transformations. Notably, redox chemistry of substituted electron-rich and electron-deficient radialenes has been investigated and charge-transfer complexes of

[3]radialenes have attracted attention due to their magnetic properties[13] and as potential organic metals.[14-16] Organometallic complexes of fulvalenes offer catalytic properties alongside novel reactivity patterns. In particular, sesquifulvalenes have attracted much attention as their organometallic complexes exhibit unusually large non-linear optical properties. The first hyperpolarizability of conjugated organic molecules is markedly increased by the presence of donor and acceptor groups at opposite end of the conjugation path. Such molecules (sesquifulvalenes) find increased application in non-linear optics as second harmonic generators and electro-optic modulators.

1.2. Fluorine – Significance as a Substituent

As a significant portion of the chemistry described herein involves the synthesis and investigation of novel fluorinated compounds, this is meant to serve as a brief overview of the significance of fluorine in organic chemistry. The introduction of fluorine into organic compounds is often far from trivial and drastically alters their physicochemical properties. These property-altering affects are well established and often advantageously exploited in biologically active compounds or novel materials.[17] Fluorine is primarily utilized to selectively modify the electronic features of a compound while maintaining its structural characteristics, as the molecular geometry does not strikingly change.

Organofluorine compounds have found numerous applications outside of their use as specialty solvents and valuable building blocks (**Figure 4**). They are used widely in materials applications as (*1*) specialized polymers, (*2*) refrigerants, (*3*) components in liquid crystal displays, and (*3*) fire-fighting foam. Their biological applications are prominent in the agrochemical and pharmaceutical industries. Fluorine substituents in agrochemicals significantly improves their efficacy. When fluorine is introduced into

some organic molecules, it enhances the biological activity as fluorine affects nearly all physical, adsorption, distribution, metabolism, and excretion properties of compounds, mainly through electrostatic interactions. Currently, 50% of agrochemicals contain at least one fluorine substituent and the same goes for 25% of pharmaceuticals.

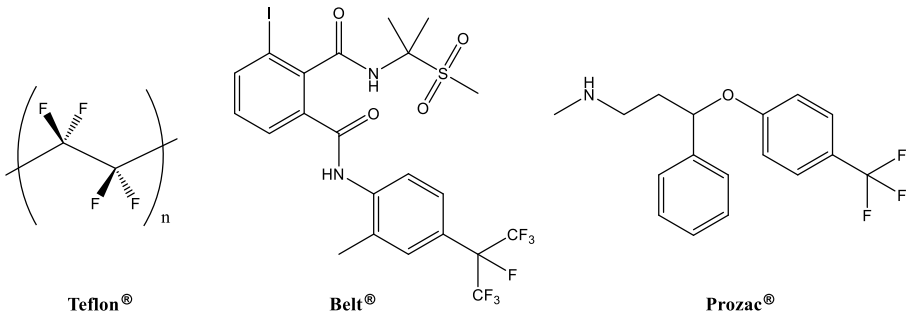

Figure 4. Organofluorine compounds with various applications; Teflon® is a specialized polymer, Belt® is a widely used herbicide, Prozac® is one of the most commonly prescribed antidepressants.

As best said by Manfred Schlosser, *"Fluorine leaves nobody indifferent; it inflames emotions be that affections or aversions. As a substituent, it is rarely boring, always good for a surprise, but often completely unpredictable."*[18] It is that unpredictability that intrigues me and guides my investigations into unique fluorinated scaffolds.

1.2.1. Properties of Fluorine

Fluorine is the most chemically reactive and electronegative element ($\chi = 4$) with an electron affinity of 328 kJ/mol. It has a vdW radius of 1.47 Å, being the smallest element after hydrogen (vdW radius: 1.20 Å) and helium (vdW radius: 1.40 Å), that allows for a 0.60 Å covalent radius. Fluorine readily forms stable compounds with most other elements, including the noble gases krypton, xenon, and radon. It is the most abundant halogen in the lithosphere and the thirteenth most abundant element in the earth's crust where it can be found in minerals, rocks, coal, and clay.

Natural sources of fluorine include fluorite (CaF_2), cryolite (Na_3AlF_6), and fluorapatite ($Ca_5(PO_4)_3F$). Fluorite is used industrially as a flux for lowering the melting point of metal ores and as a source of hydrogen fluoride. Cryolite is often used as a pesticide and an insecticide; molten cryolite is used in the refining of aluminum by way of the Hall-Héroult process. Fluorapatite can be used as a precursor for the industrial production of phosphorus and as a source of hydrogen fluoride.

The synthesis of the first organofluorine compound was reported in 1862 and was accomplished by nucleophilic halogen exchange.[19] After continuous efforts by numerous chemists, elemental fluorine was successfully isolated in 1886 by Henri Moissan through electrolysis of potassium hydrogen difluoride solution in liquid hydrogen fluoride, later earning him the Nobel Prize in Chemistry in 1906.[20] Elemental fluorine continues to be produced in this fashion to this day.

1.2.2. The Carbon-Fluorine Bond

The carbon-fluorine bond is the strongest bond in organic chemistry (105.4 kcal mol^{-1}) and this contributes significantly to the high thermal and chemical stability of organofluorine compounds. The carbon-fluorine bond is relatively short (1.35 Å) and together with the small vdW radius of fluorine this is the reason for no observed steric strain in polyfluorinated molecules. Fluorine's high electronegativity induces a polarization on the carbon-fluorine bond ($\chi_C = 2.5$), resulting in the bond having a large dipole moment ($\mu = 1.41$). It's been suggested that the strength of the carbon-fluorine bond arises from the polarization of the bond and that an attractive interaction exists between $F^{\delta-}$ and $C^{\delta+}$ rather than the classical sharing of electrons often observed in a covalent bond.[21,22] Fluorine has the lowest polarizability of all atoms (0.56×10^{-24} cm^3) that causes very weak

dispersion forces between polyfluorinated molecules and leads to the depressed boiling points often observed in fluorinated compounds as compared to their hydrocarbon counterparts. Although the exchange of fluorine for hydrogen does not significantly alter the molecular geometry of a molecule, it does have prominent effects on its physicochemical properties (**Table 1**).

Table 1. Comparison of the physicochemical properties of n-hexane with varying degrees of fluorination.

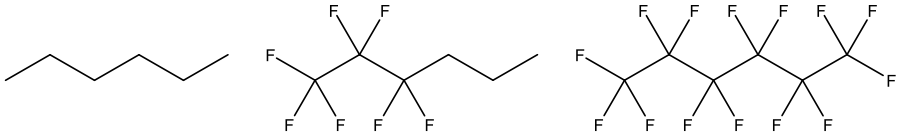

7 **8** **9**

	7	8	9
B.P. (°C)	69	64	57
density (g/mL)	0.655	1.265	1.672
ΔH (kcal/mol)	6.9	7.9	6.7
Tc (°C)	235	200	174

1.2.3. Synthetic Strategies Toward Fluorinated Compounds

Fluorine chemists have long been intrigued with the unique reactivity of organofluorine compounds; the systematic preparation and study of fluorinated compounds continues to gain popularity within the synthetic community as the benefits of fluorinated molecules continue to be recognized. The introduction of fluorine into the framework of an organic molecule is an appealing and important synthetic transformation, though far from trivial. The predominant challenges are rooted in the high reactivity and hazards of working with elemental fluorine and hydrogen fluoride. To circumvent synthetic challenges, numerous reagents and strategies have been developed to fine-tune fluorination

methodology. The synthetic route chosen for any given fluorination reaction is dependent on the degree and regioselectivity of fluorination desired, as well as the nature of the precursors.

1.2.3.1. Direct Fluorination

The exchange of a hydrogen atom for a fluorine atom appears to be conveniently achieved through direct fluorination with elemental fluorine. This methodology is useful for obtaining highly fluorinated molecules by treatment of hydrocarbons with F_2, often diluted with N_2. These reactions are non-selective because elemental fluorine is extremely reactive, possessing a very weak fluorine to fluorine bond (159 kJ) with great affinity for forming strong bonds with other atoms.[23] Such reactions also pose a significant hazard as hydrocarbons are prone to burn uncontrollably in F_2.

Even so, efforts have been made in the development of direct fluorination methods (*i.e.* F_2 in the gas phase, special conditions in the liquid phase, electrochemical fluorination)[23] that started with Bigelow in the Manhattan project.[24] In order to suppress the high reactivity and non-selectivity of direct radical fluorination, Chambers utilized strongly acidic, polar media to harness elemental fluorine and promote heterolytic fluorination.[21]

1.2.3.2. Nucleophilic Fluorination

Many difficulties in nucleophilic fluorination stem from fluorine's high electronegativity, which makes it the least nucleophilic halide. The nucleophilic displacement of other alkyl halides by fluorine is favorable due to the high thermodynamic stability of the carbon-fluorine bond formed and the poor leaving group character of fluoride. As fluorine readily forms strong hydrogen bonds, its nucleophilicity decreases in

the presence of hydrogen bond donors. However, strict absence of hydrogen bond donors increases its basicity and often leads to side reactions.

A variety of reagents are available as a source of fluoride and are employed in nucleophilic displacements. Alkali metal fluoride salts are commonly used in the fluorination of alkyl compounds (**Figure 5**). The strong lattice energy of these salts render them weakly nucleophilic with poor solubility in organic solvents, so the use of crown ethers is often necessary.

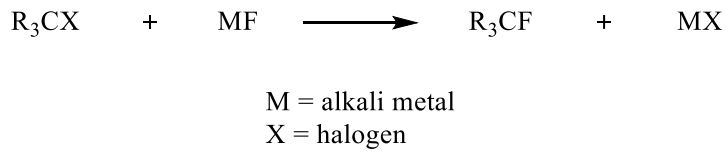

Figure 5. Nucleophilic fluorination with metal halides.

Nucleophilic aromatic substitution methods have been developed for the introduction of fluorine to an arene or heteroarene unit. Common reactions of this type are the HALEX process, Balz-Schiemann reaction, and fluorodenitration.[25]

1.2.3.3. Electrophilic Fluorination

The isolation of crystalline, benchtop-stable fluorinating reagents such as *N*-fluoro amines, amides, sulfonamides, and quaternary ammonium salts was critical to the development of selective electrophilic fluorination reagents that are functional group tolerant and can be utilized under mild reaction conditions (**Figure 6**). The organonitrogen fragments of these compounds have been fine-tuned such that they behave as a good leaving group, allowing the reactivity of fluorine with nucleophiles as a formal source of the fluoronium cation ("F^+").[26] Although *N*-fluoro reagents will behave as a source of "F^+", the nitrogen-fluorine bond is traditionally polarized with a partial negative charge on the fluorine. Mechanistically, fluorination with *N*-fluoro reagents has been debated since their

debut but two possible pathways exist: via two single-electron transfers or a concerted two-electron transfer. Xenon difluoride is also an electrophilic fluorination reagent that is commonly utilized for the selective fluorination of arenes, alkenes, and activated methylenes but it is limited by its functional group tolerance as it has a high oxidation potential.[27]

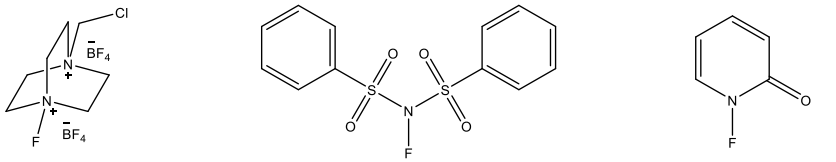

Selectfluor® Accufluor® NFSI 1-fluoro-2-pyridone

Figure 6. *N*-fluoro amines as electrophilic fluorinating reagents.

1.2.3.4. Deoxofluorination

Deoxofluorination reagents have been developed to broaden the scope of fluorination reactions to allow for the selective replacement of hydroxyl and carbonyl groups with one and two fluorine atoms, respectively (**Figure 7**). Sulfur tetrafluoride was one of the first reagents utilized to accomplish these synthetic transformations but milder reagents have since been developed to avoid use of undesirable sulfur tetrafluoride reagents.

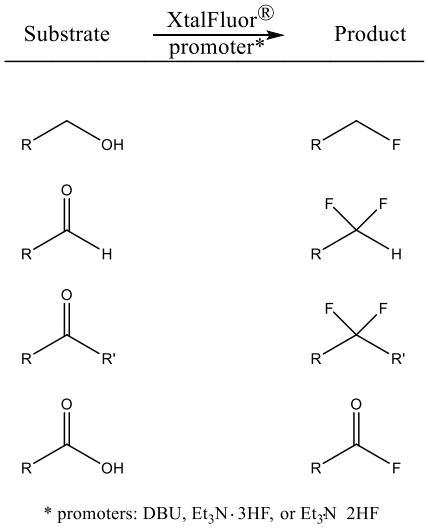

Figure 7. The scope of deoxofluorination reagents.

1.2.3.5. Fluorinated Building Blocks

The implementation of the "building block" approach in modern organofluorine synthesis is ubiquitous, as it is often more useful to assemble a complex molecule from the former rather than the introduction of fluorine substituents at a later stage in the synthetic route. Fluorinated building blocks are defined as small, readily available compounds that already contain fluorine substituents. They can be classified by the number of carbon atoms that are supplied to the target molecules, instead of simply sorted based on the number of fluorine atoms.

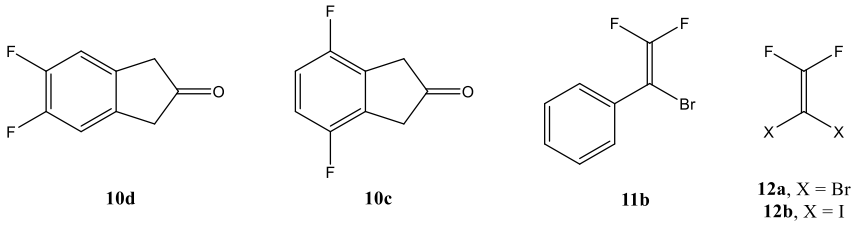

Figure 8. Fluorinated building blocks paramount to the thesis projects herein.

Several issues have encouraged the development of the fluorinated building block approach, by demand of clean synthesis (*e.g.*, without the use of chlorofluorocarbons), the desire for atom economy (*e.g.*, fluorine atoms), and utilization of methods with milder processing conditions.

CHAPTER 2: RESEARCH GOALS

While the focus of this research is synthetically driven, cross-conjugated scaffolds were targeted herein, with clear distinction between three projects: (1) "mixed" isoindenone dimers, (2) bimetallic complexes of dibenzo[b,e]fulvalenes, and (3) fluorinated dendralene derivatives. In particular, the specific research goals were formulated:

I. A small library of 2-indanone derivatives (**10**) were targeted as the necessary precursors to all polycyclic scaffolds targeted herein. These arene substituents will serve to provide electronic and steric contrast for further experimentation.

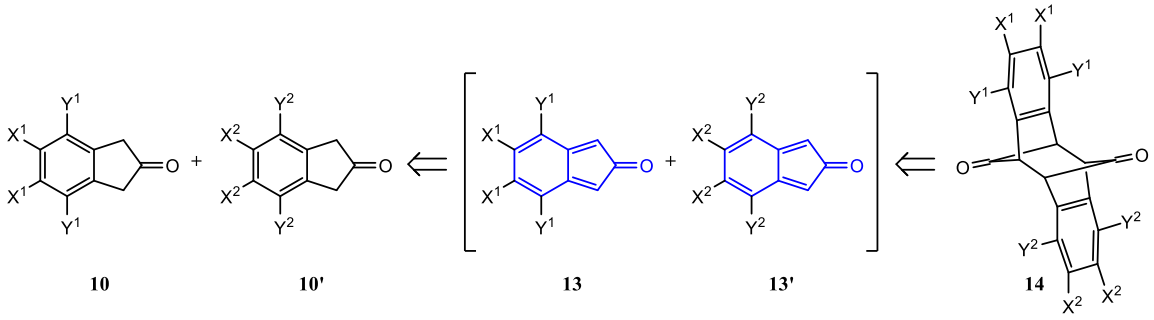

	a	*b*	*c*	*d*	*e*	*f*	*g*	*h*	*i*	*j*	*k*	*l*	*m*	*n*	*o*	*p*	*q*	*r*	*s*	*t*	*u*	*v*
X¹	H	F	H	F					H	OMe	Cl	Cl	H	H	H	H	H	H	OMe	H	H	F
X²	H	F	H	F	mono-fluoro isomers				H	OMe	Cl	Cl	H	H	H	H	Me	H	H	H	H	H
Y¹	H	F	F	H			tri-fluoro isomers		OMe	H	Cl	H	Me	Ph	H	H	H	OMe	H	F	H	H
Y²	H	F	F	H					OMe	H	Cl	H	Me	Ph	Me	OMe	OMe	H	OMe	H	F	F

Figure 9. Targeted isoindenone dimers of type **14** with a table of thesis-relevant substituent patterns.

II. Due to the failed dimerization of the formal tetrafluoro-isoindenone to its corresponding dimer **14b** through the three-step sequence optimized on the parent system **14a**, isoindenones with a spectrum of electronic structures (**13c**, **13i**, **13m**, **13n**) were targeted to ascertain structure-reactivity relationships between these fleeting intermediates.

III. Due to the failed dimerization of the formal *para*-dimethoxy-isoindenone to its corresponding dimer **14i** through the three-step sequence, even though dimers of type **14** with similar steric and electronic properties were obtained, "mixed" dimerizations of isoindenones with a spectrum of steric structures (**13a**, **13i**, **13m**) were investigated to probe potential limitations for generation and dimerization of these fleeting intermediates.

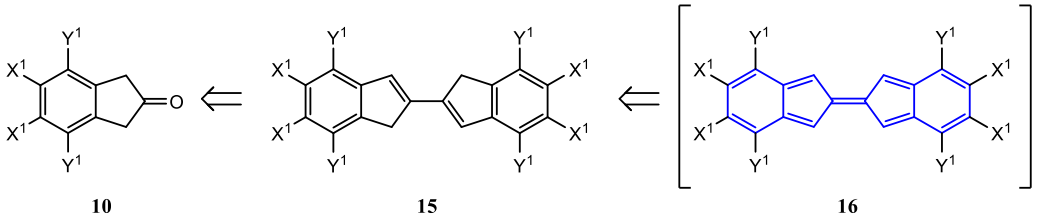

	a	*b*	*c*	*d*
X¹	H	H	H	H
Y¹	H	Me	OMe	F

Figure 10. Targeted dibenzo[b,e]fulvalenes of type **16** with a table of thesis-relevant substituent patterns.

IV. A series of dibenzo[b,e]fulvalenes of type **16** were targeted as bimetallic complexes with molybdenum because it was presumed that **16** exists only as a fleeting intermediate, based on reports of the parent system. Initially we were interested in the olefination of 2-indanone derivatives (**10**), but unexpected results prompted investigations into alternative, potentially shorter, synthetic sequences. We targeted 2,2'-biindenyl derivatives of type **15** as the direct precursor for dibenzo[b,e]fulvalene generation.

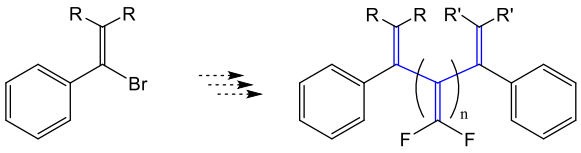

11a, R = H
11b, R = F

17a, R = R' = F
17b, R = F, R' = H

Figure 11. Targeted fluorinated dendralene derivatives of type **17**.

V. Fluorinated dendralene derivatives of type **17** were targeted for structure-reactivity comparisons to the analogous parent dendralenes. While fluorinated dendralene derivatives are expected to differ structurally only subtly from the parent compounds, the reactivity pattern of the fluorinated derivatives is anticipated to be uniquely different with potential for biological or materials applications.

CHAPTER 3: ISOINDENONES

3.1. Introduction to Isoindenones

Isoindenones, cross-conjugated 10 π-electron systems, are synthetically intriguing and have yet to be isolated due to their high reactivity and behavior as fleeting intermediates. The contributing resonance structures depicted exhibit the inherent high reactivity of these compounds as they can offer nonionic, ionic, or radical character (**Figure 12**). While isoindenones are often trapped with alkene- or alkyne-scavengers to yield

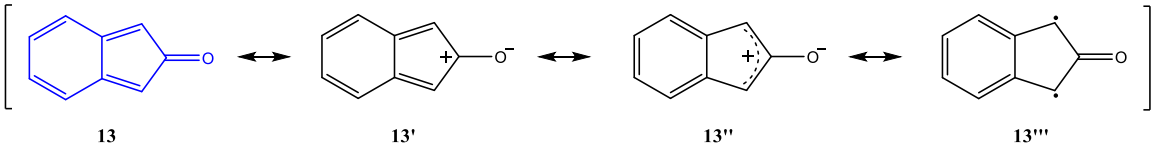

Figure 12. Selected resonance structures of isoindenone.

synthetically valuable products, in the absence of such scavengers various modes of dimerization can occur that reflect the steric demands and electronic properties of the intermediate (**Figure 13**),[28-31] making **13** an intriguing scaffold for chemists to study for its reactivity and utilization as a valuable synthetic intermediate toward novel polycyclic scaffolds.

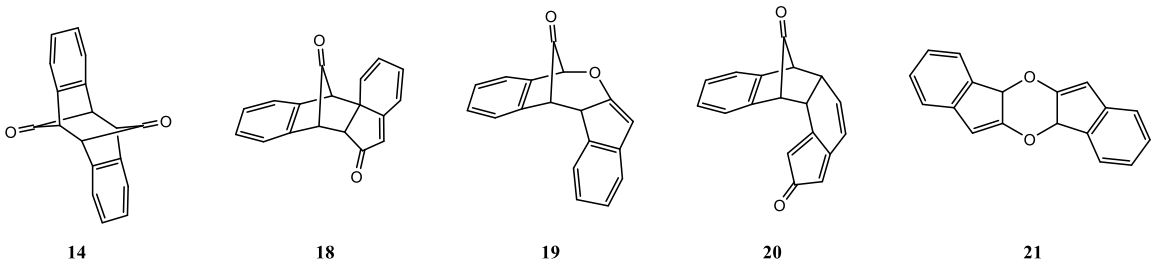

Figure 13. Dimerization modes of isoindenone **13**, substituents omitted for clarity.

Isoindenone dimers of type **18**, **19**, and **20** are easily reasoned through their corresponding [4+2], [6+4], and [4+2] π cycloaddition mechanisms. Dimers of type **14** and **21** are formal orbital symmetry forbidden [4+4] and [6+6] π dimers, respectively. The radical character of isoindenone resonance structure **13‴** and ionic 2π character of **13″** seemingly allow for plausible mechanistic pathways to structures of type **14** or **21** but no experimental evidence has been obtained for contributions from either structure to the resonance hybrid. A recent theoretical study provides evidence that the structure of isoindenone most closely resembles **13** through nucleus independent chemical shift (NCIS) calculations that predict a weakly anti-aromatic six-membered ring and strongly anti-aromatic five-membered ring.[32] Furthermore, the generation of isoindenone derivatives in the presence of various dienophiles has provided no evidence for either resonance structure. If biradical resonance form **13‴** contributed significantly to the resonance hybrid formal [4+2] π cycloaddition reactions should proceed non-stereoselectively, however, trapping experiments with *cis*- or *trans*-alkenes produced defined products through suprafacial orbital interactions according to Woodward-Hoffman rules.[31]

Isoindenones have been extensively studied by several groups, mainly to exploit their reactivity toward the generation of polycyclic scaffolds or to obtain kinetically stable derivatives through the introduction of sterically or electronically stabilizing substituents. Three groups (Jones [Leeds],[33,34] Fuchs [Tel Aviv],[30,35] Hoffman [Darmstadt][36]) focused investigations on obtaining persistent isoindenone derivatives through the introduction of sterically or electronically stabilizing substituents. Steric effects were probed by the introduction of bulky substituents in the α,α'-positions and the attempt towards electronic stabilization was examined by the introduction of fused rings to the arene unit (**Figure 14**).

A novel approach by Jones combined the introduction of bulky *o*-tolyl α,α'-substituents, that hindered isoindenone conjugation due to the nonplanarity of these groups, and alkoxy stabilization with methoxy substituents on the arene unit, to afford 5,6-dimethoxy-1,3-di-*o*-tolyl-isoindenone (**23**).[29]

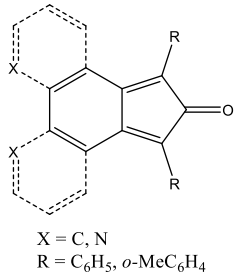

22

Figure 14. Steric and electronic stabilization of isoindenones.

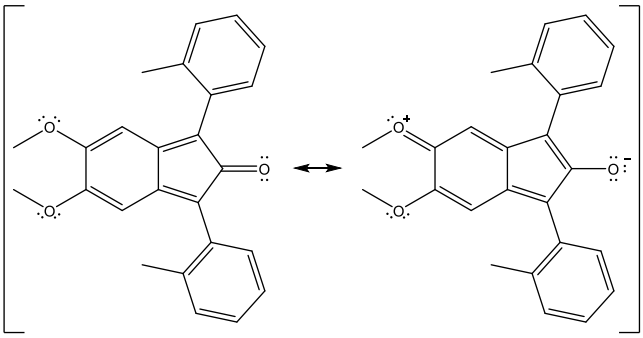

23

Figure 15. Persistent push-pull stabilized isoindenone **23**.

3.1.1. Isoindenone Generation and Dimerization

Various routes for the generation of isoindenones have been applied to an array of derivatives, each originating with the corresponding saturated isoindanones (**Figure 16**). One of the routes suggests the generation of isoindenone from treatment of a monobromo derivative of type **24** with a base. Treatment of 1,3-dibromo-isoindanone derivatives of type **25** with NaI in acetone or Zn in DMF will undergo reduction to generate the corresponding isoindenone.[33] The dehydration of alcohol derivatives of type **26** have only been successful on 1,3-diaryl-cyclopentaphenanthren-2-ones.[34] The three proceeding procedures were not reproducible in our hands, but we found success in the mild and elegant procedure pioneered by the Jones' group that exploits the strong fluorine-silicon bond for the fluoride induced cleavage of bromo silyl enol ethers of type **27** to afford the

10 π-electron cross-conjugated isoindenone intermediate.[28] The most attractive feature of Jones' methodology is its tolerance towards a variety of substituents that allows for prior arene functionalization of the isoindanone scaffold.

3.1.2. "Simple" Isoindenones and Their Respective Dimers

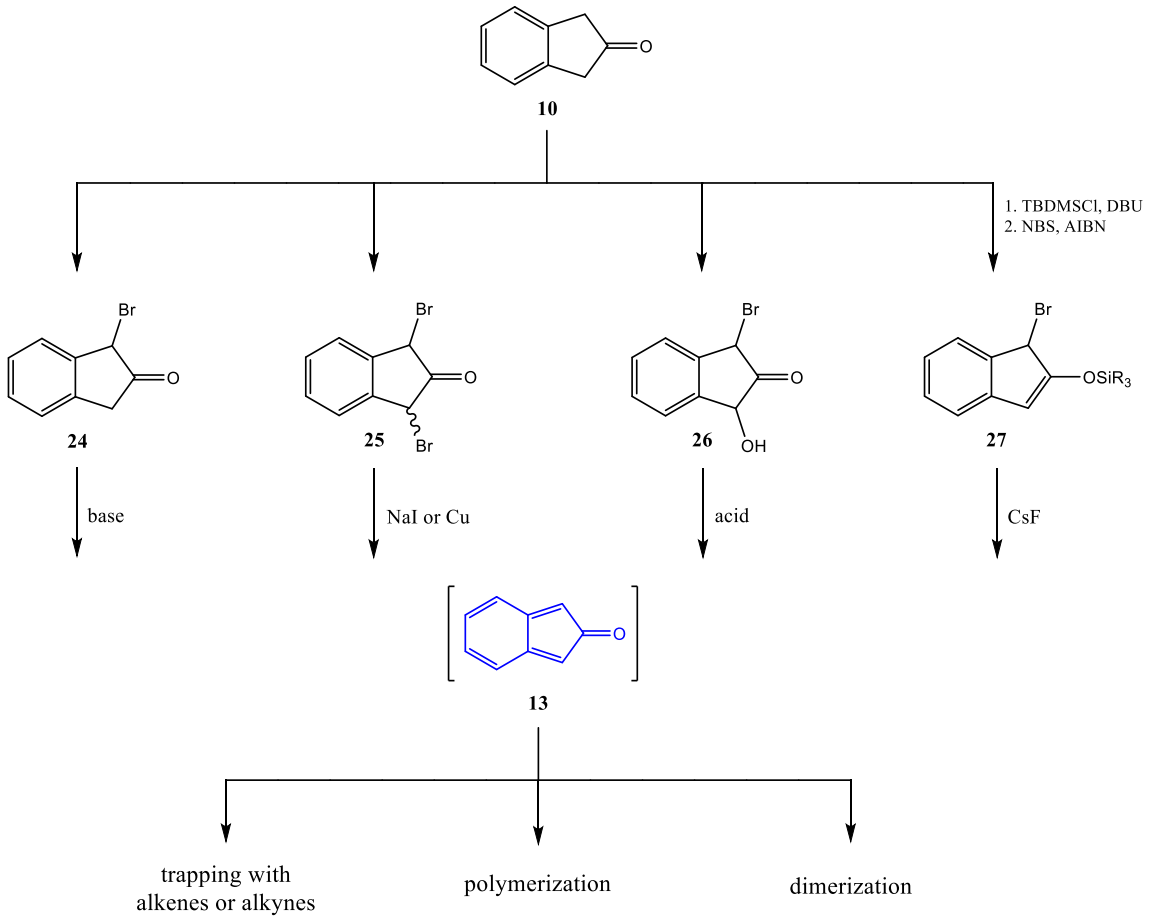

Figure 16. Strategies for isoindenone generation.

Although isoindenone chemistry is somewhat established, only three halogenated derivatives have been postulated[30] and to date there are no reports for the preparation of fluorinated isoindenones. "Simple" isoindenones, lacking conjugative stabilization or steric protection in the α,α'-positions, are prominently absent in the experimental literature. Several isoindenones have been dimerized in the absence of trapping agents, nevertheless,

"simple" arene-substituted dimers of type **14** are rare. In optimizing Jones' two-step procedure, our group has built a small library of symmetrical isoindenone dimers of type **14** donning either electron-withdrawing or electron-donating substituents on the arene unit (**Figure 17**). Through these efforts we have been able to suggest general reactivity trends of isoindenones bearing various substituent patterns on the arene unit.

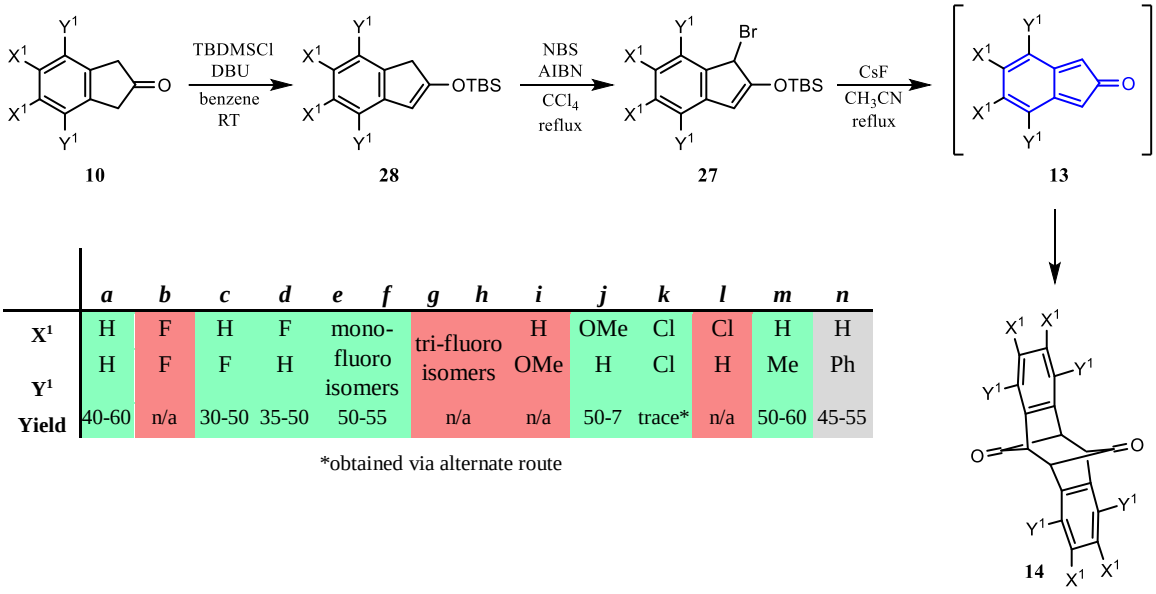

	a	*b*	*c*	*d*	*e*	*f*	*g*	*h*	*i*	*j*	*k*	*l*	*m*	*n*
X¹	H	F	H	F	mono-		tri-fluoro		H	OMe	Cl	Cl	H	H
Y¹	H	F	F	H	fluoro isomers		isomers		OMe	H	Cl	H	Me	Ph
Yield	40-60	n/a	30-50	35-50	50-55		n/a		n/a	50-7	trace*	n/a	50-60	45-55

*obtained via alternate route

Figure 17. Generation and dimerization of simple isoindenones including a table with substituent patterns that delivered desired dimer **14** (green), did not (red), or remains inconclusive (grey).

3.1.3. Alternate Route to *anti*-Dibenzo Dimer

An alternative method to obtain scaffolds of type **14** was previously explored by our group through the benzannulation of dienedione **32**.[37] Cylcopentadiene was oxidized and dimerized to the *endo* Diels-Alder product (**31**). Photochemical isomerization of **31** afforded the *anti*-dienedione (**32**); to circumvent rapid thermal isomerization of **32** to **31**, hydroxyketone **33** was prepared as the dienophile substrate for Diels-Alder cycloaddition. Utilizing tetrachlorothiophene dioxide (**34**) as the diene, the *anti*-dibenzo dimer **14k** was

prepared in a seven-step procedure. Although only trace quantities of poorly soluble **14k** were accessible via this route, full characterization was obtained.

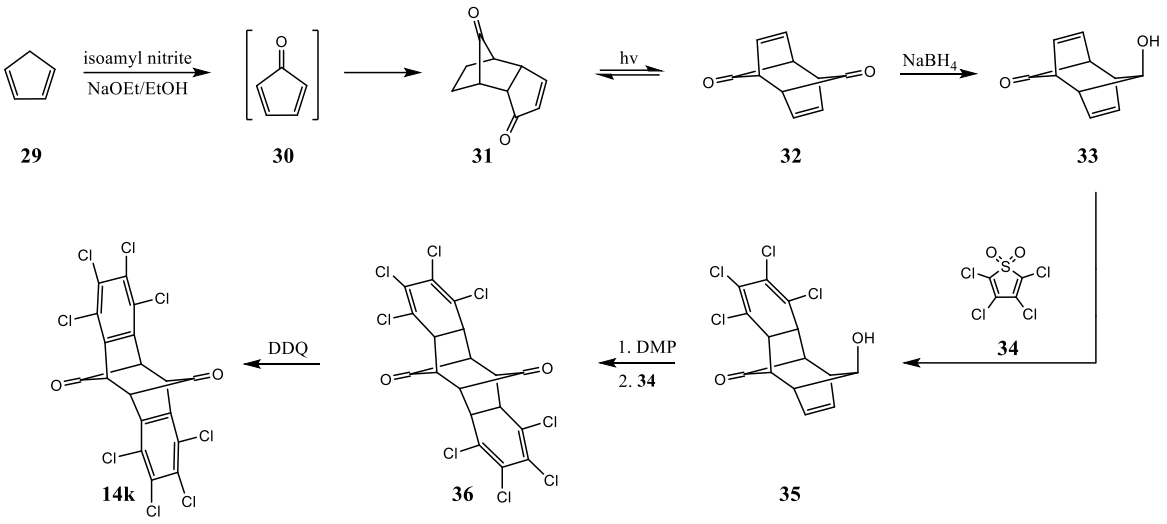

Figure 18. Reported synthesis of the formal octachloro-*anti*dibenzo dimer **14k** through a Diels-Alder approach.

3.2. Results and Discussion

3.2.1. Syntheses, Characterization, and Structures of Select 2-Indanone Derivatives

A variety of 2-indanone derivatives have been reported in the literature as precursors to functional organic materials or biologically active compounds. The synthetic methodologies described to obtain these valuable building blocks vary with the unique reactivities inherent to the substituent pattern. Access to the thesis-relevant *para*-disubstitued 2-indanones of type **10** are discussed below.

3.2.1.1. Synthesis of 4,7-Difluoro-2-indanone

We previously optimized an eight-step sequence to afford 5,6-difluoro-2-indanone from the corresponding 3,4-difluorobenzaldehye.[38] For the practicality of employing familiar reaction conditions and to probe the applicability of this sequence toward the *para*-difluoro isomer we applied the optimized protocols to 2,5-difluorobenzaldehyde (**37c**).

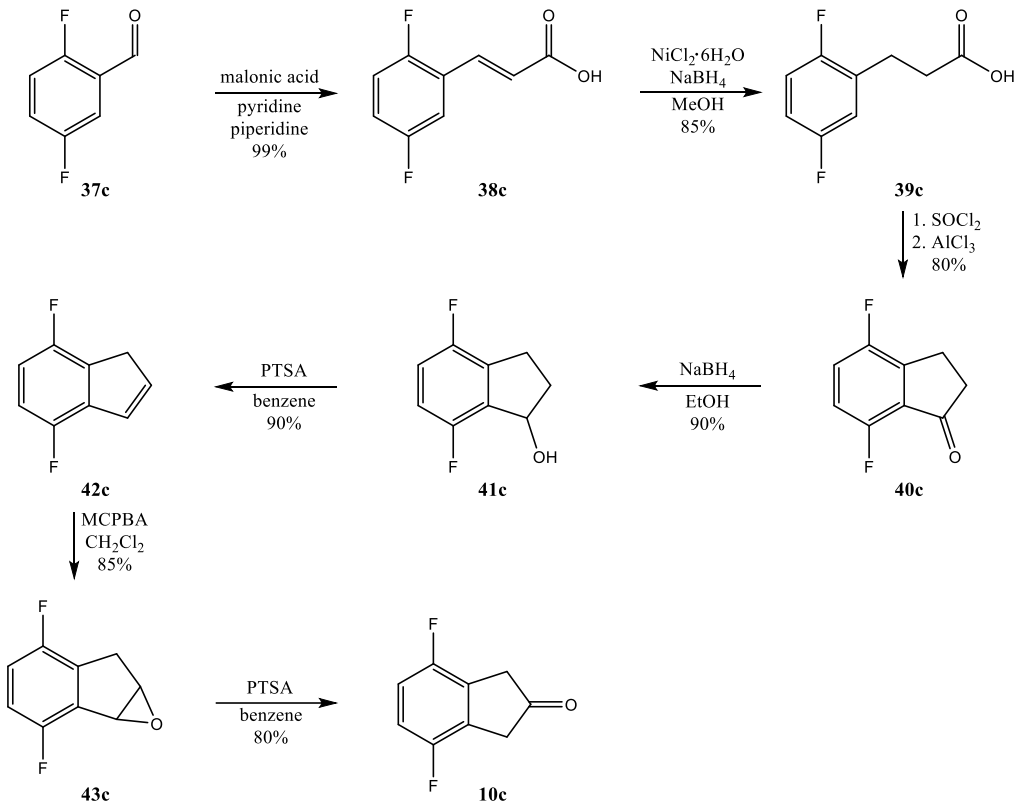

Figure 19. Optimized synthetic route to 4,7-difluoro-2-indanone (**10c**).

Commercially available 2,5-difluorobenzaldehyde (**37c**) was subjected to a Knoevenagel condensation with malonic acid under standard conditions[39] to afford the corresponding cinnamic acid **38c** quantitatively. The subsequent reduction of the aliphatic double bond was accomplished by reaction of **38c** with *in situ* generated nickel boride[40] to afford propionic acid **39c** in 85% yield. Subsequent PPA mediated cyclization did not deliver the corresponding 1-indanone and mostly unreacted **39c** was recovered after aqueous workup. Although deviation from strict reaction conditions often led to an undesirable aldol condensation on the *ortho*-difluoro system,[38] when both the temperature and reaction time are significantly increased in attempts to force cyclization of **39c** there is no further conversion toward the desired product or subsequent formation of the aldol dimer or other side products. We postulate that the carbocation intermediate for

electrophilic aromatic substitution is destabilized due to the position of the fluorine substituents on the aromatic ring, necessitating more forcing reaction conditions. To increase the ease of cyclization we first synthesized the corresponding acyl chloride. Conversion of **39c** to the acyl chloride proceeded quickly at 70 °C, the reaction was monitored by visualizing gas evolution and was complete when gas evolution ceased. The crude acyl chloride was added to a vigorously stirring solution of $AlBr_3$ in CS_2 to afford 1-indanone (**40c**) in good yield.[41] An alternative methodology was equally successful in our hands, while avoiding the use of CS_2. The corresponding acyl chloride was prepared at room temperature overnight and the crude product was subjected to a neat reaction with $AlCl_3$ at high temperature to afford clean **40c** in comparable yield.[42]

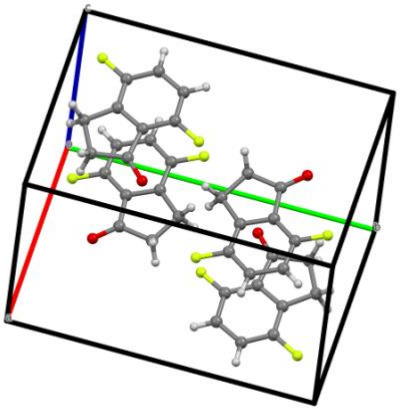

Figure 20. Crystal structure and unit cell of 4,7-difluoro-1-indanone (**40c**).

The ketone transposition of various 1-indanone derivatives to the corresponding 2-indanone has been examined and is typically accomplished via acid-catalyzed ring opening of epoxide intermediates.[43,44] The sodium borohydride reduction of **40c** and subsequent elimination with PTSA to afford indene **42c** proceeded smoothly to yield clean product in 80% yield over the two steps. Implementing our optimized one-pot, two-step Organic Synthesis procedure:[43] **42c** was epoxidized to **43c** via *in situ* generation of

peroxyformic acid. Excess formic acid within the reaction readily ring-opened epoxide **43c** to the formate ester intermediate (**44c**). Subsequent hydrolysis and dehydration to afford 2-indanone **10c** was achieved through a modified steam distillation. In lieu of the traditional steam distillation that introduces steam from an external source, refluxing the crude formate ester intermediate in aqueous acid condenses the clean product without

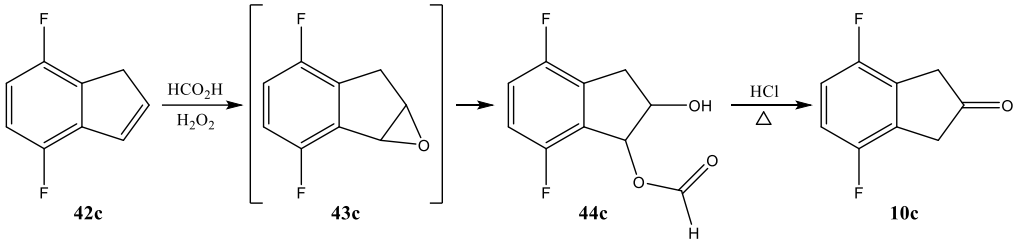

Figure 21. Two-step, one pot reaction to afford isoindanone **10c** from the corresponding indene derivative (**42c**).

running water in the condenser unit. If water was running through the condenser unit the product would solidify in the distillation bridge and prevent further product from being pulled over. If this occurred the bridge was rinsed with a small amount of dichloromethane and the distillation resumed. The previously optimized protocol utilized 7% aqueous sulfuric acid for the hydrolysis and dehydration step,[43] yet again more forcing reaction conditions were necessary for the *para*-fluorinated isomer and with the use of half concentrated hydrochloric acid we obtained 2-indanone **10c**. This modified protocol gives clean **10c** in 50% yield over the two-steps and was scalable up to a 2 gram batch.

Although this vetted synthetic route provided reliable access to clean 4,7-difluoro-2-indanone (**10c**) in gram quantities, we wanted to search for milder reaction conditions and probe the effect of the fluorine substituent pattern toward previously unsuccessful attempts at epoxidation of the 5,6-difluoro-indene.[38] MCPBA epoxidation of **42c** at room temperature initially appeared by ^{1}H NMR to deliver the desired epoxide with significant

impurities and side products (**Figure 22**). However, upon thorough analytical analysis it was found that our crude material contained the isomeric mixture of the corresponding diols that were formed during the reaction by ring-opening of the epoxide with residual

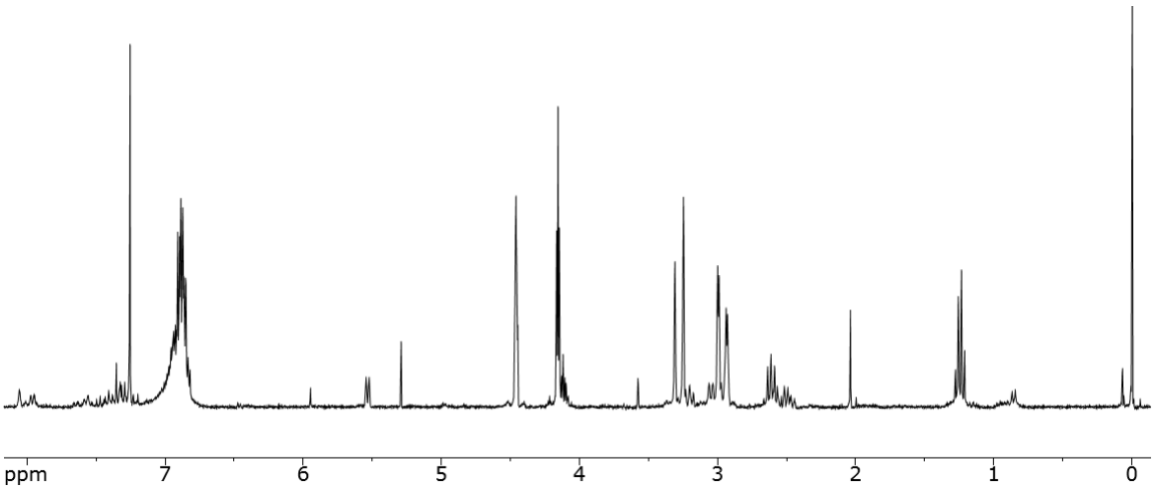

Figure 22. Crude ^{1}H NMR after epoxidation of **42c** with MCPBA.

water in the reaction from the MCPBA reagent. The subsequent rearrangement to 2-indanone **10c** was attempted utilizing zinc iodide at the Lewis acid catalyst[44] but no reaction was observed, which was not surprising due to the predominant presence of the isomeric diol mixture. We ultimately found promise in a PTSA catalyzed dehydration of the crude epoxidation material to afford 2-indanone **10c** in 68% yield over the two steps. Through this optimized sequence we are able to obtain **10c** in gram quantities with milder reaction conditions.

3.2.1.2. Synthesis of 4,7-Dimethoxy-2-indanone

4,7-Dimethoxy-2-indanone (**10i**) has been reported in the literature as a synthetic intermediate for pharmaceuticals[45] and agrochemicals.[46] Following our previously optimized procedure for the synthesis of propionic acid derivatives of type **39** from the corresponding benzaldehyde, we could access 4,7-dimethoxy-propionic acid (**39i**) in

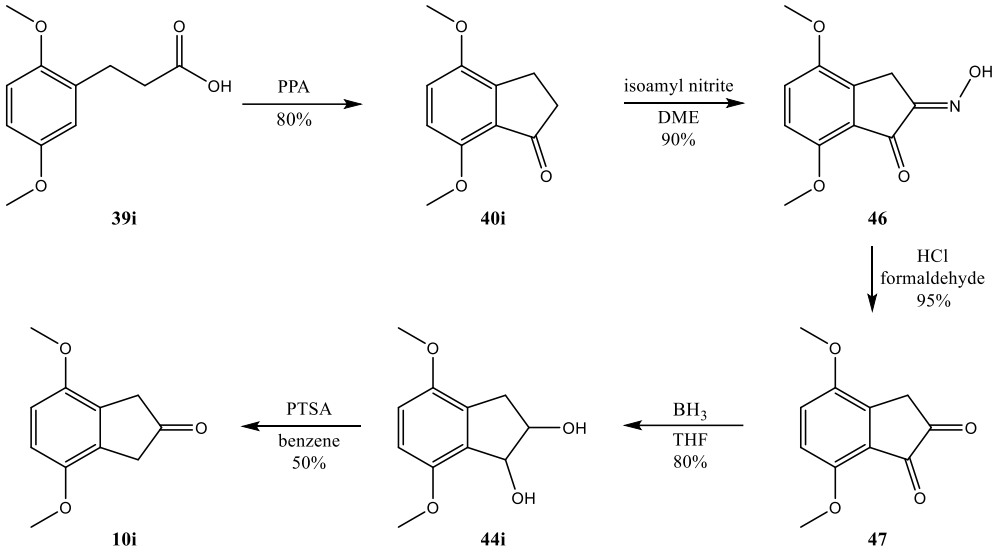

Figure 23. Optimized synthetic route to 4,7-dimethoxy-2-indanone (**10i**).

nearly quantitative yield over the two-step sequence. Subsequent cyclization via Friedel-Crafts acylation occurs readily with PPA but strict reaction conditions must be adhered otherwise the yield and purity of the product decreases rapidly. Although an increase in reaction temperature often lead to undesired aldol dimerization for other derivatives, that has not been observed with occasional overheating of 4,7-dimethoxy-1-indanone (**40i**) cyclization reactions. In an isolated incident we observed clean conversion to the corresponding aldol dimer, however, with a gross oversight in the protocol this particular batch was heated at 100 °C for over 24 h. We observed that the size of the RBF and the size and shape of the magnetic stir-bar also make an impact on reaction success; for optimal results a wide neck 100 mL RBF should be utilized with a 1 inch stir-bar that is not football shaped.

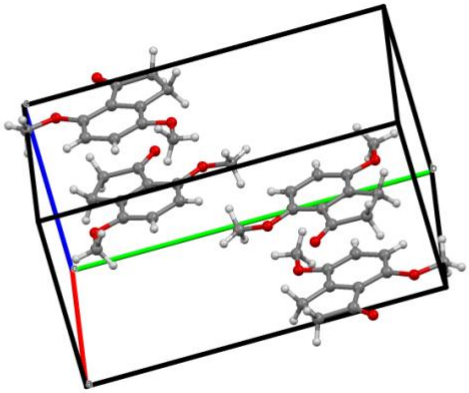

Figure 24. Crystal structure and unit cell of 4,7-dimethoxy-1-indanone (**40i**).

The subsequent ketone transposition was achieved over a four-step sequence in 34% yield, along a modified literature protocol that obtained milligram quantities of 5,6-dimethoxy-2-indanone by preparatory TLC.[47] The final synthetic transformation was the bottleneck reaction that primarily accounts for the overall low yield. Oximation of 1-indanone **40i** occurred readily at room temperature with isoamylnitrite to afford the clean product in 90% yield as a tan solid that was collected via suction filtration. Hydrolysis of oxime **46** to the corresponding diketone (**47**) was accomplished with concentrated hydrochloric acid and formaldehyde in nearly quantitative yield to give clean **47** as a brown solid that was also collected via suction filtration. Subsequent reduction of **47** utilized boron as the reducing agent and necessitated two days for complete conversion to afford diol **44i** in 80% yield as a tan crystalline solid. PTSA catalyzed dehydration of **44i** was sluggish and required refluxing for a minimum of 12 hours to obtain optimal conversion without significant increase in undesired side products. The crude product was purified by trituration with diethyl ether to afford clean **10i** as a beige solid in 50% yield.

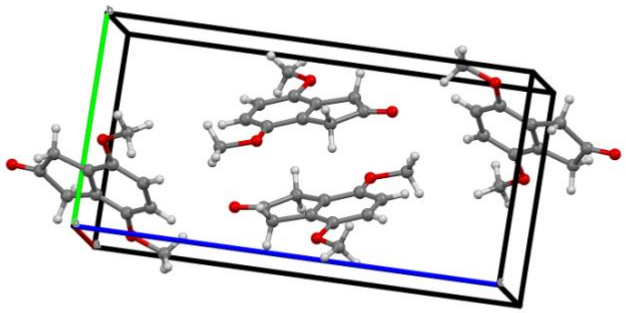

Figure 25. Crystal structure and unit cell of 4,7-dimethoxy-2-indanone (**10i**).

3.2.1.3. Synthesis of 4,7-Dimethyl-2-indanone

4,7-Dimethyl-2-indanone (**10m**) has been utilized as a synthetic intermediate for the regioselective synthesis of ellipticine[48] and the preparation of organometallic complexes for catalysis[49] and cytotoxic activities.[50] The literature reported preparations of **10m** follow synthetic routes for the oxidation of the preceding indene (**42m**).

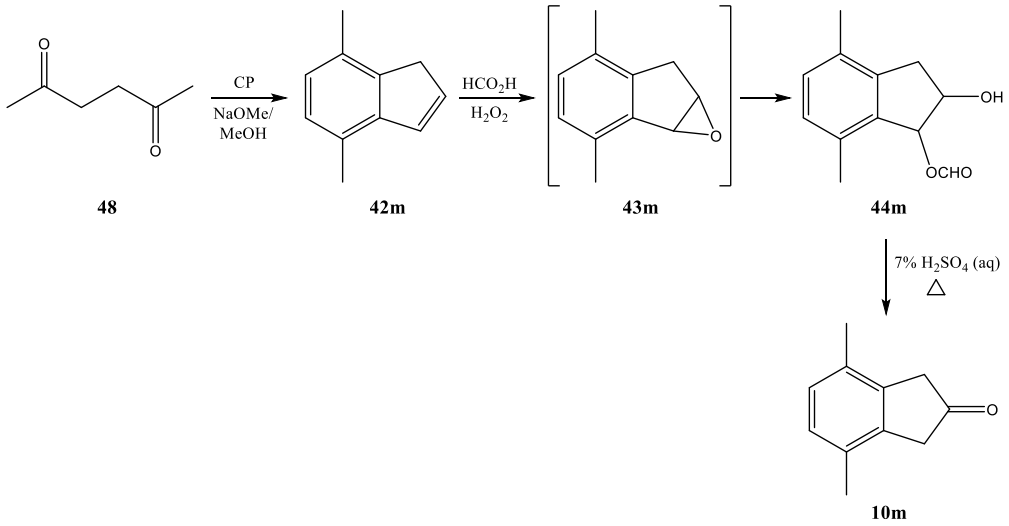

Figure 26. Synthesis of 4,7-dimethyl-2-indanone (**10m**).

We obtained multi-gram quantities of **10m** through a three-step sequence. Commercially available hexa-2,5-dione was subjected to cyclization with cyclopentadiene

under basic conditions to afford indene **42m** in 85% yield.[51] A two-step, one-pot Organic Synthesis procedure[43] that was vetted for the conversion of parent indene to the corresponding 2-indanone was employed to afford epoxide **43m** via *in situ* generation of peroxyformic acid. Excess formic acid within the reaction readily ring-opened epoxide **43m** to the formate ester intermediate **44m**. Subsequent hydrolysis and dehydration to afford 2-indanone **10m** was achieved through a modified steam distillation. In lieu of the traditional steam distillation that introduces steam from an external source, refluxing **44m** in 7% aqueous sulfuric acid condensed the clean product on the distillation bridge without running water. This modified protocol gives clean **10m** in 50% yield over the two-steps and can be scaled up to 10 grams.

Alternatively, epoxidation of **42m** with MCPBA gave a complex mixture of the desired epoxide with the enantiomeric mixture of the ring-opened diols in quantitative yield. Subsequent PTSA catalyzed dehydration on the crude epoxidation mixture affords clean **10m** in 65% yield. Although this methodology affords a higher yield with milder reaction conditions, it was only successfully scalable to a 2 gram batch before considerable decrease in conversion and overall yield was observed.

3.2.1.4. Synthesis of 4,7-Diphenyl-2-indanone

Analogous to the methodology applied to obtain 4,7-dimethyl-2-indanone (**10m**), we targeted the appropriate dione (**51**) for subsequent cyclization and oxidation to 4,7-diphenyl-2-indanone (**10n**).

NBS bromination of acetophenone **49** proceeded smoothly with a catalytic amount of PTSA along a literature described protocol.[52] Following aqueous workup the crude material contained primarily the desired brominated product (**50**) with trace amounts of residual starting material. Recrystallization from a chloroform:hexane (4:1) mixture affords clean **50** as a tan crystalline solid in 90% yield. Subsequent homocoupling of **50** was accomplished with zinc dust in the presence of a catalytic amount of iodide through a zinc stabilized enolate intermediate. The crude product was often a mixture of the desired dibenzoylethane (**51**) and up to 10% **49** that forms via zinc-mediated reduction of **50**.

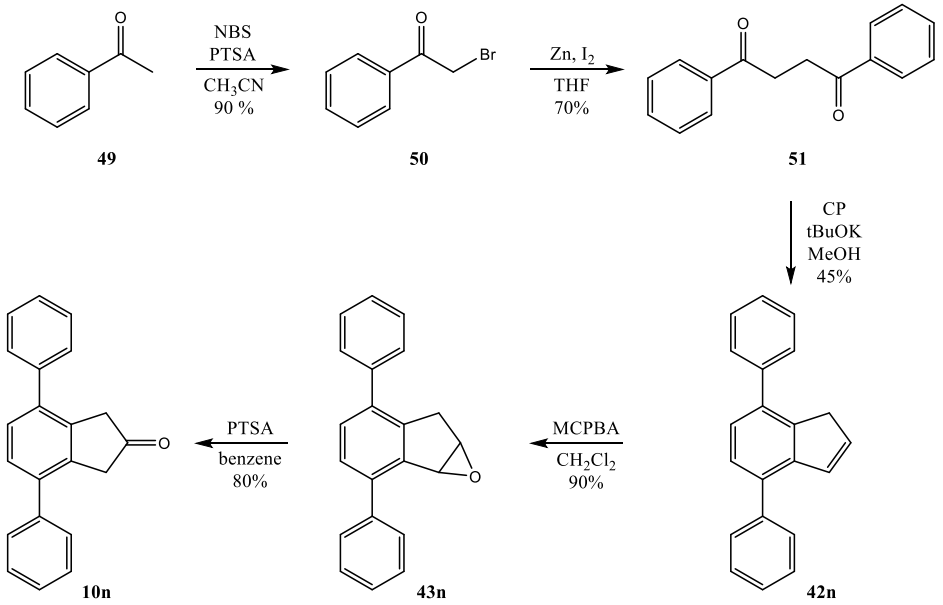

Figure 27. Optimized synthesis of 4,7-diphenyl-2-indanone (**10n**).

Cyclization of **51** was accomplished with cyclopentadiene under basic conditions, following a literature reported protocol.[53] After several attempts, we were unable to obtain a satisfactory yield in comparison to the reported results and probed alternative reaction conditions (**Table 2**). Under our optimized conditions, gentle heating of the reaction to 40 °C increased the conversion to the desired indene (**42n**) by 50%. Column

chromatography on silica gel with pentane:ethyl acetate (5:1) affords clean **10n** as a colorless solid in 40% yield.

Table 2. Probed reaction conditions for the cyclization to 4,7-diphenyl-indene (**42n**) with product ratios observed in GC-MS.

Solvent	Base	Base Equivalent	T (°C)	t (d)	Observed Conversion (%)
THF	NaH	1.1	RT	4	0
Et_2O	NaH	1.1	RT	4	< 5
EtOH	NaOEt	1.1	RT	4	< 5
MeOH	NaOMe	1.1	RT	4	< 15
MeOH	NaOMe	1.5	RT	4	< 15
MeOH	tBuOK	0.5	RT	4	< 5
MeOH	tBuOK	0.5	40	4	45-50
MeOH	tBuOK	1	RT	4	< 5
MeOH	tBuOK	1	40	4	45-50

Due to the additional phenyl substituents, we did not anticipate that the Organic Synthesis procedure would be a feasible route to the desired 2-indanone. Therefore, we employed the previously mentioned alternative route utilized on 4,7-dimethyl-indene (**42m**). Epoxidation of **42n** proceeded in quantitative yield, analogous to other indene derivatives of type **42**. Subsequent PTSA catalyzed dehydration afforded clean **10n** as a beige solid in 78% yield.

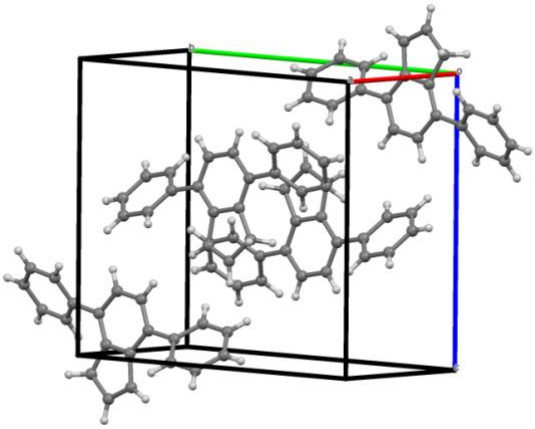

Figure 28. Crystal structure and unit cell of 4,7-diphenyl-indene (**42m**).

3.2.2. "Simple" Isoindenone Dimers

While the parent isoindenone dimer and several derivatives thereof can be readily prepared, the formal tetrafluoro-isoindenone dimer (**14b**) remained an elusive target for our group, in lieu of exhaustive investigations through a variety of synthetic routes. Notably, the route pioneered by Jones *et al.* for isoindenone generation and dimerization was applied towards our target.[28] Through the three-step procedure starting with 4,5,6,7-tetrafluoro-2-indanone (**10b**), only poorly characterized, presumably polymeric, material was obtained. Although Jones' report claimed the dimerization of parent isoindenone, they provided no analytical details for characterization. We reproduced and optimized this sequence on the parent system to serve as a control and obtained full characterization of the parent dimer (**14a**) for the first time. This prompted our investigation into the generation and dimerization of isoindenones (**13**) with an array of electronic and steric properties to probe the reactivity of these fleeting intermediates. Discussed below are the thesis-relevant *para*-substituted systems.

3.2.2.1. "Simple" Isoindenone Dimers Incorporating Electron-Donating Substituents

We anticipated that applying the optimized route to 4,7-dimethyl-2-indanone (**10m**) would deliver results analogous to the parent system. The corresponding silyl enol ether (**28m**) was prepared utilizing DBU to generate the enolate intermediate, instead of LDA, to avoid the necessity of low temperatures. Subsequent NBS radical bromination at reflux proceeded quickly to afford the corresponding bromo silyl enol ether **27m** in less than 10 minutes. The crude bromo silyl enol ether was notably susceptible to hydrolysis so to avoid this it was quickly taken up in acetonitrile and added slowly to a refluxing suspension of cesium fluoride in acetonitrile. The slow addition is imperative to minimize

polymerization of the highly reactive isoindenone intermediate (**13m**). Following aqueous workup, the crude product shows mostly the desired dimer **14m** with minor impurities. The crude material was taken up in acetone and precipitation with pentane afforded the clean dimer (**14m**) as a colorless solid in 55% yield.

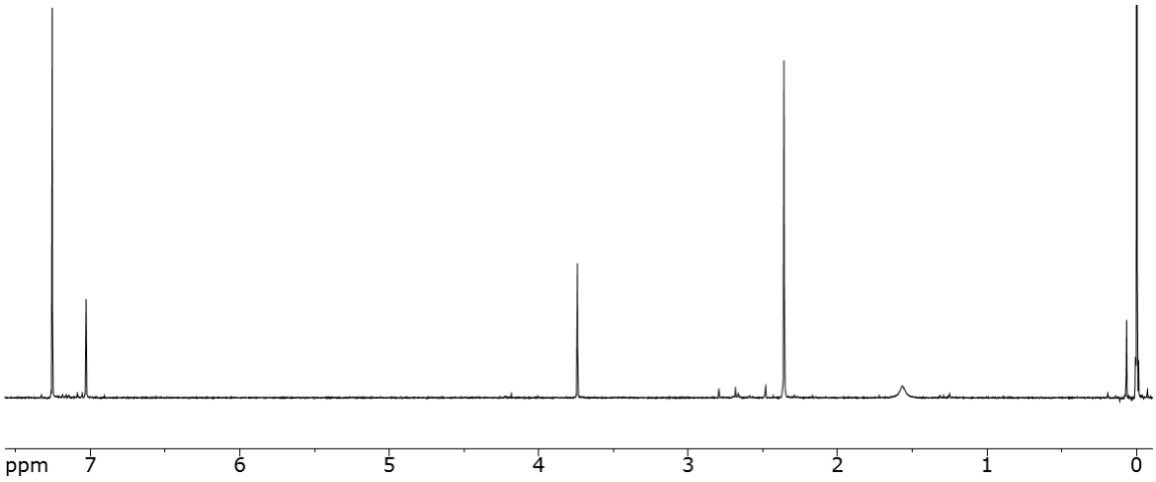

Figure 29. ^{1}H NMR spectrum of the formal 4,7-dimethyl-isoindenone dimer (**14m**).

To probe the applicability of this sequence toward systems with electron-donating substituents on the arene unit we applied it to two dimethoxy isoindanone derivatives (**10i** and **10j**). We obtained the corresponding isoindenone dimer (**14j**) for the *ortho*-substituted isomer in 55% yield[38] but were unable to obtain the desired dimer from the *para*-substituted system. Silylation of 4,7-dimethoxy-2-indanone (**10i**) proceeded smoothly with DBU at room temperature. The crude product was an orange oil that was characterized by ^{1}H NMR. Unlike the other silyl enol ethers previously obtained, GC-MS data for the dimethoxy derivatives could not be obtained. The subsequent NBS bromination proceeded quickly and did not require reflux, or any heating, for the reaction to occur. The crude bromo silyl enol ether (**27i**) was obtained quantitatively with high purity as an orange sticky solid. Trace amounts of carried over TBDMSCl was present but there were no significant

side products or impurities. Bromo silyl enol ether **27i** was particularly stable, unlike other bromo silyl enol ethers obtained, with no hydrolysis observed within 24 hours at room temperature. A solution of **27i** in acetonitrile was added to refluxing cesium fluoride in acetonitrile slowly, via syringe pump. The reaction mixture became turbid and turned brown over time. Following aqueous workup, the crude product did not contain the anticipated ^{1}H NMR signals for the diagnostic bridgehead protons but was a more complex product. We obtained MS data from direct injection that gave a molecular weight of 334 g mol^{-1}, which does not correlate to the isoindenone dimer but could correlate to some

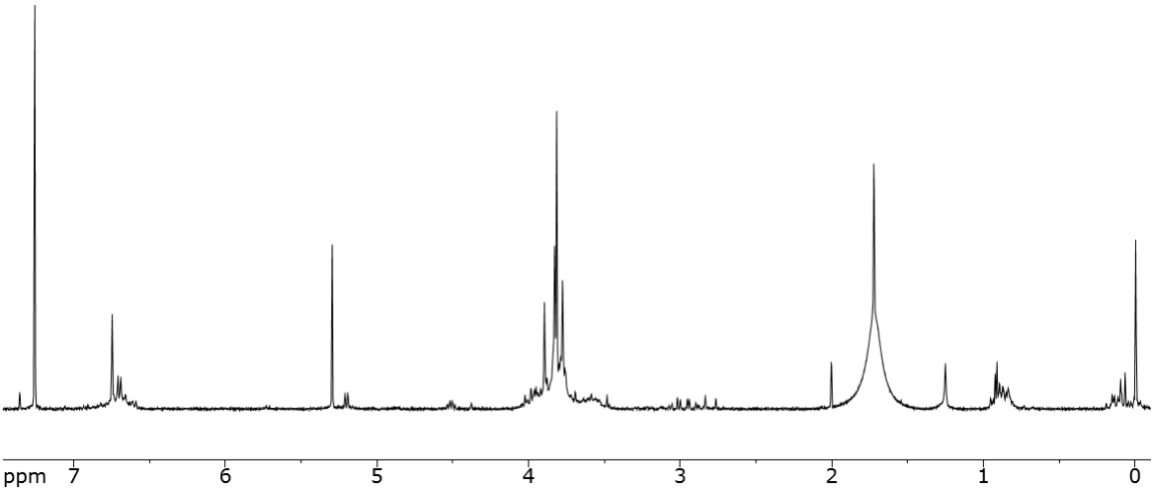

Figure 30. Crude ^{1}H NMR after attempted generation and dimerization of 4,7-dimethoxy-isoindenone (**13i**).

other dimerization product. Unfortunately, we were unable to assign the exact structure of the compound but it did leave us to question why we did not obtain the isoindenone dimer (**14i**) even though we obtained the direct precursor **27i** in high yield and purity.

We also targeted a diphenylated system by employing this sequence to 4,7-diphenyl-2-indanone (**10n**). We obtained silyl enol ether **28n** in 90% yield as a brown oil and characterized it by ^{1}H NMR and GC-MS. The subsequent NBS bromination also proceeded quickly to afford **27n** quantitatively as a brown sticky solid. A solution of **27n**

in acetonitrile was added to refluxing cesium fluoride in acetonitrile slowly. The reaction mixture became turbid and turned dark brown over time. Following aqueous workup, the crude product did not contain any defined signals but had significantly broad signals in the aromatic region that were largely under the chloroform solvent peak and a singlet at 4.39 ppm, in the anticipated bridgehead region. A ^{1}H NMR in methylene chloride allowed for the integration of all peaks that we anticipated were our desired product, although the aromatic region was still just two broad signals. We attempted a low temperature ^{1}H NMR to see if we could get any definition to the signal structures to no avail. Integration of the broad aromatic signals did correlate to the relative integration ratios of 5:1 that we would expect in the aromatic region for isoindenone dimer **14n**. We were unable to obtain a GC-

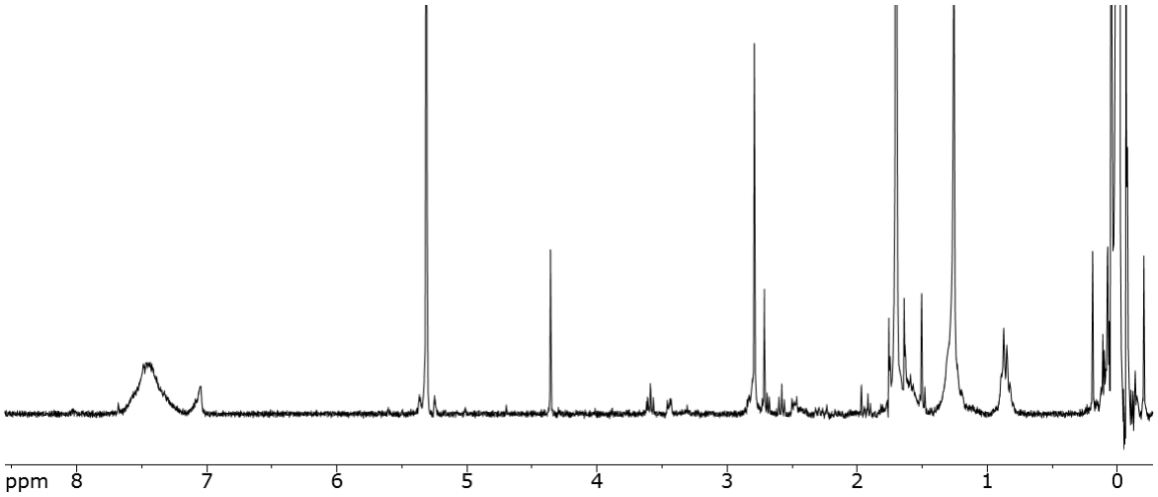

Figure 31. Crude ^{1}H NMR after reaction for generation and dimerization of 4,7-diphenyl-isoindenone (**13n**).

MS but we did acquire MALDI-TOF data that we felt strongly suggests that we actually obtained **14n**. The MALDI-TOF showed the apparent parent peak to be 508 *m/z*, which corresponds to the loss of two carbonyls from the isoindenone dimer. Although this is not what we have typically observed with these molecules, this directly correlates to the trend observed for the base peak with all of the isoindenone dimers obtained to date. MALDI is

an ionization technique that employs a laser energy absorbing matrix to generate ions of large molecules with minimal fragmentation. Due to this, it is not surprising that with this technique we observed the most stable ion of the isoindenone dimer as the apparent parent peak.

3.2.2.2. Fluorinated "Simple" Isoindenone Dimers

The inability to obtain the tetrafluoro-isoindenone dimer (**14b**) led us to question whether the degree of fluorination and/or the position of fluorine substituents on the arene unit contributed to the failed dimerization. This prompted investigation into the generation and dimerization of fluorinated isoindenones with varying degrees of fluorination and substituent patterns on the arene unit.

Employing our optimized sequence to two difluorinated isoindanone isomers (**10c**/**10d**) we obtained both corresponding isoindenone dimers (**14c**/**14d**) in 30-50% yield as light brown solids.[38] The fluorinated bromo silyl enol ethers (**28c**/**28d**) also exhibited hydrolytic lability with minor amounts of the corresponding 1-bromo-2-indanone derivative present following workup. It was imperative to immediately react the bromo silyl enol ethers before significant hydrolysis occurred. Purification of **14c** and **14d** was accomplished by taking the crude material up in a small amount of acetone and precipitation of the clean dimer with pentane.

With success on the difluorinated systems we investigated select isomers along the full spectrum with respect to the degree of fluorination on the aromatic unit of 2-indanones. We subjected 4-fluoro-2-indanone (**10e**) and 5-fluoro-2-indanone (**10f**) to the three-step sequence to deliver their expected *anti*-benzo scaffolds (**14**). Selective dimerization of the unsymmetrical monofluorinated systems was anticipated to provide information on the

potential electronic effects of the fluorine substituent at either position, but both possible isomers were obtained on both systems. The isomeric products observed in each monofluorinated dimerization were obtained in nearly equal amounts, reflecting the high reactivity, and non-selective nature, of the fleeting isoindenone intermediate.

Both trifluorinated isomers 4,5,6-trifluoro-2-indanone (**11g**) and 4,5,7-trifluoro-2-indanone (**11h**) were subjected to the same protocol and no distinguishable products were obtained. Only broad signals in the aromatic region were observed in the ^{1}H NMR for each system. Unfortunately, no specific reactivity trends could be drawn from our extensive investigations on these seven fluorinated systems. We found that the position of fluorine substituents on the aromatic ring does not seem to affect its reactivity but the degree of fluorination does, isoindenones possessing three or more fluorine substituents on the arene unit do not deliver defined products.

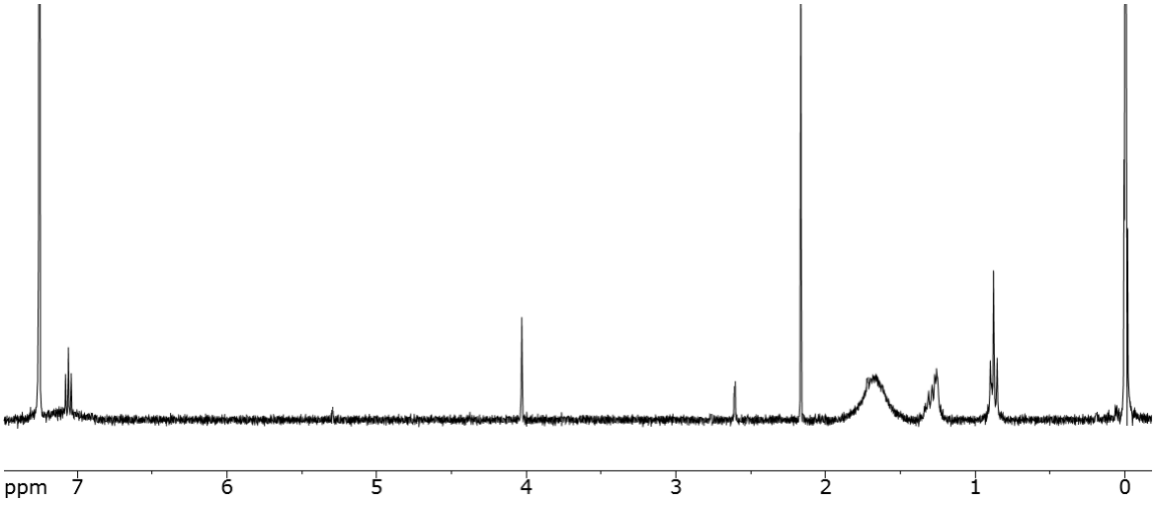

Figure 32. ^{1}H NMR spectrum of the formal 4,7-difluoro-isoindenone dimer (**14c**).

3.2.3. Toward the Formal Tetrafluoro-Isoindenone Dimer

All previous attempts by our group to obtain the formal tetrafluoro-isoindenone dimer (**14b**) through isoindenone generation and subsequent dimerization have failed even

though we have successfully obtained the direct precursor (**27b**) in high yield and purity. We postulate that this is the result of a destabilized isoindenone intermediate due to the significant electron deficiency of the arene unit bearing four fluorine substituents. In previous efforts by our group, we obtained and characterized the octachloro-*anti*dibenzo dimer (**14k**) through an alternative method via the benzannulation of dienedione (**32**). At that time, an appropriate C_4F_4 synthon was not accessible to employ in this benzannulation method.

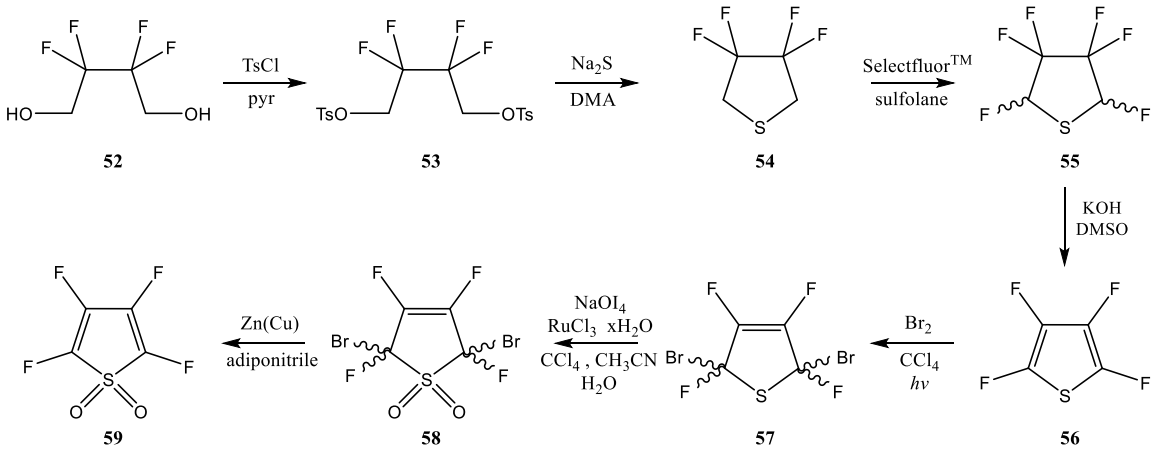

Figure 33. Reported synthetic route to tetrafluorothiophene S,S-dioxide (**59**).

Recently, a sophisticated route that affords tetrafluorothiophene S,S-dioxide (**59**) was reported by Lemal *et al.* (**Figure 33**) that appears as a promising C_4F_4 synthon, although its synthesis is arduous and has a meager 18% overall yield.[55] This seven-step procedure begins with the tosylation of commercially available 2,2,3,3-tetrafluorobutane-1,4-diol (**52**) with tosyl chloride to afford ditosylate **53** as a tan solid in quantitative yield. The subsequent cyclization to 3,3,4,4-tetrafluorothiolane (**54**) was accomplished by stirring **53** with sodium sulfide hydrate in a high boiling solvent to allow for product isolation by vacuum transfer. The liquid N_2-cooled trap-to-trap vacuum transfer was originally

reported to be carried out at a pressure of 16 mbar at 70 ºC, however, as the pressure was reduced to 25 mbar there was significant burping of the reaction mixture observed. The vacuum pressure was increased to 40 mbar and brought down slowly over one hour to reach 16 mbar without noticeable burping. After holding the vacuum pressure at 16 mbar for 20 minutes, the u-tube trap was warmed to room temperature and the contents were pipetted into a pear-shaped flask.

The phase separation between the product and any accompanying water was not apparent to the naked eye and it was reported that a small drop of red food coloring was often utilized to visualize the layers.[55] Upon addition of minimal red food coloring, it continued to appear as a homogenous sample with no clear distinction between the two phases making separation of the desired product from water increasingly difficult. Based solely on the crude mass balance and anticipated yield, an appropriate amount of concentrated sulfuric acid was added to sequester the water and the thiolane was short-path distilled to remove any residual solvent to afford thiolane **54** as a colorless liquid in 55% yield.

Fluorination to *cis*- and *trans*-2,3,3,4,4,5-hexafluorothiolane (**55**) was achieved with Selectfluor® via a tandem fluoro-Pummerer rearrangement.[55] The product mixture was isolated by a liquid N_2-cooled trap-to-trap vacuum transfer and subsequently short-path distilled without water in the condenser to afford the hexafluorothiolane **55** as a colorless liquid in 50% yield. Dehydrofluorination of **55** occurs readily upon the addition of powdered potassium hydroxide. Again, the product is isolated by a liquid N_2-cooled trap-to-trap vacuum transfer to afford tetrafluorothiophene (**56**) as a colorless liquid in 75% yield.

The reaction of bromine with tetrafluorothiophene has been reported to be considerably sluggish,[56] therefore, the bromination of **56** was facilitated by irradiation with a 5.5 W UV lamp. Conversion is monitored by ^{19}F NMR with C_6D_6 as the internal standard and is typically complete in under three hours to afford a mixture of the *cis* and *trans* isomers (**57**) in 90% yield. The oxidation of *cis*- and *trans*-2,5-dibromo-2,3,4,5-tetrafluorothiol-3-ene was reported to occur without difficulty in 23 hours. Repeating this reaction under exact literature conditions,[55] we were unable to obtain the desired dioxide **58** after multiple attempts. Even with the most vigorous stirring we always observed a clearly biphasic mixture, which also made monitoring the reaction by ^{19}F NMR exceedingly difficult. Attempts were made to check each of the two phases independent of each other but the NMR was consistently unable to lock onto either sample. Ultimately, we proceeded with the aqueous workup after the reported 23 hour reaction time without prior ^{19}F NMR confirmation.

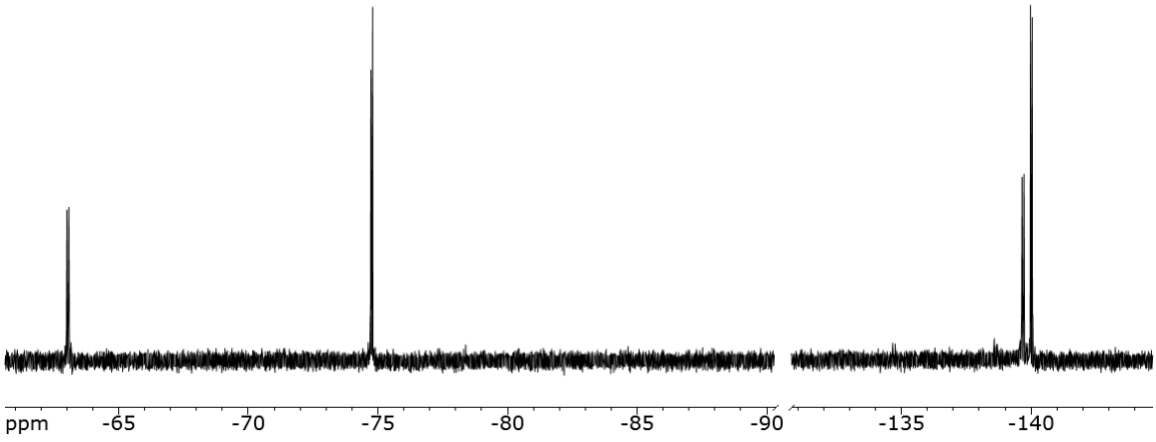

Figure 34. ^{19}F NMR of 2,5-dibromo-2,3,4,5-tetrafluorothiol-3-ene (**57**), both *cis* and *trans* isomers.

In all five attempts, we were unable to obtain evidence for the desired dioxide but we did isolate the same unidentified product(s) reproducibly each time. The unidentified product(s) did not correlate to the formation of the mono oxidized species and its structure(s) could not be identified as poor solubility did not allow for ^{13}C NMR data to be obtained. The ^{19}F NMR had four peaks: two apparent doublets at -143.0 and -143.16 ppm and two apparent triplets at -144.07 and -144.24 ppm. There were no peaks observed in the GC-MS but we were able to obtain a molecular weight of 391 by ESI. We are unsure what led to the demise of this reaction, considering that we obtained the direct precursor both visually and spectrally clean per literature reports (**Figure 34**).[55] Ultimately, after using all of the available precursor and not obtaining the necessary dioxide **58** it became unfeasible to continue our efforts toward the tetrafluorothiophene S,S-dioxide (**59**) along this route.

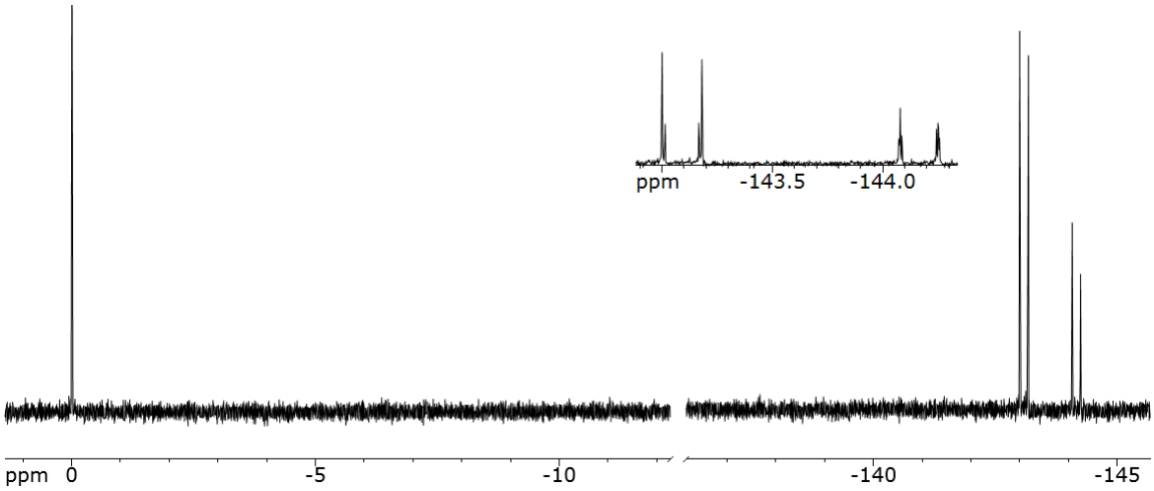

Figure 35. Crude ^{19}F NMR obtained after the attempted oxidation of 2,5-dibromo-2,3,4,5-tetrafluorothiol-3-ene (**57**).

3.2.4. Novel "Mixed" Isoindenone Dimers

Our group has previously established a small library of "simple", symmetrical isoindenone dimers of type **14**, where the arene unit is functionalized with either electron-donating or electron-withdrawing substituents. Our inability to obtain the corresponding isoindenone dimers for a handful of derivatives (**12b**, **12i**, and **12l**), that are similar electronically or sterically to other isoindenone dimers we have successfully obtained, propelled us to investigate "mixed" dimerizations between isoindenones bearing different substituents and/or substituent patterns.

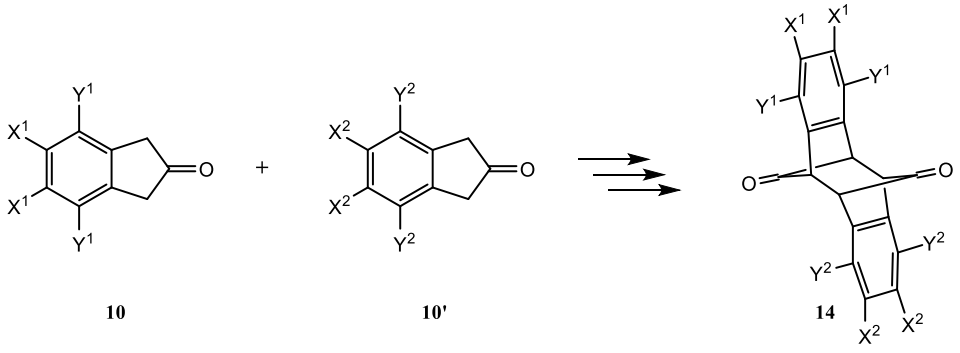

	X¹	Y¹	X²	Y²	Observed Products	GCMS Yield Ratios for Mixtures
o	H	H	H	Me	***a, m, o***	1:1:3 (a:m:o)
p	H	H	H	OMe	***a, p***	3:2 (a:p)
q	H	Me	H	OMe	***m, q***	1:1 (m:q)
r	H	H	OMe	H	*not yet attempted*	
s	OMe	H	H	OMe	***j***	N/A
t	H	H	F	H	***a, d, t***	1:2:1 (a:d:t)
u	H	H	H	F	***a***	N/A
v	F	H	H	F	***d***	N/A

Figure 36. Targeted "mixed" isoindenone dimers including a table with substituent patterns that delivered desired mixed dimer of type **14** (green) or did not (red).

3.2.4.1. "Mixed" Isoindenone Dimers Incorporating Electron-Donating Substituents

Previous investigations into isoindenone dimers of type **14** that possess electron-donating substituents on the arene unit have not delivered conclusive reactivity trends of

the various intermediates as nearly all of the attempted systems have delivered the desirable symmetrical isoindenone dimer in comparable and satisfactory yields. However, our inability to obtain the formal *para*-dimethoxy isoindenone dimer, even though we obtained the direct precursor **27i** in high yield and purity, lead us to question whether the methoxy substituents were sterically prohibiting the self-dimerization or if electronic effects prevented the generation of the corresponding isoindenone intermediate. To further probe whether the failure was attributed to sterics or electronics, we launched investigations into mixed dimerizations.

We initially targeted the mixed dimerization between the easily accessible parent and *para*-dimethyl isoindenones. Stoichiometric amounts of parent 2-indanone (**10a**) and 4,7-dimethyl-2-indanone (**10m**) were subjected, in parallel, to an optimized three-step procedure that Jones' reported for the generation and dimerization of the parent isoindenone to afford the desired dimer of type **14**. The corresponding silyl enol ethers of type **28** were prepared utilizing DBU to generate the enolate intermediate, instead of LDA, to avoid the necessity of low temperatures. Subsequent NBS radical bromination at reflux proceeded quickly to afford the corresponding bromo silyl enol ethers of type **27** in less than ten minutes. The crude bromo silyl enol ethers were combined in a homogenous solution with acetonitrile and added slowly, via syringe pump, to a refluxing suspension of cesium fluoride in acetonitrile. The slow addition is imperative to minimize the polymerization of the highly reactive intermediate. Following aqueous workup, the crude product showed a mixture of the three possible dimers: the parent isoindenone dimer (**14a**), the *para*-dimethyl isoindenone dimer (**14m**), and the desired mixed dimer (**14o**) in a roughly 1:1:3 ratio, by GC-MS, favoring the formation of the mixed dimer (**Figure 37**).

Taking the mixture up in acetone and precipitating with a minimal amount of pentane, a purification method previously utilized on the symmetrical isoindenone dimers, showed enrichment of the desired mixed dimer in the mother liquor but does not achieve complete separation.

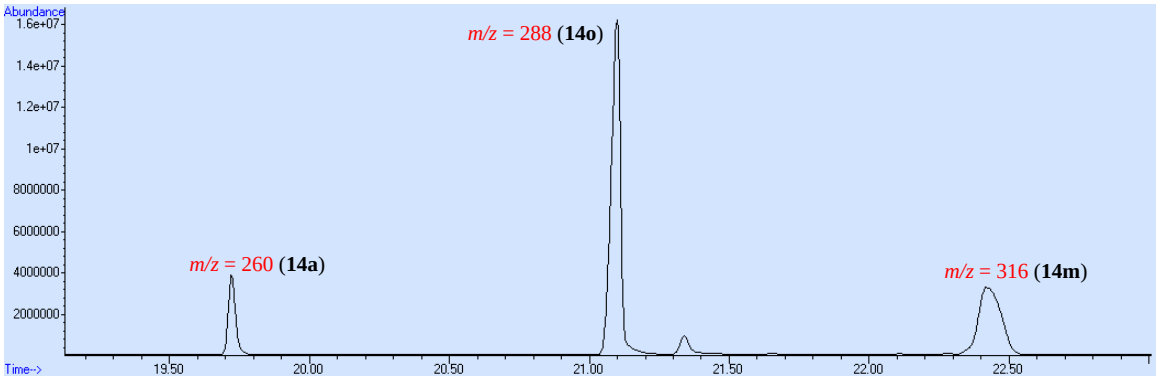

Figure 37. Gas Chromatogram of the crude product obtained from a mixed dimerization between the parent and *p*-dimethyl isoindenones.

With success in obtaining the mixed dimerization product between the parent and *para*-dimethyl isoindenones, we targeted investigations on the elusive *para*-dimethoxy system. To probe any electronic effects that may prevent isoindenone generation, we performed a mixed dimerization between the parent and *para*-dimethoxy systems. Much to our delight, we obtained the desired mixed dimer (**14p**) in a 3:1 ratio, by GC-MS, with the parent isoindenone dimer (**14a**), favoring the formation of the mixed dimer (**Figure 38**). This suggests that the *para*-dimethoxy isoindenone intermediate (**13i**) is indeed formed, but further raises the question as to why it does not self-dimerize; leading us to hypothesize that it may most likely be a steric effect. The traditional methodology of purification for these compounds is to take the crude material up in acetone and precipitate the product from a minimal amount of pentane. Generally, with a triplicate attempt clean product is obtained but this particular mixed system could not be purified with this method, with no observed enrichment of the precipitate or the mother liquor. A column

chromatography with hexane:ethyl acetate (4:1) was attempted and resulted in the separation of the mixed dimer from the parent dimer, but the fractions containing the mixed dimer still contained unidentified impurities that we were unable to remove through subsequent purification attempts.

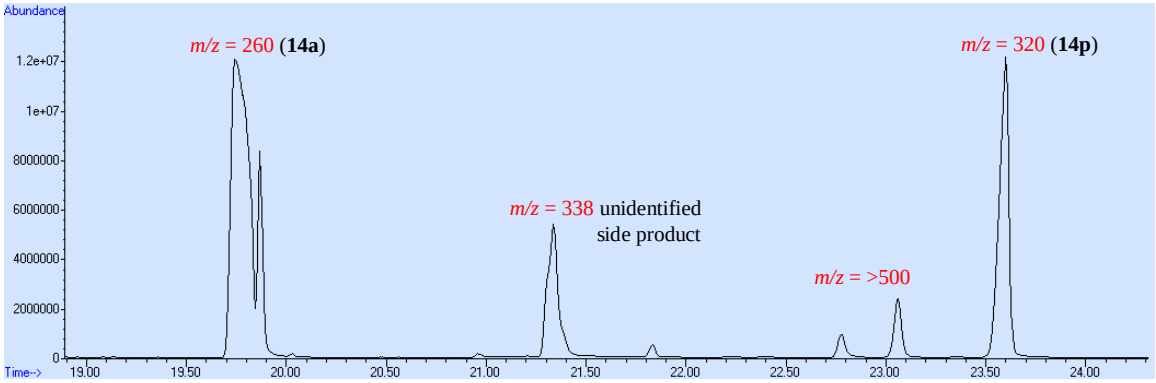

Figure 38. Gas Chromatogram of the crude product obtained from a mixed dimerization between the parent and *p*-dimethoxy isoindenones.

To probe the potential steric effects on the dimerization of *para*-dimethoxy isoindenone (**13i**), we performed a mixed dimerization between the *para*-dimethoxy and *para*-dimethyl systems. To our surprise, we obtained the mixed dimer (**14q**) in roughly a 1:1 ratio, by GC-MS, with the *para*-dimethyl isoindenone dimer (**14m**) (**Figure 39**). Although the methyl substituents do not provide equal steric encumbrance as a methoxy substituent, we felt confident to assume sterics were not the primary driving force behind the failed self-dimerization attempts. As observed with some of the other mixed systems, our traditional purification methodology did not allow for separation of the dimers and a column chromatography on silica gel was attempted. The desired dimer **14q** stuck to the column but was recovered in a methanol wash with other impurities.

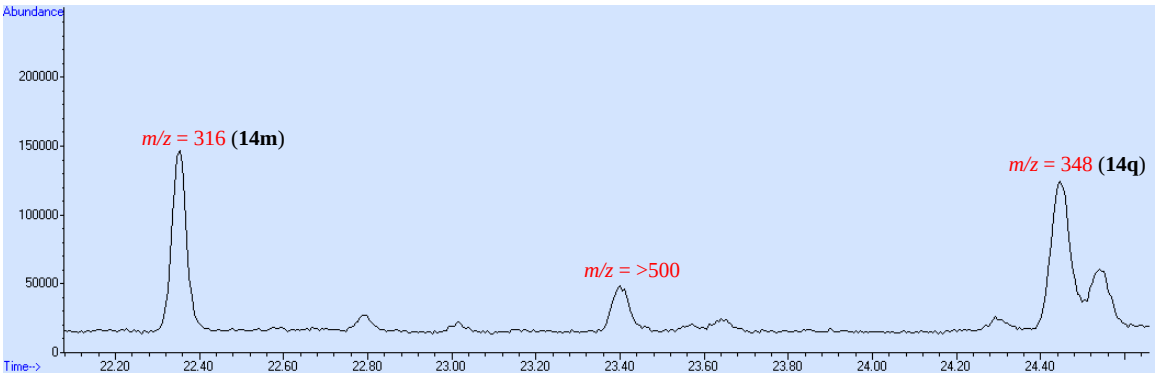

Figure 39. Gas Chromatogram of the crude product obtained from a mixed dimerization between the *p*-dimethyl and *p*-dimethoxy isoindenones.

With no significant evidence to substantiate the claim that sterics are the only factor preventing the self-dimerization of **13i**, we proceeded to further probe the effect of the electronics by attempting a mixed dimerization between the two dimethoxy isoindenone isomers. In these attempts, only the *ortho*-methoxy isoindenone dimer (**14j**) was obtained. With the inability to obtain the mixed dimer between these two intermediates, we propose that there is an electronic effect prohibiting the self-dimerization of **13i** as it also does not dimerize with the *ortho*-dimethoxy isomer **13j**.

3.2.4.2. Fluorinated "Mixed" Isoindenone Dimers

Previous investigations into fluorinated isoindenone dimers of type **14** with varying degrees of fluorination allowed for general reactivity trends to be postulated. Unsymmetrical monofluorinated systems afforded both possible dimeric isomers in nearly equal amounts, showing no distinct regioselectivity of the highly reactive intermediates. The two symmetrical difluorinated systems afforded their corresponding dimers in satisfactory, comparable yields showing that the position of the fluorine substituents on the arene unit did not substantially affect reactivity of the isoindenone intermediate. However, dimerization attempts of the two trifluorinated isomers and the tetrafluorinated system failed without any evidence of defined products that could result from their isoindenone

intermediates. While the position of fluorine substituents on the arene unit does not seem to affect reactivity, the degree of fluorination of the arene unit does. As the degree of fluorination increases, the aromatic ring becomes significantly electron deficient and this could lead to destabilization of the reactive intermediate either disfavoring the generation of the isoindenone intermediate or resulting in immediate polymerization.

Stoichiometric amounts of parent 2-indanone (**10a**) and 5,6-difluoro-2-indanone (**10d**) were subjected, in parallel, to the optimized three-step sequence for isoindenone generation and dimerization. Following aqueous workup, a mixture of three dimers was observed in a nearly quantitative yield over the three-step sequence. The parent isoindenone dimer (**14a**), the *o*-difluoro isoindenone dimer (**14d**), and the desired mixed dimer (**14t**) were formed in a 1:2:1 ratio, obtained by GCMS (**Figure 40**). This suggests that the *o*-difluoro isoindenone intermediate has a higher reactivity than the parent isoindenone intermediate. The fluorine substituents on the arene unit pulling electron density may result in further destabilization of the *o*-difluoro isoindenone intermediate, thus increasing its reactivity.

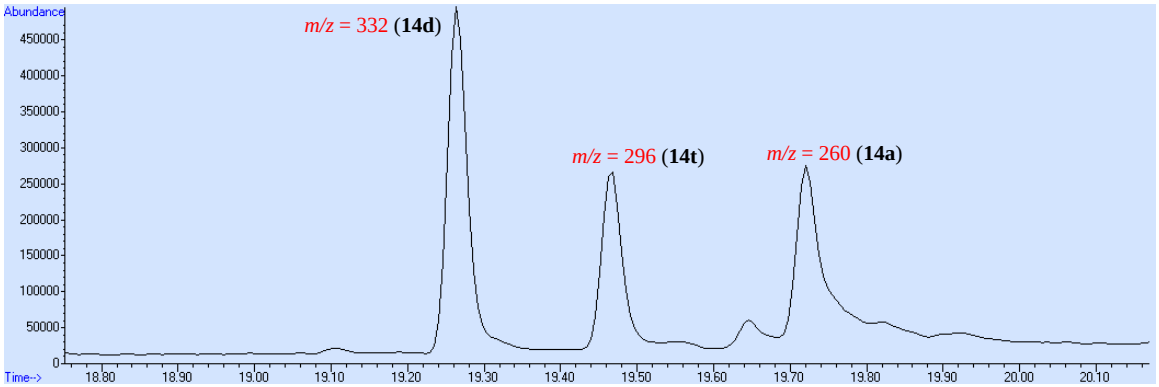

Figure 40. Gas Chromatogram of the crude product obtained from a mixed dimerization between the parent and *p*-difluoro isoindenones.

With the *ortho*-difluoro isoindenone dimer (**14d**) and *para*-difluoro isoindenone dimer (**14c**) both isolated in decent yields, we anticipated that a mixed syringe pump with

stoichiometric amounts of the corresponding bromo silyl enol ethers would afford an equal distribution of the three possible dimers as the intermediate reactivity of the difluorinated isoindenone isomers was assumed to be comparable. However, we only observed the formation of the *ortho*-difluoro isoindenone dimer (**14d**). Considering that we obtained and characterized the *para*-difluoro isoindenone dimer, we were puzzled as to why we did not observe its formation, in any quantity, during the mixed dimerization. With these results being reproducible in triplicate, we can only presume that they *para*-difluoro isoindenone immediately polymerized during the mixed dimerizations although we cannot postulate why that would be at this time.

With the inability to obtain the mixed isoindenone dimer between the *ortho*-difluoro and *para*-difluoro systems, even though both self-dimerizations have yielded the corresponding isoindenone dimers of type **14**, we wanted to probe the reactivity of the combined *para*-difluoro bromo silyl enol ether (**27c**) and parent bromo silyl enol ether (**27a**). Again, we were unable to obtain the mixed dimer and only observed the parent isoindenone dimer. Due to these reproducible, unexpected results we utilized the same 4,7-difluoro-2-indanone (**10c**) batch to perform a self-dimerization and we did obtain **14c** in nearly 50% yield. After confirming the generation and dimerization of the *para*-difluoro isoindenone (**13c**), we were unable to reason why the mixed dimerizations did not deliver any dimers containing the *para*-difluoro substitution pattern; we expected to obtain the *para*-difluoro isoindenone dimer, at the least. We can only presume that during the mixed dimerizations, the *para*-difluoro isoindenone polymerized but we are unable to reason why at this time.

CHAPTER 4: DIBENZOFULVALENES

4.1. Introduction to Dibenzofulvalenes

Dibenzofulvalenes, cross-conjugated 18 π-electron systems, are synthetically alluring compounds that are prominently absent from the experimental literature. Fulvalene (**60**) is a highly reactive 10 π-electron polyene that is non-isolable but spectroscopically characterizable in a highly dilute solution. Upon standing, fulvalene solutions readily form dimers and polymers.[57] The bonds of parent fulvalene are explicitly labeled as shown (**Figure 41**) with dibenzofulvalenes being named according to which bonds are benzannulated. Dibenzofulvalenes may offer significantly increased stability over fulvalene without compromising subsequent reactivity.

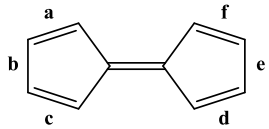

60

Figure 41. Bond labeling of parent fulvalene utilized for naming dibenzofulvalenes.

4.1.1. Dibenzofulvalene Synthetic Strategies

The first literature described compound in this class was dibenzo[a,f]fulvalene **61** that was reported as an unexpected byproduct isolated along efforts to synthesize a novel aromatic system via photosensitized dimerization of indene.[58] Though attempts have been made to synthesize dibenzofulvalenes, reports of their isolation and full characterization are rare. Many of the dibenzofulvalenes reported to date are generated in situ, immediately complexed with transition metal species, and characterized as the

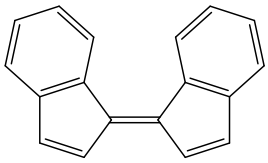

61

Figure 42. The first literature reported dibenzofulvalene **61.**

dibenzofulvalene metal complex. This commonly employed methodology circumvents the necessity of isolation and purification of the ligand, and avoids challenges that may arise with potentially unstable or reactive intermediates.

Dibenzo[a,d]fulvalene (**64**) was the first compound in its class to be synthetically targeted, isolated, and characterized.[57,59] Deprotonation of 1,1'-biindenyl (**62**) in THF followed by oxidative coupling with $CuCl_2$ or $AgBF_4$ at low temperature was reported to afford **64** in modest yields.[57] However, this synthetic strategy was not found to be reproducible by other groups and alternative reaction conditions were explored. There are two additional described methods in the literature for the synthesis and isolation of dibenzo[a,d]fulvalene, each proceeding through a tetra-brominated intermediate (**63**).[59]

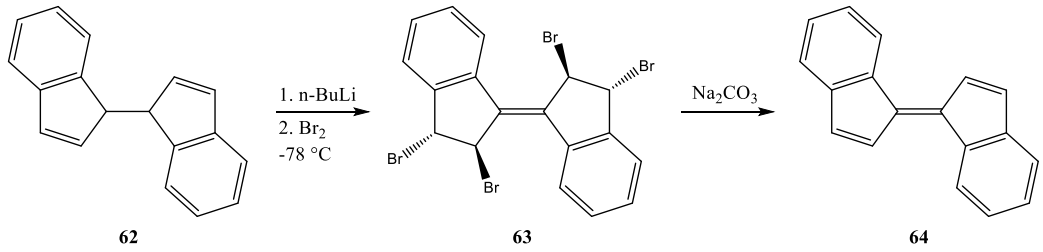

Figure 43. Optimized two-step synthesis reported for dibenzo[a,d]fulvalene **64** from 1,1'-biindenyl (**62**).[59]

First, the double deprotonation of **62** followed by bromination at low temperature for 5.5 hours results in the brominated compound (**63**) that was isolated and could be purified by column chromatography followed by recrystallization to afford the tetra-brominated intermediate. Often the crude residue was utilized without purification and the subsequent reduction with sodium carbonate and sodium iodide affords the target compound **64** reasonably clean after column chromatography.[59] Although this two-step

synthetic route allowed reliable access to **64**, the meager 24% yield left more to be desired in optimization of reaction conditions.

In an attempt for optimization of this sequence to increase overall yields, the bromination at low temperature was allowed to stir for only 2 hours. In lieu of isolating brominated intermediate **63**, after aqueous work-up the organic layer was sharply roto-evaporated over anhydrous sodium carbonate. The crude residue was subjected to column chromatography to afford the target compound **64**.[59] Through a shorter reaction time, foregoing isolation of the brominated intermediate, and allowing for the reduction with sodium carbonate during the workup they successfully increased the overall yield of isolated dibenzo[a,d]fulvalene two-fold. Notably, dibenzo[a,d]fulvalene is stable enough to survive column chromatography and with the optimized procedure does so in

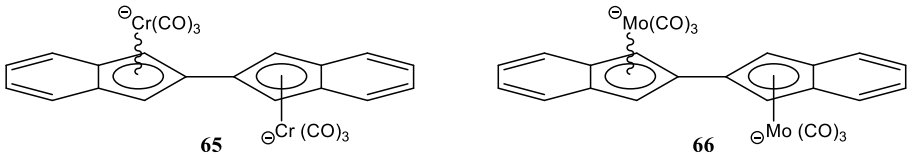

65 **66**

Figure 44. Literature reported dianionic bimetallic complexes of dibenzo[b,e]fulvalene with chromium and molybdenum carbonyl moieties.[59]

satisfactory yield.

Currently there are no literature reports toward dibenzo[a,e]fulvalene or its corresponding bimetallic complexes and reports on the [b,e] isomer are rare. To date dibenzo[b,e]fulvalene has only been reported and characterized as a dianionic bimetallic complex with chromium or molybdenum,[59] a neutral bimetallic complex with molybdenum,[65] and as various silicon-based bridged ligands of organorhodium compounds.[66]

The neutral (dibenzo[b,e]fulvalene)$Mo_2(CO)_6$ complex (**69**) was prepared in a three-step sequence starting with readily available 2,2'-biindenyl (**67**).[65] The treatment of **67** with $Mo(CO)_3Py_3$ in the presence of boron trifluoride diethyl etherate delivers **68**, where the molybdenum tricarbonyl moieties are complexed to each of the arene units either in an *s-cis* or *s-trans* conformation. Double deprotonation of **68** results in a migration of both molybdenum tricarbonyl moieties to the five-membered rings resulting in the bis- η^5-dianonionc complex (**66**). Subsequent treatment of **66** with ferrocenium tetrafluoroborate at low temperature allows for conversion to the desired metal-metal bonded bimetallic complex (dibenzo[b,e]fulvalene)$Mo_2(CO)_6$ (**69**).[65]

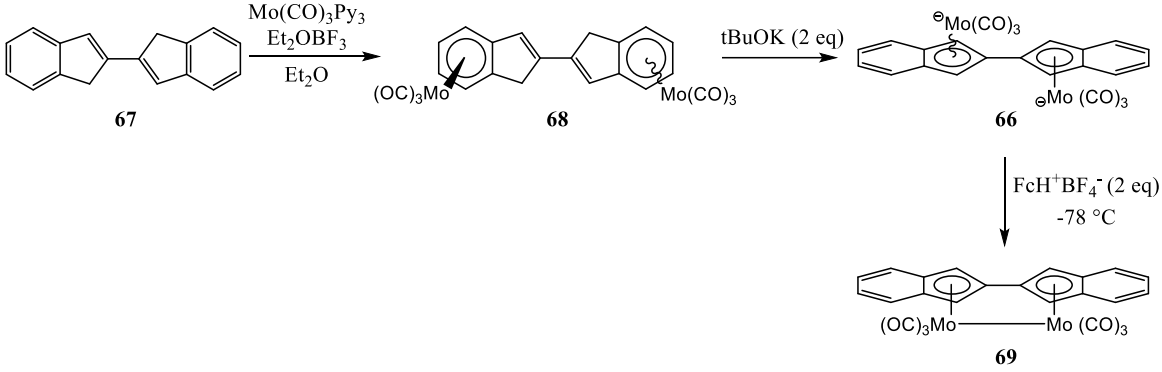

Figure 45. Three-step synthetic route reported for the neutral metal-metal bonded bimetallic complex of dibenzo[b,e]fulvalene (**69**).[65]

4.1.2. Dibenzofulvalene Reactivity

Bimetallic complexes have attracted significant attention due to the notion that concerted effects of two metals in close proximity should result in novel reactions useful in stoichiometric synthesis and in catalysis.[60] Relative to mononuclear complexes, bimetallic compounds exhibit an increased binding capacity for ligands, including the ability to form μ-bridged intermediates. Furthermore, an expanded range of oxidation

states is accessible to bimetallic complexes as a result of stabilizing metal-metal interactions.

Fulvalene **60** has provided the foundation for many bimetallic complexes[61,62] in part due to the strong binding of its cyclopentadienyl rings to early and middle transition metals. In contrast to the well-studied cyclopentadienyl carbonyl dimers, the fulvalene-bridged analogues are expected to show, and have shown in several cases, enhanced reactivity. This can be attributed to the ability of the fulvalene ligand to allow for metal-metal bond cleavage while inhibiting fragmentation to mononuclear complexes; the potential for metal-metal cooperativity is maintained thru relative proximity and possibly by communication through the π-bond system of the fulvalene ligand.[63]

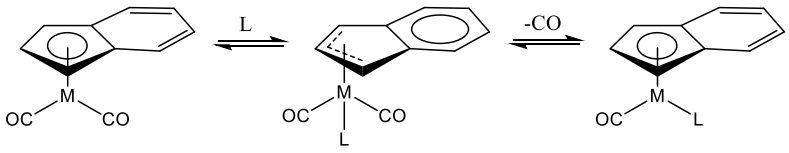

Figure 46. Illustration of the "indenyl effect" that can enhance reactivity during ligand substitution reactions.

A shortcoming of fulvalene as a bridging ligand is that the persistent η^5 bonding of its cyclopentadienyl rings leads to kinetic inertia and leaves little room for additional ligands in the case of late transition metals.[64] In contrast, (η^5-indenyl)-metal compounds often display enhanced reactivity in ligand substitution reactions. This phenomenon, termed the "indenyl effect", is attributed to the ease of slippage from a nominally 18-electron η^5 structure to a 16-electron η^3 structure, assisted by restoration of full aromaticity to the benzene ring (**Figure 46**). For this reason, dibenzofulvalenes have become intriguing targets for bridging ligands in bimetallic complexes.

4.1.2.1. Bimetallic Complexes of Dibenzofulvalenes

Efforts to enhance the reactivity of fulvalene bimetallic complexes have been accomplished through the preparation of several bimetallic complexes of dibenzofulvalenes, successfully exploiting the "indenyl effect".[64] Kerber et al. targeted the neutral metal-metal bonded complexes of dibenzofulvalenes with group 6 transition metals (Cr, Mo, W).[59] From 1,1'-biindenyl they were able to generate (dibenzo[a,d]fulvalene)$M_2(CO)_6$ complexes (where M = Cr, Mo, W), (dibenzo[b,e]fulvalene)$Mo_2(CO)_6$, and (dibenzo[a,f]fulvalene)$Mo_2(CO)_6$ in a one-pot, three-step sequence via double deprotonation, migration, and oxidation.

The reactivity of (dibenzo[b,e]fulvalene)$Mo_2(CO)_6$ (**69**) was investigated in comparison to the fulvalene analog, $FvMo_2CO_6$. Bimetallic molybdenum complex **69** reacts instantly with slightly more than one equivalent of $P(CH_3)_3$ at 0 °C to give a precipitate whose spectral data was consistent with the anticipated (dibenzo[b,e]fulvalene)$Mo(CO)_2(P(CH_3)_3)$. The presence of *cis*-$Mo(CO)_4(P(CH_3)_3)_2$ and *fac*-$Mo(CO)_3(P(CH_3)_3)_3$ in the soluble portion of the crude reaction mixture reveals the fate of the other molybdenum tricarbonyl moiety. Reaction of $FvMo_2CO_6$ with two equivalents of $P(CH_3)_3$ under similar reaction conditions did not show conversion after three days, conversion to the anticipated analogous substitution product was achieved after a six-fold excess of $P(CH_3)_3$ with two additional days of reaction in acetonitrile.[65] The disparity in the reaction rates between these two compounds is compelling evidence for the indenyl effect enhancing ligand substitution reactions for bimetallic complexes that contain the benzannulated fulvalene derivatives.

Comparative studies utilizing various dimolybdenum complexes as catalysts in the Kharasch-type reaction for the addition of carbon tetrachloride to 1-hexene to afford 1,1,1,3-tetrachloroheptane (**Table 3**). Compound **69** proved to be the most effective catalyst, while the fulvalene analog was found to be inert.[65]

Table 3. Experimental yields from the addition of carbon tetrachloride to 1-hexene catalyzed by dimolybdenum complexes.[65]

dimolybdenum complex	% yield
(dibenzo[b,e]fulvalene)Mo_2CO_6	21
$[CpMo(CO)_3]_2$	5.6
(dibenzo[a,d]fulvalene)Mo_2CO_6	< 0.20
$FvMo_2(CO)_6$	< 0.16

4.2. Results and Discussion

4.2.1. Olefination of Select 2-Indanone Derivatives

Olefination is an important synthetic transformation and carbonyl olefination is one of the most fundamental conversions in organic synthesis. A multitude of synthetic methodologies have been developed for application on various carbonyl derivatives, reflecting steric and electronic demands, to achieve the formation of a carbon-carbon double bond. For the chemistry described below, we targeted the olefination of isoindanone to derivatives of type **70** directly via the McMurry reaction and indirectly via pinacol coupling.[67,68]

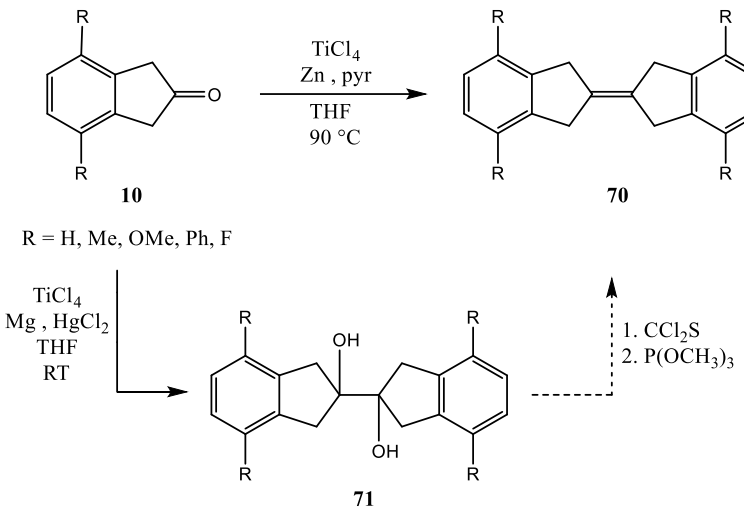

Figure 47. Methodologies to accomplish olefination of isoindanone **10**.

4.2.1.1. McMurry Reaction of 2-Indanone Derivatives

The McMurry reaction reductively couples carbonyls to an alkene utilizing low valent titanium species. Although several mechanisms have been postulated, it is widely accepted and viewed as a two-step reaction: first the formation of a 1,2-diolate (pinacolate) complex and secondly the deoxygenation gives the desired alkene. This second step exploits the oxophilicity of titanium.[69] This methodology is preferable for the olefination of sterically encumbered carbonyls.

Following a literature protocol that was reproducible on parent isoindanone **10a** in our hands,[67] we targeted olefination of *para*-disubstituted isoindanone to derivatives of type **70** with a spectrum of steric and electronic properties. We first focused our investigations on 4,7-dimethyl-2-indanone (**10m**) as it was anticipated to behave analogous to the parent system. After the addition of **10m** to a suspension of Zn and $TiCl_4$, the mixture was heated to 90 °C and stirred overnight. The reaction mixture turned to deep purple that almost appeared black. Following workup, the crude material was nearly clean pinacol

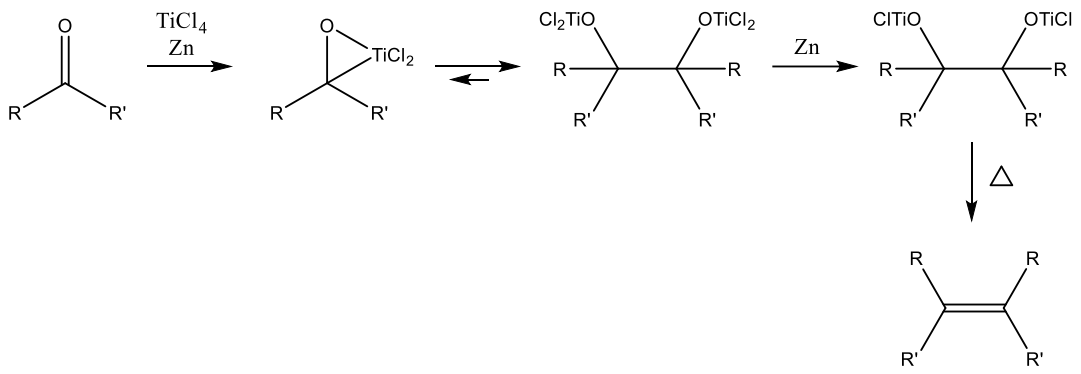

Figure 48. Proposed reaction mechanism for McMurry reaction with $TiCl_4$ and Zn.

product (**71b**) with small amounts of 4,7-dimethyl-indene (**72m**) and 4,7-dimethyl-2-indanol (**73m**), mechanistically reasoned and expected side products. There was only trace evidence for targeted olefin **70b**, which is surprising because the harsher reaction conditions are meant to facilitate the deoxygenation step to favor the olefination product. These results were reproducible and the reaction was easily scaled to gram batches. Although the pinacol was not our intended target, it is still a valuable intermediate that could be utilized toward the olefinated target. Purification was accomplished by trituration with diethyl ether and afforded clean **71b** as a beige solid in 78% yield. We fully characterized the novel pinacol derivative (**71b**) and obtained the crystal structure by XRD.

When this procedure was applied to 4,7-dimethoxy-2-indanone (**10i**), we obtained a similar product mixture with the major product being pinacol **71c** and side products 4,7-dimethoxy-2-indanol (**72i**) and 4,7-dimethoxy-indane (**73i**). In this case, the product distribution contained a substantial amount of the side products in comparison to the methylated case, which lead us to believe that sterics may have played a role in limiting the conversion to the coupled product. Again, there was no evidence for targeted olefin **70c**. Synthetic challenges limited our access to **10i**, therefore, we were not able to scale

this reaction beyond 400 mg batches. Purification was accomplished by trituration with diethyl ether to afford clean **71c** as a beige solid in 55% yield.

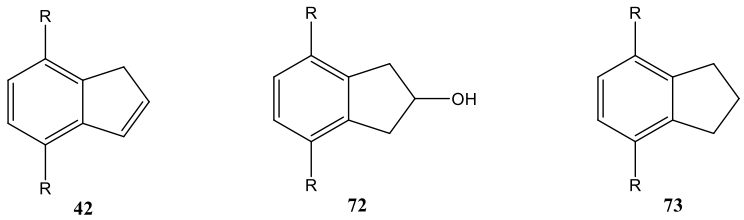

Figure 49. Side products observed for olefination reactions.

To probe the applicability of this protocol to isoindanone derivatives containing electron-withdrawing substituents we applied it to 4,7-difluoro-2-indanone (**10c**). In all three attempts, we did not obtain any fluorinated products. Although frustrating, this result was not overly surprising. It can be reasoned that the addition of an electron to the aromatic ring results in a radical anion which extrudes a fluoride ion to afford an aryl radical. This radical is expected to easily accept another electron to form an aryl carbanion that subsequently becomes protonated.[70]

Table 4. Experimental results obtained from McMurry reactions carried out on isoindanones of type **10**, with relative product distributions obtained by GC-MS.

R	batch size	crude mass	indene	indane	indanol	olefin	pinacol
H	1 g	821 mg	0%	1%	30%	25%	44%
CH_3	1 g	895 mg	5%	0%	11%	1%	83%
OMe	0.40 g	318 mg	0%	2%	39%	0%	59%
F	0.50 g	249 mg*	-	-	-	-	-

*did not deliver any fluorinated products

4.2.1.2. Pinacol Coupling of 2-Indanone Derivatives

The Pinacol coupling reaction is a free radical process that homocouples carbonyls to the corresponding vicinal diol. Mechanistically, the first step in the reaction is a one electron reduction of the carbonyl group by a reducing agent to a ketyl radical anion species. Subsequently, two ketyl radical anions couple to give a vicinal diol with deprotonated hydroxyl groups. Quenching with water or another suitable proton donor delivers the diol. When magnesium is the electron donor, the first step results in a 5-membered cyclic intermediate with the two oxygen atoms coordinated to the oxidized Mg^{2+} ion. This complex is readily hydrolyzed to afford the diol.

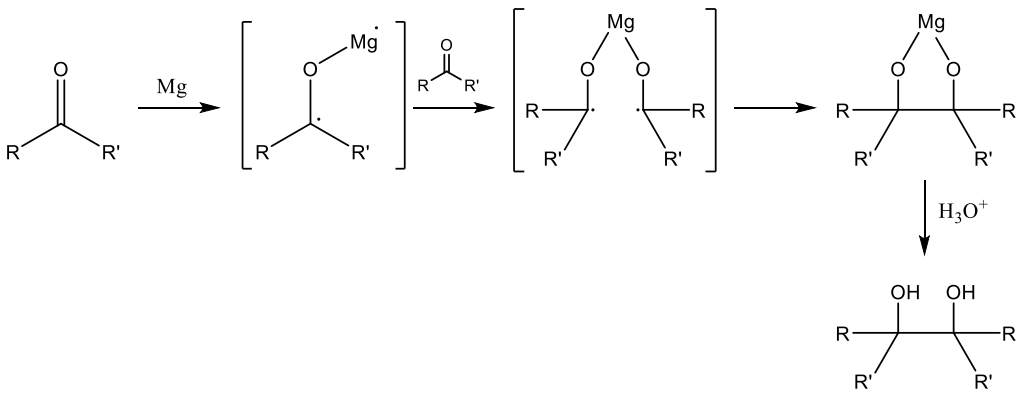

Figure 50. Reaction mechanism for Pinacol coupling reaction with Mg.

Even though we inadvertently obtained the pinacol derivatives for the *para*-dimethyl and *para*-dimethoxy systems as the major product from the McMurry coupling reactions, we continued with our investigation into the targeted pinacol coupling reaction that is carried out under milder reaction conditions. The parent pinacol **71a** has been mentioned in the literature,[71] but with no reports of its preparation or characterization. After the addition of parent isoindanone to a suspension of $TiCl_4$ and a mercury/magnesium amalgam,[72] the mixture was stirred at room temperature. The reaction mixture eventually

turned the same deep purple, nearly black, that was observed in the McMurry reaction but the changes in visual appearance took significantly longer to occur. Following aqueous workup, the crude material was a complex mixture of the desired pinacol **71a**, olefin **70a**, and anticipated side products **42a**, **72a**, and **73a**, among other impurities (**Figure 51**). Purification attempts to isolate parent pinacol **71a** included trituration with diethyl ether; though this method proved successful on the *para*-dimethyl and *para*-dimethoxy systems it did not translate to the parent system. Recrystallization attempts from various solvents and solvent mixtures also did not allow for further purification. Despite preliminary TLC analysis, column chromatography on silica gel with hexane:ethyl acetate (7:1) was unsuccessful. However, through these efforts we stumbled across the poor solubility of olefin **70a** in acetone and utilized this as an effective means for its isolation from the complex mixture.

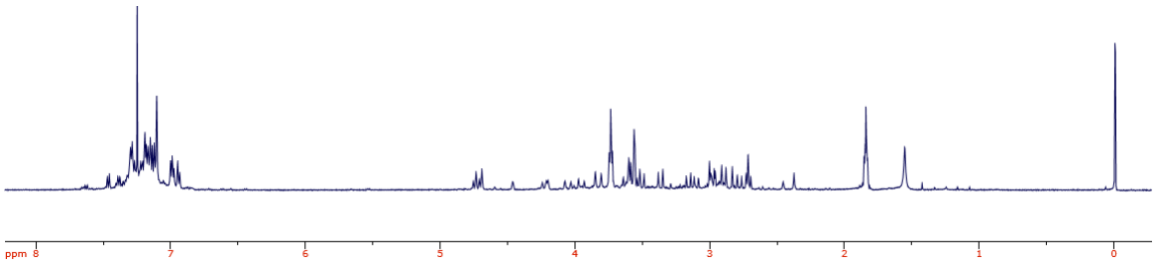

Figure 51. Crude ^{1}H NMR spectrum from the targeted Pinacol coupling of **10a**.

Applying the same procedure to 4,7-dimethyl-2-indanone (**10m**), we obtained a cleaner, more defined product mixture than with the parent system. As expected, the major product was pinacol **71b** along with side products **42m**, **72m**, and **73m**. Interestingly this methodology also delivered olefin **70b** that was not obtained from the direct olefination attempts via the McMurry reaction. Trituration of the crude product with diethyl ether affords clean pinacol **71b** in 55% yield as a beige solid. The diethyl ether mother liquor was then concentrated and the resulting sticky solid was triturated with acetone to afford

clean olefin **70b** in 10% yield as a colorless crystalline solid. We fully characterized the novel olefin (**70b**) and obtained the crystal structure by XRD.

Similarly, the *para*-methoxy system also delivered a clean and defined product mixture with the major product being pincaol **71c**, with side products **72i** and **73i**. Again, it was interesting that we obtained olefin **70c** that was not observed in the direct olefination attempts via the McMurry reaction.

To probe the milder reaction conditions of pinacol coupling toward derivatives with fluorine arene substituents we applied the procedure to 4,7-difluoro-2-indanone (**10c**). Unfortunately, we observed a similar outcome to the MuMurry Reaction that resulted in no fluorinated products. Although the pinacol coupling implements milder reaction conditions, it still proceeded through a metal mediated radical intermediate that allowed for the extrusion of fluoride from the aromatic unit.

Table 5. Experimental results obtained from targeted Pinacol coupling reactions carried out on isoindanones of type **10**, with relative product distributions obtained by GC-MS.

R	batch size	crude mass	indene	indane	indanol	olefin	pinacol
H	1 g	860 mg	2 %	3 %	15 %	8 %	72 %
CH_3	1 g	745 mg	10 %	1 %	20 %	11 %	58 %
OMe	0.25 g	180 mg	0 %	3 %	30 %	15 %	53 %
F	0.50 g	205 mg*	-	-	-	-	-

*did not deliver any fluorinated products

4.2.2. Toward 2,2'-Biindenyl Derivatives

Attempts toward olefination of 2-indanone derivatives of type **10** consistently yielded the corresponding pinacol derivatives of type **71**; though we initially intended to employ the Corey-Winter olefin synthesis to the pinacol derivatives to afford the desired olefins of type **70**,[73] we shifted our focus toward the elimination to afford 2,2'-biindenyl derivatives of type **15** as this method utilizes milder reaction conditions and was anticipated to shorten the overall synthetic sequence to the final target compounds. Due to limited access to 4,7-dimethoxy-2-indanone (**10i**) and unsuccessful attempts toward olefination of 4,7-difluoro-2-indanone (**10c**), we targeted 2,2'-biindenyls of type **15** from either the corresponding indene or 1-indanone derivatives of types **42** and **40**, respectively.

Table 6. Calculated HOMO and LUMO energies for select 2,2'-biindenyl derivatives **(15)** using Spartan '16: B3LYP/6-31G*.

R	point group	E HOMO (eV)	E LUMO (eV)
H	D_{2h}	-4.96	-3.46
CH_3	C_{2v}	-4.84	-3.30
OMe	C_1	-4.45	-3.33
F	D_{2h}	-5.37	-3.97

.

4.2.2.1. Elimination of Pinacol Derivatives

Since the attempts toward olefination of isoindanone derivatives of type **10** predominantly yielded the corresponding pinacol derivatives of type **71**, we investigated their subsequent elimination toward 2,2'-biidenyls of type **15**. Initially we proposed the olefination of pinacol derivatives via the Corey-Winter Synthesis,[73] but PTSA catalyzed dehydration allowed the use a familiar reaction with significantly milder reaction

conditions to be utilized. Access to 2,2'-biindenyls of type **15** would ultimately shorten our synthetic sequence to target compound **69**.

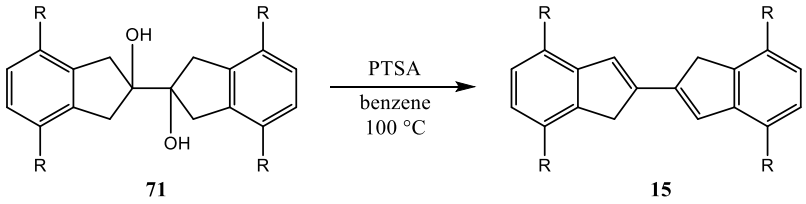

Figure 52. PTSA catalyzed elimination of pinacol derivatives of type **71** to afford 2,2'-biindenyls of type **15**.

The para-methyl pinacol derivative **71b** was subjected to PTSA catalyzed dehydration and after refluxing 45 min a GC-MS sample was drawn and indicated no remaining pinacol **71b** with an observed mixture of the hydroxyalkene intermediate and desired **15b** in roughly a 1:1 ratio. This suggests that the elimination of the first hydroxyl group happens quickly while the second elimination proceeds at a slower rate. In an attempt to push the reaction to completion, more PTSA was added and the reaction was refluxed for an additional hour. A GC-MS sample revealed approximately 20% increased conversion. Ultimately we found the conversion to peak at around 75% after refluxing for 4 hours. Following workup, the crude product was purified by trituration with acetone to afford clean **15b** as a beige crystalline solid in 70% yield.

4.2.2.2. Coupling of 2-Bromo-Indene Derivatives

Due to the inability to obtain the desired fluorinated McMurry or Pinacol coupling products, we sought an alternative synthetic route that starts with the corresponding indene derivative of type **42**. Following literature reported protocols,[74,75] we reproduced the three-step sequence on 4,7-dimethyl-indene (**42m**). Generation of a bromonium intermediate that was subsequently ring-opened by water proceeded smoothly at room temperature to

deliver the corresponding bromohydrin **74m** in 87% yield as a yellow crystalline solid that was collected by suction filtration. PTSA catalyzed dehydration of **74m** delivered the corresponding 2-bromo-indene of type **75** in 75% yield as a brown solid. The following dehalogenative homocoupling was achieved by nickel(0)-assisted dehalogenative coupling to afford clean biindenyl **15b** in 85% yield as a beige crystalline solid. For nickel(0)-assisted dehalogenative coupling of aryl or alkenyl halides the consecutive steps of oxidative addition, disproportionation, and reductive elimination constitute the reaction pathway. This is a well-established cycle for organotransition-metal chemistry. In the reaction we carried out, the nickel(II) generated during the disproportionation step reacted further with excess zinc powder in the presence of potassium iodide to regenerate the nickel(0) and ensure the catalytic cycle.[76]

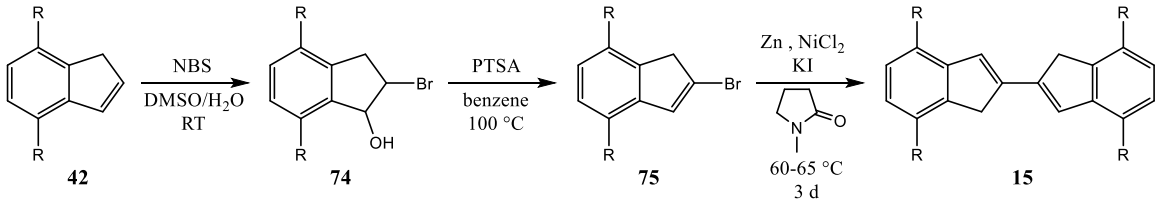

Figure 53. Reported synthetic route to 2,2'-biindenyls of type **15** from the corresponding indenes of type **42**.

Our optimized sequence to 4,7-dimethoxy-2-indanone (**10i**) did not go through the indene because we previously faced challenges targeting the indene derivative on the *ortho*-dimethoxy system as the cation intermediate was particular stable due to increased resonance and subsequently reacted with an indene molecule to afford a previously reported dimer.[38] Ultimately an alternative synthetic sequence was investigated and that procedure was applied to the *para*-dimethoxy system from the beginning.[47] To probe the applicability of bromo-indene homocoupling to substrates with differing arene

substituents, we targeted 4,7-dimethoxy-indene (**42i**). The reduction of **40i** was accomplished with sodium borohydride to afford indanol **41i** in 90% yield as a beige solid. The subsequent elimination proved problematic in our hands. First, we attempted to translate our general PTSA catalyzed dehydration to **41i** but after allowing the reaction to stir at 100 °C overnight there was minimal conversion to **42i** and noticeable unidentified side product formation. Deeming this methodology unfit for the elimination we investigated alternative reaction conditions. Following a literature protocol,[77] we added PTSA to a solution of **41i** in chloroform and stirred at room temperature. After 2.5 hours no conversion was observed and additional PTSA was added in an attempt to drive the reaction forward. The reaction was monitored by TLC and once conversion was observed a sample for GC-MS was drawn from the reaction. Unfortunately, we did not observe any indication for the desired indene (**42i**) and were unable to reproduce this procedure.[77] This result was not surprising as we observed only minimal conversion when refluxing with PTSA overnight. While the reaction was monitored by TLC, we observed what we assumed to be conversion to the product with a new spot developing. However, a GC-MS sample showed that there was no conversion and only unreacted starting material in the reaction. We proposed that the elimination could have taken place on the silica during TLC analysis and we probed this by the addition of silica to a solution of indanol **41i** in methylene chloride. This mixture was stirred at room temperature for 24 h and checked multiple times over this period to no avail.

With reliable access to 4,7-difluoro-indene (**42c**), we investigated the three-step sequence toward the corresponding 2,2'-biindenyl **15d**. Generation of the bromonium intermediate that was subsequently ring-opened by water proceeded smoothly at room

temperature, however, bromohydrin **74c** was not a solid and could not be filtered from the reaction mixture and necessitated an aqueous workup. This proved challenging for isolation of clean **74c** due to the difficulty of removing the solvent, DMSO. We took the crude product up in 100 mL benzene and washed with copious amounts of water (~300 mL) three times and although inconvenient, this proved effective in removing 95% of the DMSO that allowed for NMR characterization of novel bromohydrin **74c**. Subsequent PTSA catalyzed elimination to the corresponding 2-bromo-indene **75c** did not behave as anticipated on this system. After refluxing overnight, we observed approximately 50% conversion to **75c** and upon the addition of more PTSA or increased reaction time we are unable to improve this yield. Following aqueous workup, a complex product mixture is obtained and purification by column chromatography on silica gel with hexane:ethyl acetate (20:1) afforded clean **75c** as a yellow liquid in only 15% yield.

Application of the dehalogenative homocoupling procedure to **75c** in an isolated event, on the first attempt, delivered a fluorinated crude product. It was not the desired 2,2 ' -biindenyl **15d**, but appeared to be a dibrominated dimer by GC-MS (*m/z* = 463) that we were unable to unequivocally assign a structure. In three subsequent attempts, we were unable to reproduce these results and only obtained presumably polymeric material that we were unable to characterize due to exceedingly poor solubility.

4.2.2.3. Coupling of 1-Indanone Derivatives

Faced with seemingly unsurmountable synthetic challenges along the *para*-dimethoxy and *para*-difluoro sequences toward the corresponding biindenyls of type **15** along the procedures discussed above, we sought to probe a literature protocol for the oxidative coupling of 1-indanone that we successfully reproduced on the parent 1-indanone (**40a**).[78]

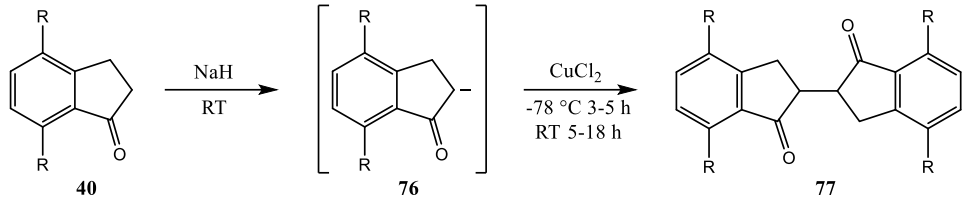

Figure 54. Reaction scheme of the oxidative coupling of indanone **42**.

Application of the oxidative coupling to **40c** was our last effort toward fluorinated 2,2'-biindenyl derivative **15d**. The generation of enolate **76c** occurred readily at room temperature, notably faster than on the parent system based solely on observation of hydrogen gas evolution. This can be attributed to the increased acidity of the protons alpha to the carbonyl due to the sigma-withdrawing nature of the fluorine substituents on the arene unit. Subsequent oxidative coupling at -78 °C with $CuCl_2$ delivered crude material that contained the expected isomeric mixture of bisketone **77c** as well as chlorinated side products. Although TLC analysis appeared to allow for good separation, column chromatography of the crude material on silica gel with hexane:ethyl acetate (2:1) was not successful for the purification of **77c**. The column did effectively separate the chlorinated side products but was not able to separate residual 1-indanone from the bisketone isomers because the 1-indanone streaked through every fraction.

4.2.3. Molybdenum Chemistry on 2,2'-Biindenyl Derivatives

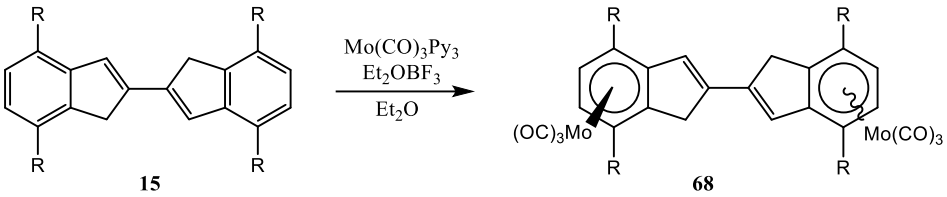

Figure 55. Reaction of **15** for the addition of molybdenum tricarbonyl moieties to the six-membered aromatic rings.[59]

Addition of molybdenum tricarbonyl moieties to the six-membered aromatic rings of **15b** was accomplished with freshly prepared $Mo(CO)_3(py)_3$[79] in the presence of boron trifluoride diethyl etherate.[59] Confirmation of **68b** was not trivial as standard organic spectroscopic techniques proved problematic. NMR spectroscopy was not feasible as **68b** was insoluble in most common solvents. Minor solubility in DMSO showed decomposition to **15b**, which was not surprising as the lability of (arene)$Mo(CO)_3$ is highly precedented.[80] ^{1}H NMR of the crude material in chloroform did not show any peaks that confirmed it did not contain any free 2,2'-biindenyl **15b**, as it is highly soluble and was NMR characterized in chloroform. A GC-MS sample did not show any peaks and this could be attributed to the high molecular weight of **68b** potentially making it nonvolatile and therefore not suitable for gas phase analysis. Although it is not a conclusive means for absolute identification purposes, we ultimately relied on IR

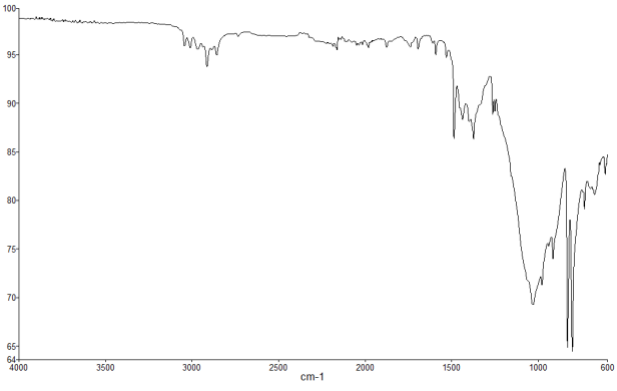

Figure 56. IR spectrum of the free ligand, 2,2'-biindenyl **15b**.

spectroscopy to determine the formation of **68b**. We recorded the IR spectra for the free ligand (**15b**), freshly prepared $Mo(CO)_3(py)_3$, and the crude product.

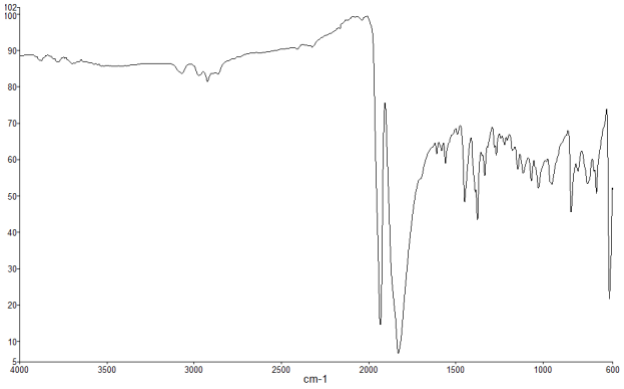

Figure 57. IR spectrum of $Mo(CO)_3(py)_3$.

Double deprotonation of **68b** was reported with potassium *tert*-butoxide[65] but in our hands this base was not sufficient for deprotonation of our arene substituted scaffold, which necessitated the use of *tert*-butyllithium. The color change observed during this transformation was incredibly subtle, unlike the notable color change reported on the parent system,[65] the mixture turned slightly lighter and this was only apparent when splashing was observed on the side walls of the reaction flask that left a lighter residue. Subsequent oxidation of the dianionic intermediate to the metal-metal bonded complex **69b** was accomplished at low temperature with the addition of ferrocenium tetrafluoroborate all at once and the reaction mixture turned dark blue. Following workup, the crude product was a dark blue crystalline

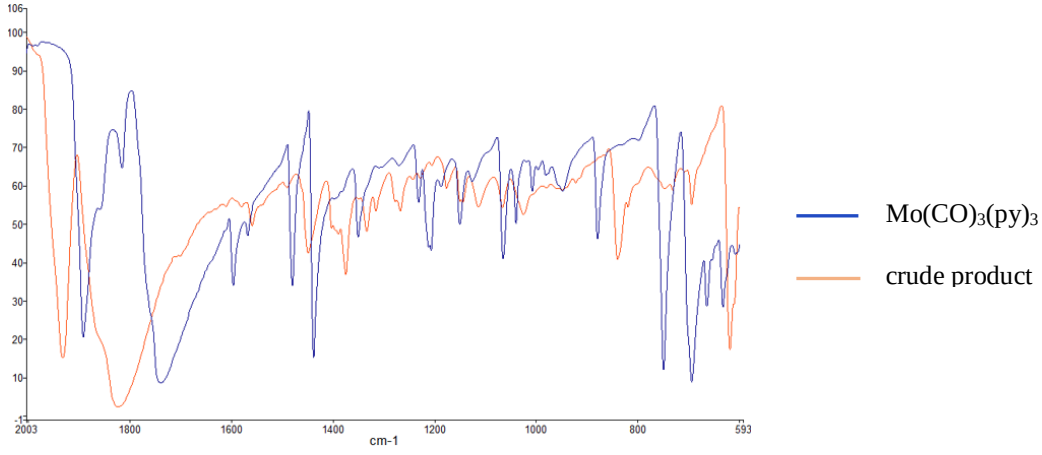

Figure 58. Overlaid IR spectra of $Mo(CO)_3(py)_3$ and crude product obtained through the three-step sequence to **68b**.

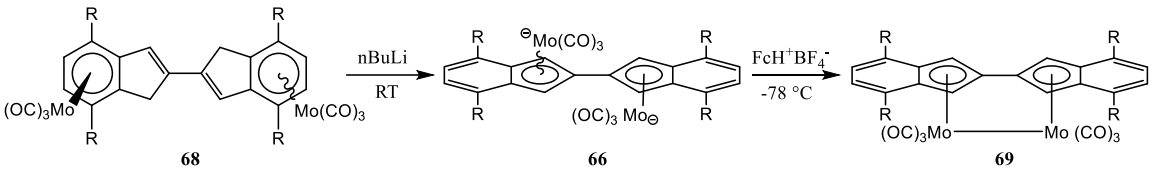

Figure 59. Two-step, one pot sequence for the migration of molybdenum moieties and oxidation to the desired complex **69**.

material with limited solubility. ^{1}H NMR in chloroform gives evidence for the desired bimetallic complex **69b** as a mixture with free ligand **15b** in nearly a 1:1 ratio (**Figure 60**). Three singlets at 6.78, 5.21, and 2.24 ppm with relative integrations of 1:1:3, respectively, correlate with the expectations for the proton NMR spectrum of the desired complex.

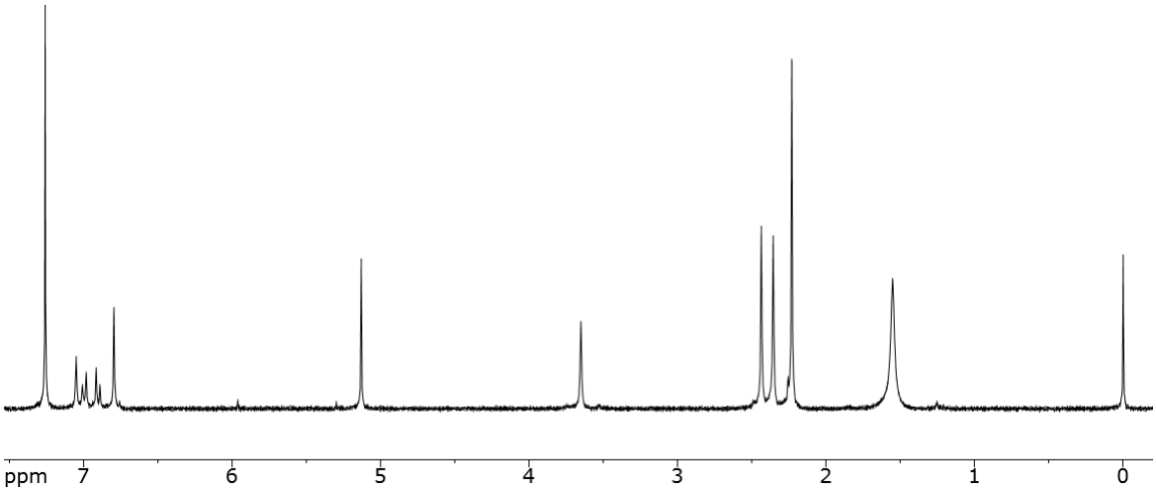

Figure 60. Crude ^{1}H NMR after the three-step sequence toward desired bimetallic complex **69b**.

CHAPTER 5: DENDRALENES

5.1. Introduction to Dendralenes

Dendralenes are a unique family of π-bond rich hydrocarbons that are discrete, acyclic, cross-conjugated polyenes. They are colloquially named as an [*n*]dendralene, where n equals the number of cross-conjugated alkene units along the backbone (**Figure 61**). These compounds are often separated into their odd and even parity's, which due to conformational effects behave differently. The odd parity dendralenes exhibit much less stability and subsequently higher reactivity than their even counterparts.[81] The history of chemical syntheses and unveiled synthetic applications of the dendralenes are as unique and intriguing as the molecules themselves.

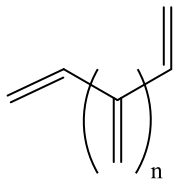

Figure 61. General dendralene structure.

5.1.1. Dendralene Synthetic Strategies

The preparation of [3]- and [4]dendralene were first reported in 1955 and 1962, respectively.[82,83] Classical flow tube pyrolysis methods were performed on the appropriate acetate precursors. Pyrolysis is the thermochemical decomposition of organic material in the absence of oxygen. This method involves the simultaneous change of chemical composition and physical phase, rendering it irreversible. At the time of these experiments, more advanced synthetic methodologies were lacking and the necessity of harsh reaction conditions often afforded poor yields and complex product mixtures. The resulting dendralenes were isolated in mere milligram quantities and deemed highly reactive, unstable compounds that readily polymerized at -5 °C in under 36 hours.[83] Due to these

accounts, and reports of being difficult to handle in the laboratory, further investigations on these scaffolds were abandoned at the time.

Nearly four decades later, a general synthesis for the dendralenes was reported by Sherburn's group.[84] The assumed instability of these compounds was taken into account from the beginning and the synthetic approach was designed employing a "storage concept" that masked the dendralene structure as 3-sulfolene derivatives. A Stille cross-coupling reaction delivered the masked dendralene, where subsequent pyrolysis at 450 °C resulted in the cheletropic extrusion of sulfur dioxide to afford the pure dendralene (**Figure 62**). Although this improved synthetic route allowed for the isolation and characterization of dendralenes 3-8, it still necessitated temporary protection and harsh reaction conditions.

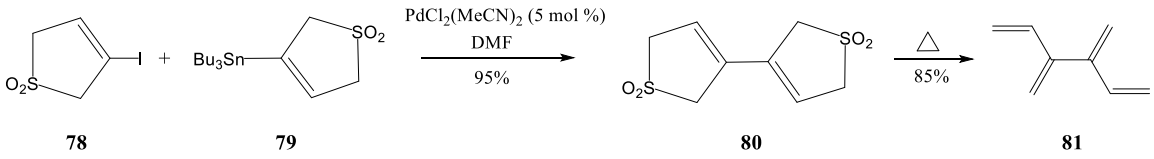

Figure 62. General route of the first practical syntheses of dendralenes via Stille Coupling.

Sherburn's group continued investigations into dendralenes and the development of more practical syntheses. In 2009, they reported their successful new approach that employed transition metal-catalyzed cross-coupling reactions, of the Kumada and Negishi type, which utilized the chloroprene Grignard reagent as a readily available starting material (**Figure 63**).[81] These routes allow rapid access to the dendralenes in synthetically useful amounts, up to 5 grams. This paved the

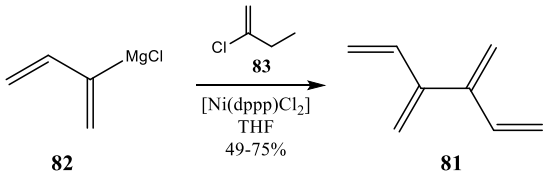

Figure 63. Practical synthesis of [4]dendralene via Kumada cross-coupling.

way for the first fundamental investigations into the properties and reactivity of these compounds. One of the most important findings in the search for practical syntheses has been that the postulated extreme instability and high reactivity of the dendralenes was nothing more than a mere myth.

5.1.2. Dendralene Reactivity

The dendralenes are often separated into their odd and even parity's based on inherent differences in behavior and subsequent reactivity. The odd dendralenes exhibit less stability, and subsequent higher reactivity, in comparison to their even counterparts that can be attributed to conformational effects. This alternation in behavior is more pronounced in the smaller analogs (n=3-8).[86] When analyzing the DFT lowest energy conformations for [4]- and [5]dendralene, which are representative of the even and odd parity's, respectively, [4]dendralene contains s-*trans* dienes that are nearly orthogonal to each other, whereas [5]dendralene possesses a terminal s-*cis* diene (**Figure 64**).[87] This aids in the explanation of observed differences in reactivity of the odd and even parity's of these compounds, most notably in diene-transmissive Diels-Alder reactions that require a *cis* conformation of the diene.

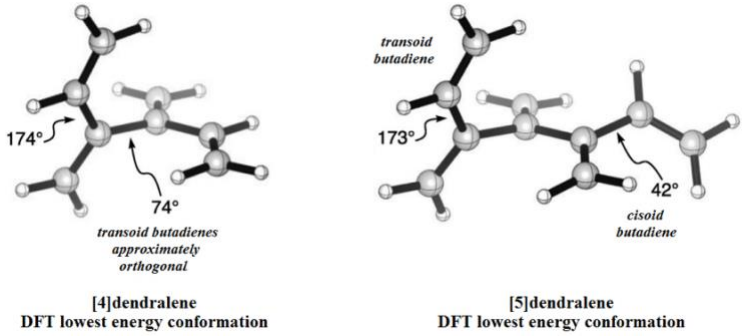

Figure 64. DFT lowest energy conformations for [4]- and [5]dendralene.[87]

5.1.2.1. Reactivity as Multidienes

Dendralenes may function as multidienes, with the ability to undergo Diene-Transmissive Diels-Alder (DTDA) reactions. Although the odd parity's undergo these reactions more rapidly due to conformational effects, the even parity still proceed to completion. These reactions consist of sequential Diels-Alder (DA) reactions that begin with the first cycloaddition to the terminal site of a dendralene followed by a subsequent DA reaction utilizing the newly formed diene. This generates complex polycyclic frameworks in remarkably short step count total synthesis.[88] An [*n*]dendralene can participate in n-1 DTDA reactions, forming multiple new carbon-carbon bonds and stereocenters in a single reaction; [4]dendralene will undergo three DTDA reactions with N-methylmaleimide to form six new carbon-carbon bonds and eight new stereocenters (**Figure 65**), offering significant structural complexity in a one pot reaction.[89] These types of reactions are often used for target synthesis of complex biological compounds, such as cortisone and tetracycline, and align with industry standards as they actively strive to move toward syntheses with atom- and step-economy.

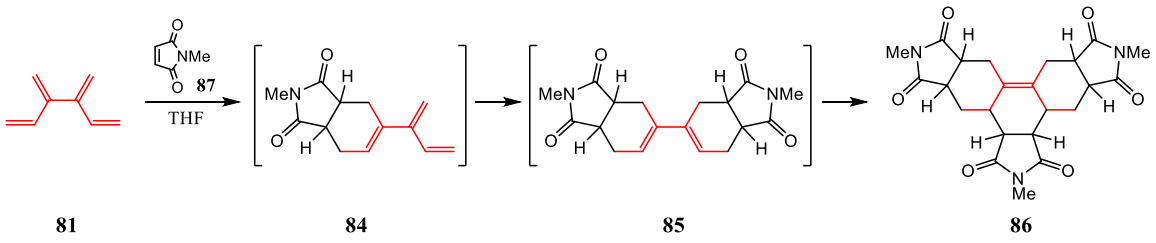

Figure 65. [4]-dendralene (**81**) undergoing DTDA reaction with N-methylmaleimide, with the dendralene backbone highlighted in red.

5.1.2.2. Reactivity as Multialkenes

Dendralenes may also function as multidienes, allowing for the direct synthesis of polyols and oligo-cyclopropanes, the latter are colloquially known as ivyanes for the hydrocarbon derivatives. The ivyanes are named analogous to their corresponding dendralene; [8]dendralene (**87**) can undergo an 8-fold cyclopropanation to form sixteen new carbon-carbon bonds to afford [8]ivyane (**88**) (**Figure 66**).

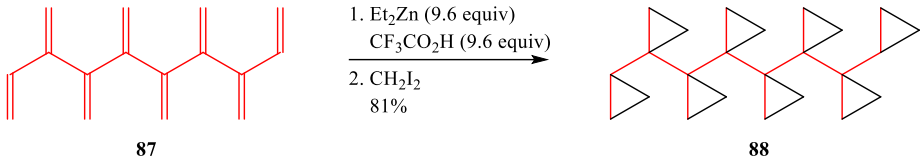

Figure 66. [8]dendralene (**87**) undergoing 8-fold cyclopropanation to afford [8]ivyane, with the dendralene backbone highlighted in red.

The ivyanes are 1,1-linked oligo-cyclopropanes that adopt chiral helical conformations in both solid and liquid phases, showing enantioisomerization through a helix twist (**Figure 67**).[90] These compounds have unique optical properties, with an unusually high specific rotation, making them attractive target compounds for material applications. Despite their high energy strain (cyclopropane has strain energy of *ca.* 115 kJ mol^{-1}),[91] these compounds are kinetically stable to moderate temperatures.[90] [6]ivyane is kinetically stable to *ca.* 200 °C and its experimental heat of combustion was found to be

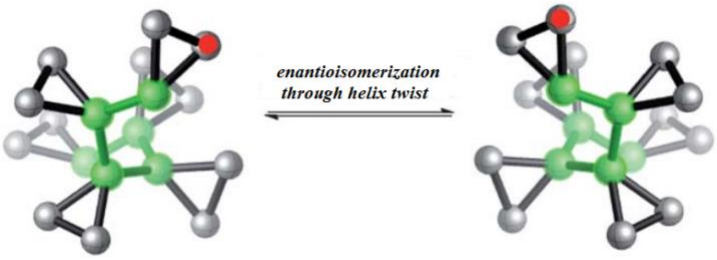

Figure 67. Structure of [6]-dendralene illustrating interconversion between the two enantiomers through a helix twist with the labeled methylene in red, hydrogen atoms are omitted for clarity.[90]

12.3 ± 0.6 MJ mol^{-1},[92] one of the highest reported for a hydrocarbon and significantly higher than that of cubane.[91] [6]Ivyanes molar heat of combustion is nearly six times greater than that of cyclopropane (2.1 MJ mol^{-1}),[17] with comparable thermodynamic strain energies in isolated and covalently bonded cyclopropane rings it is reasoned that the connected nature of the ivyane structure does not lead to a decrease in kinetic stability.

5.2.2. Results and Discussion

5.2.2.1. Synthesis of Fluorinated Building Blocks

The challenges of directly fluorinating *exo*-methylene units or incorporating fluorinated methylene units to an existing hydrocarbon backbone are anticipated to be insurmountable. With this in mind, the necessity of obtaining appropriate fluorinated building blocks became paramount to this project. The two primary building blocks that we targeted were synthetically useful fluorinated styryl derivatives (**11**) and *gem*-difluoroethylenes (**12**).

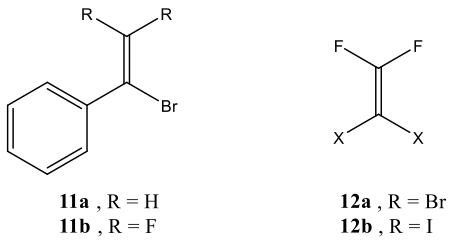

11a , R = H
11b , R = F

12a , R = Br
12b , R = I

Figure 68. Fluorinated building blocks **11** and **12** targeted for dendralene synthesis.

The incorporation of a terminal phenyl substituent was important synthetically, as it is anticipated to lower the potential volatility of the resulting intermediates and products that will make isolation, purification, and further reactivity more manageable. The intention was to synthesize all initial dendralene derivatives utilizing this phenylated building block and carrying out sequential, known metal-mediated cross-coupling reactions with an appropriate fluorinated ethylene of type **12** to construct the dendralene backbone. Our first synthesis of the desired α-bromo-β,β-difluorostyrene (**11a**) was accomplished via Suzuki-Miyaura coupling of phenyl boronic acid with 1,1-dibromo-2,2-

difluoroethylene (**12a**).[92] Although this methodology reliably produced the product in excellent yield, it quickly consumes our costly building block **12a**. To avoid excessive and unnecessary use of **12a**, we explored an alternative method for the synthesis of (**11a**).

Beginning with benzaldehyde (**89**), the synthetic transformation to α-bromo-β,β-difluorostyrene (**11b**) was accomplished in a three-step procedure. First, the deoxygenative difluoromethylenation of the carbonyl through a Witting-type reaction was attempted along literature protocols utilizing $TMSCF_3$.[93] Following the reported (optimized) reaction conditions, we were unable to obtain the desired product (**90**) and observed no conversion of the starting material after 24 hours. When the reaction was allowed to run four days we observed a 17% conversion to the desired product, deeming these conditions unsuitable as an efficient route. We have found that in our hands the reaction is most successful when run in a solvent mixture of 8% DMF in CH_3CN.[93]

Table 7. Probed reaction conditions for the deoxygenative difluoromethylenation of benzaldehyde **89**.[93]

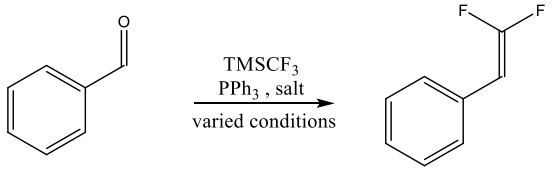

89 **90**

Solvent	T (°C)	t (h)	Salt (equiv)	Reported Conversion (%)	Observed Conversion (%)
8% DMF/dioxane	120	24	LiI (2.0)	83	17 (4 d)
THF	70	10	NaI (0.6)	64	28 *
THF	110	10	NaI (6.0)	69	45 *
5% DMF/THF	110	24	LiI (2.0)	77	45 *
8% DMF/CH_3CN	120	24	LiI (2.0)	78	100
16% DMF/toluene	120	15	LiI (2.0)	83	0

* Reaction also gives three additional, unidentified side products by GC-MS

Furthermore, we often observed that the amount of isolated product was significantly diminished after completing the described workup and often contained significant amounts of residual triphenylphosphine and the triphenylphosphine oxide byproduct. Investigation into this showed that the product was more volatile than described and was being pulled over with the diethyl ether on the rotovap, which we ultimately used to our advantage as it proved to be an effective means of separating the β,β-difluorostyrene (**90**) from the other organic compounds. We did not attempt the isolation of **90** from the diethyl ether as the next reaction along this pathway could be run in an ethereal solvent without sacrifice. This compound was found to be stable in solution at ambient conditions up to one week, possibly longer or even indefinitely but we always proceeded within one week time toward the next reaction.

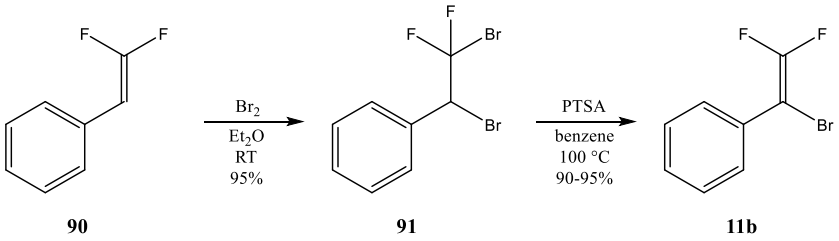

90 **91** **11b**

Figure 69. Synthetic transformation to **11b**.

Subsequently, the addition of bromine over the styryl alkene unit delivered (1,2-dibromo-2,2-difluoroethyl)benzene (**91**), as a sticky orange solid. Due to the presumed instability of this compound, the crude material was immediately reacted without any attempt of purification. Elimination with DBU[94] proceeded quickly at room temperature to afford the desired product (**11b**) in an 85% crude yield over the three-step sequence. A column chromatography with pentane on silica gel affords the clean product as a colorless liquid.

Fluorinated ethylenes of type **12** were targeted as the primary building block that can be utilized in metal-mediated cross-coupling reactions for the synthesis and extension of the cross-conjugated dendralene backbone. Commercially available 1,1-dibromo-2,2-difluoroethylene (**12a**) was initially the prime candidate for this role, however, it is of considerable price when taking inherent synthetic challenges into account that will ultimately require large gram quantities of this building block throughout the duration of the project.

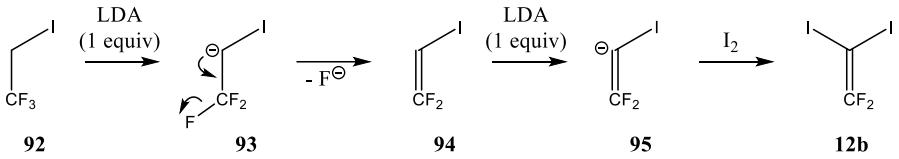

Figure 70. Synthetic route toward target building block **12b**.

For a more cost-effective approach, we targeted the synthesis of the 1,1-difluoro-2,2-diiodoethylene (**12b**) along a reported procedure[94] from the commercially available 1-iodo-2,2,2-trifluoroethane (**92**) precursor. In the presence of 2 equivalents of LDA, **92** was deprotonated and the formation of a double bond extruded a fluoride to form intermediate **94** that was then deprotonated to generate the reactive vinylic anion (**95**) that in the presence of iodine afforded **12b** (**Figure 70**). Complete removal of solvent, THF, from the crude product proved challenging as the product exhibited a similar boiling point and at low pressure began to come over on the rotovap. Since the subsequent cross-coupling reactions were to be carried out in an ethereal solvent we did not investigate the complete removal of solvent. Increased lability of the carbon-iodide bond, in comparison to the carbon-bromine bond, was anticipated to increase ease of subsequent cross-coupling reactions.

5.2.2.2. Metal-Catalyzed Cross-Coupling Reactions

Until the early 1970's, metal-mediated carbon-carbon bond formation was mostly accomplished via the use of alkali and alkaline earth metals, commonly lithium and magnesium. Unfortunately, organometallic intermediates that contain only these metals are not typically applicable for the formation of carbon-carbon bonds with unsaturated organic electrophiles such as C(sp^2)-X or C(sp)-X, where X is a halogen or notable leaving group. This synthetic limitation has been fundamentally overcome through the incorporation of d-block transition metals as components of catalytic reagents (**Figure 71**). The transition metal-catalyzed cross-coupling reactions that were investigated toward novel fluorinated dendralene derivatives herein are Negishi, Kumada, Stille, and Suzuki.

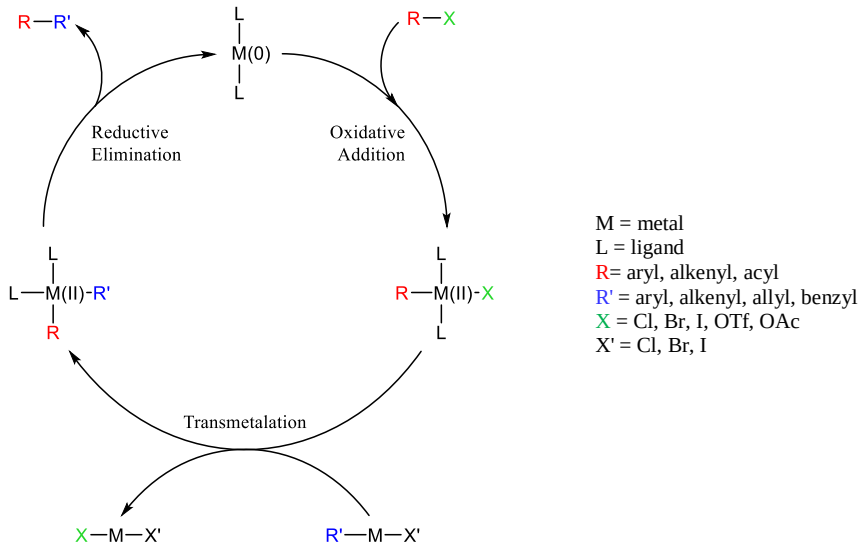

Figure 71. General catalytic cycle for metal-mediated cross coupling reactions.

5.2.2.2.1. Negishi Coupling

Negishi coupling is commonly utilized in total synthesis methods as it allows for selective formation of carbon-carbon bonds between complex synthetic intermediates. The Negishi cross-coupling reaction utilizes an organozinc intermediate that is coupled to an sp^2 or sp hybridized organic halide or triflate. Typically, the metal catalyst is a palladium(0) species, although sometimes nickel is used. Organozinc compounds are more reactive than most other cross-coupling adducts (*e.g.*, organostannanes and organoborates) that allows for faster reaction times. The largest drawback to Negishi coupling is that organozinc compounds are incredibly sensitive to both moisture and air, necessitating all reactions to be carried out strictly in water- and oxygen-free environments. For this reason, most industrial applications do not employ Negishi coupling as there are other effective

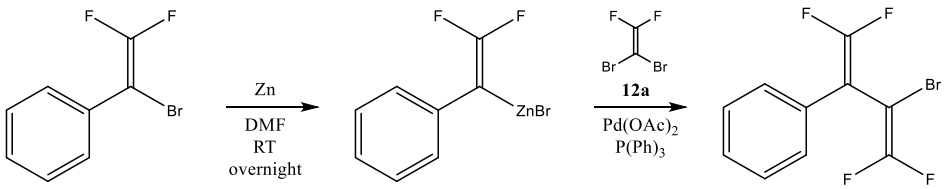

Figure 72. Proposed Negishi cross-coupling toward fluorinated dendralenes.

cross-coupling reactions that require less restricting reaction conditions.

To begin our investigation into metal-catalyzed cross-coupling reactions we focused on Negishi coupling reactions as the most recent and relevant literature reports on cross-coupling of fluorinated vinylic derivatives utilize this methodology.[95-97] Although there are a handful of literature protocols for the generation and subsequent coupling of organozinc intermediates on fluorinated compounds, their generation has proved far from trivial in our hands. We initially attempted the cross-coupling of α-bromo-β,β-

difluorostyrene (**11b**) with dibromodifluoroethylene (**12a**) by generating the organozinc intermediate with **11b**. We chose to generate this intermediate as we can easily synthesize gram quantities of this compound as needed. Along a literature procedure,[95] we vigorously stirred **11b** with zinc dust in DMF at room temperature then proceeded with the subsequent cross-coupling with **12a** in the presence of palladium acetate and triphenylphosphine. Following aqueous workup, we quantitatively obtained clean, unreacted starting material suggesting that we were unsuccessful in generating the critical organozinc intermediate for the coupling. Considering the generation of this highly reactive intermediate depends solely on the insertion of zinc into the vinylic carbon-bromine bond, we postulated that increasing the reactivity on the surface of the zinc would facilitate the reactivity toward insertion. Thus, we activated zinc dust via acid washing with concentrated hydrochloric acid immediately prior to use in the reaction; the results of these attempts were identical to those of the unactivated zinc dust, we recovered unreacted starting material. In a final attempt to force the organozinc generation, we prepared Reike zinc[98] but again we obtained

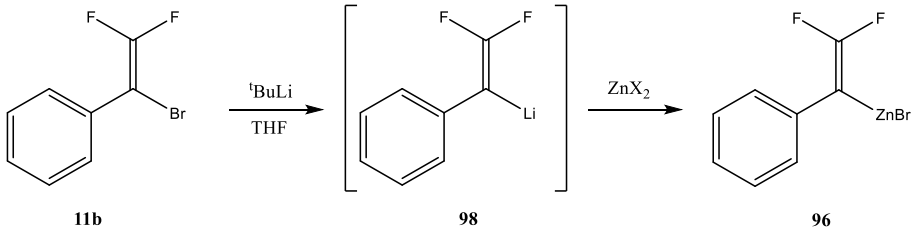

Figure 73. Attempted organozinc intermediate generation.

only unreacted starting material.

With no success along the direct insertion of zinc into the vinylic carbon-bromine bond we probed alternative methodologies to obtain the targeted organozinc intermediate. Lithiation of the substrate followed by subsequent transmetalation with an appropriate zinc salt was anticipated to generate the desired reactive intermediate. We attempted the

lithiation of **11b** with n-BuLi and subsequent transmetalation with $ZnBr_2$ to no avail, next we tried more forcing conditions with the treatment of *tert*-butyllithium that rendered the same results. Changing the zinc salt to $ZnCl_2$ did not deliver a different outcome. Ultimately, we presumed that even though we worked under strict Schlenk conditions that it was not sufficient enough to ensure that our reagents and reaction remained completely air and moisture free, which is paramount to the success of reactions with organozinc intermediates. With the highly hygroscopic nature of zinc salts, even weighing and quickly transferring them to our reaction we could have introduced sufficient moisture to ensure reaction failure. Utilizing a glove box to guarantee an air and moisture free environment may have been all that was necessary to have successful generation of the targeted organozinc intermediates.

5.2.2.2.2. Kumada Coupling

Kumada coupling was among the first reported catalytic cross-coupling reactions and despite the continued development of alternative methodologies it continues to be employed in various industrial synthetic applications, such as the production of Aliskiren® (a hypertension medication) and polythiophenes that are useful in organic electronic devices. The Kumada cross-coupling reaction utilizes a Grignard reagent that reacts with a vinyl halide. Generally, palladium(II) or nickel(II) metal catalysts are utilized to couple a combination of alkyl, vinyl, or aryl groups.

Kumada coupling was paramount in the development of practical syntheses for the parent dendralenes.[81] It was anticipated that the translation of this methodology to fluorinated analogs would allow quick access to our target frameworks of type **17**. Generation of Grignard **99** was accomplished by refluxing α-bromostyrene (**11a**) and

magnesium turnings overnight with a catalytic amount of 1,2-dibromoethane. Freshly prepared **99** was added to a suspension of dibromodifluoroethylene (**12a**) and Ni(dppp)Cl_2 at -20 °C.[99] Following aqueous workup, styrene was the only observed product that resulted as the hydrolysis of **99**. Residual **12a** was not observed after workup and due to its high volatility was likely pulled over during solvent evaporation. To determine whether or not the oxidative addition of **12a** to the nickel catalyst occurred, we repeated the reaction and prior to aqueous workup a GC sample was drawn. GC-MS analysis of the reaction mixture showed Grignard **99** and unreacted **12a**, leading us to believe that the reaction failed because oxidative addition did not occur. The reaction was repeated and the suspension of **12a** and Ni(dppp)Cl_2 was allowed to stir three hours, in comparison to roughly 20 minutes, to probe whether increased time would promote the oxidative addition.

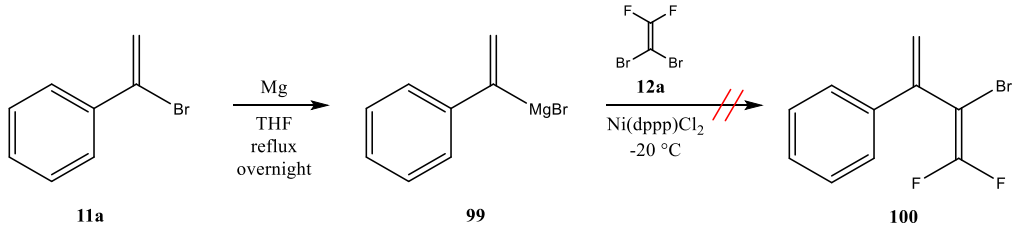

Figure 74. Proposed Kumada cross-coupling toward fluorinated dendralenes.

Unfortunately, we did not observe any conversion with the increased reaction time.

We attempted to increase the chances for oxidative addition of **12a** to the transition metal catalyst with the use of a palladium catalyst. Along the literature protocol for the parent system,[81] we employed the use of Pd(PPh_3)$_4$ as the transition metal catalyst and unfortunately obtained the same reaction failure results. It seemed that the oxidative addition was the failing step of the sequence along our efforts.

5.2.2.2.3. Suzuki Coupling

The Suzuki reaction is widely utilized to synthesize poly-olefins, styrenes, and substituted biphenyls. Being easily scalable and cost-effective, it is ideal for use in the synthesis of intermediates for pharmaceuticals or fine chemicals. The Suzuki reaction utilizes an organoboron species that is coupled to an sp^3 or sp^2 hybridized organohalide or pseudohalide using a palladium catalyst in the presence of a base. The availability of common boronic acids, low toxicity, mild reaction conditions, and its use of relatively inexpensive reagents make Suzuki coupling rather attractive over similar reactions.

The isolation and purification of boronic acids is reputably challenging due to their polar (and often amphiphilic) character. When extracting boronic acids from aqueous solutions, ideally the pH of the aqueous phase should be adjusted to a slightly acidic level and a polar organic solvent should be utilized for an efficient partition. However, with prior success employing the Suzuki reaction to couple phenyl boronic acid with **12a** to afford one of our target building blocks **11b**, we were interested in the synthesis of the styryl boronic acid derivative for use in subsequent coupling reactions. Along a literature protocol,[100] lithiation of α-bromostyrene was accomplished at low temperature with *tert*-butyllithium. Triisopropyl borate was added and the reaction was stirred at low temperature for an additional 2 hours and then at room temperature overnight. The following workup was executed strictly to the literature report. We did not obtain the desired boronic acid and could not find evidence for it in any of the various organic and aqueous phases from the work up. We repeated the reaction utilizing trimethyl borate, to perturb any potential challenges attributed to steric effects. Unfortunately, these attempts did not deliver targeted the boronic acid. Due to the well-known challenges in the isolation of boronic acids, we did not press further toward the styryl boronic acid.

5.2.2.2.4. Stille Coupling

Stille coupling is widely employed in organic syntheses, predominantly in the synthesis of natural products. The Stille cross-coupling reaction utilizes an organostannane compound that is coupled to an organic halide or pseudohalide; the reactive carbon center is sp^2 hybridized. Organostannanes are robust compounds that are both air and moisture stable, making them of considerable interest as reactive intermediates as they can be synthesized in large quantities, isolated, and stored.

Due to the challenges faced along other cross-coupling reactions discussed above, our final efforts toward fluorinated dendralene derivatives focused on Stille coupling. Following a literature reported protocol,[101] the synthesis of tributylstannylstyrene was accomplished by the generation of Grignard **99** and subsequent transmetallation with tributyltin chloride. The subsequent cross-coupling was attempted with dibromodifluoroethylene (**12a**) utilizing $Pd(PPh_3)_4$ in the presence of copper iodide. Following aqueous workup, we obtained nearly pristine unreacted tributylstannylstyrene. After triplicate attempts with the same disheartening results, we concluded that failure of the oxidative addition of **12a** to our transition metal catalyst was preventing the cross-coupling reaction. Faced with significant synthetic challenges along various methodologies, we had to conclude our investigations into novel fluorinated dendralenes at this time.

Table 8. Thesis relevant metal-catalyzed cross-coupling reactions general overview.

Reaction	Reactant A		Reactant B		Catalyst
Negishi	R-Zn-X	sp^3, sp^2, sp	R-X	sp^3, sp^2	Pd or Ni
Kumada	R-Mg-X	sp^3, sp^2	R-X	sp^2	Pd or Ni
Stille	R-SnR_3	sp^3, sp^2, sp	R-X	sp^2	Pd
Suzuki	R-$B(OR)_2$	sp^2	R-X	sp^3, sp^2	Pd or Ni

CHAPTER 6: SUMMARY AND OUTLOOK

Through this synthetically driven project, cross-conjugated intermediates were investigated as building blocks for novel polycyclic scaffolds and overall cross-conjugated frameworks were targeted with potentially biological and materials applications and academic investigations.

Arene substituted 2-indanone derivatives (**10**) were synthesized as precursors to all novel polycyclic frameworks targeted herein. Their synthetic routes were individually optimized based on electronic demands to produce multigram quantities.

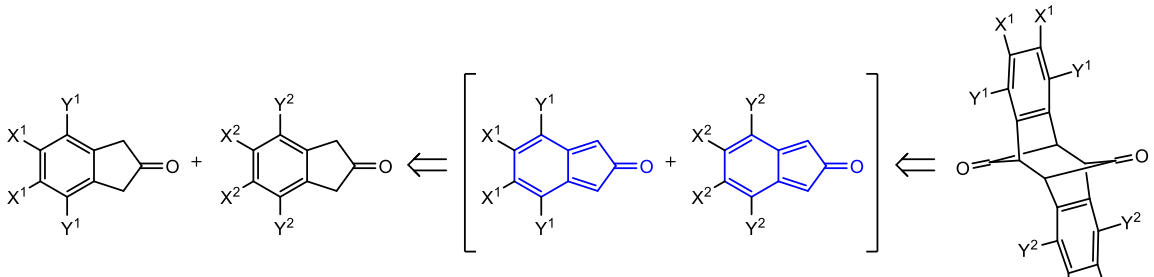

	a	*b*	*c*	*d*	*e*	*f*	*g*	*h*	*i*	*j*	*k*	*l*	*m*	*n*	*o*	*p*	*q*	*r*	*s*	*t*	*u*	*v*
X¹	H	F	H	F					H	OMe	Cl	Cl	H	H	H	H	H	H	OMe	H	H	F
X²	H	F	H	F	mono-fluoro isomers			tri-fluoro isomers	H	OMe	Cl	Cl	H	H	H	H	Me	H	H	H	H	H
Y¹	H	F	F	H					OMe	H	Cl	H	Me	Ph	H	H	H	OMe	H	F	H	H
Y²	H	F	F	H					OMe	H	Cl	H	Me	Ph	Me	OMe	OMe	H	OMe	H	F	F

Figure 9. Targeted isoindenone dimers of type **14** with a table of thesis-relevant substituent patterns.

The generation and subsequent dimerization of isoindenone derivatives (**13**) was investigated employing the synthetic sequence developed by Jones and optimized in our group. Since we were previously unable to obtain the tetramethoxy-isoindenone dimer **14i** along this methodology, even though we obtained isoindenone dimers with similar electronic and steric demands, "mixed" dimerizations were investigated to further probe whether **14i** was inaccessible due to steric or electronic properties. Through our efforts we currently presume that the self dimerization of **13i** fails predominantly due to electronics. However, investigations into the *para*-diethyl and *para*-diisopropyl isoindenone derivatives would further disprove a steric effect. We currently have collaborators working to calculate the transition energy states of the various isoindenones (**13**) and we anticipate that these theoretical calculations, along with our experimental data, will shed light on the peculiarities we have observed in select systems (notably: **13b**, **13i**, **13l**). Preliminary data

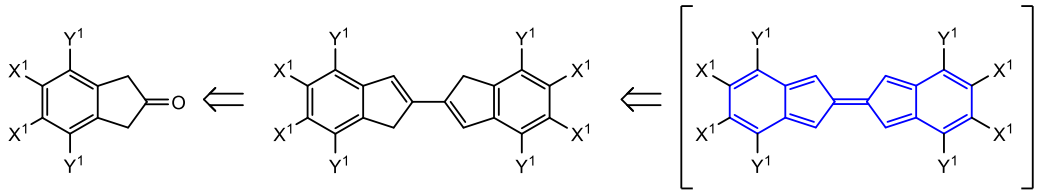

10 **15** **16**

on the parent system indicates that these scaffolds may undergo cycloreversion reactions as reported for some 1,3-disubstituted systems. It would be of interest to trap intermediates of these transformations to gain insight to mechanistic pathways and to probe substituent effects on these pathways.

	a	***b***	***c***	***d***
X^1	H	H	H	H
Y^1	H	Me	OMe	F

Figure 10. Targeted dibenzo[b,e]fulvalenes of type **16** with a table of thesis-relevant substituent patterns.

Dibenzo[b,e]fulvalene derivatives (**16**) were targeted as bimetallic complexes with molybdenum carbonyl moieties. Initially we targeted olefination products (**70**) through McMurry Reaction and pinacol coupling. Through our investigations we had unexpected results, we did not obtain the desired olefins at all with the McMurry Reaction but trace amounts were obtained during pinacol coupling. Fluorinated derivatives did not successfully undergo either of these reactions, we did not observe any fluorinated products. With these challenges we altered our targeted synthetic sequence and ultimately found a shorter route via synthetically useful 2,2'-biindenyl derivatives (**15**). Through these efforts we established reliable protocols to **15b** and **15c**. The Etzkorn group is currently working toward **15d** with promising results along the oxidative homocoupling of 4,7-difluoro-1-

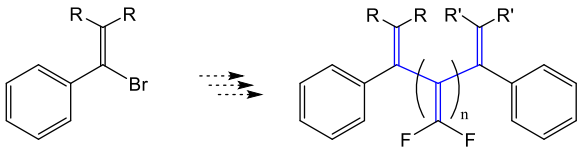

11a, R = H
11b, R = F

17a, R = R' = F
17b, R = F, R' = H

indanone **40c** to the corresponding bisketone **77**. We anticipate **77** can be reduced to the corresponding diol and eliminated to afford **15d**. Once **15d** is obtained molybdenum chemistry will be probed, however, we postulate that a more electron-rich metal will be necessary and in this case we will investigate the reactivity with iron carbonyls.

Fluorinated dendralene derivatives of type **17** were targeted but their syntheses eluded our efforts. We observed difficulties in the generation of reactive intermediates styryl boronic acid and organozinc derivatives **96**. The challenges of isolating alkenyl boronic acids are well-known and we anticipate that with additional time and dedication to

Figure 11. Targeted fluorinated dendralene derivatives of type **17**.

close attention to detail that the styryl boronic acid can be obtained. For the organozinc intermediates, it would be beneficial to repeat our attempts in a glove box to ensure strict absence of air and moisture to both the zinc salts and the reaction vessel. Although we followed strict Schlenk conditions we presume that this may not be sufficient for these incredibly sensitive intermediates. We anticipate that this may be just the trick to move forward with Negishi coupling reactions. We also faced challenges with the oxidative addition of **12a** to our metal catalysts and with mention of the oxidative addition of fluorinated alkenes to transition metal catalysts prominently absent from the experimental literature, we presume that significantly electron deficient alkenes are not suitable for this step of the catalytic cycle. With this in mind we envision that utilizing a non-fluorinated compound, such as α-bromostyrene (**11a**), as the alkene that undergoes oxidative addition and generating the reactive intermediates with the fluorinated building blocks may prove more successful, although not without its limitations. Generation of fluorinated Grignard reagents, with R-MgBr being the target Grignard, may pose challenges as this methodology is often utilized to generate fluorinated Grignard reagents.

CHAPTER 7: EXPERIMENTAL

7.1. Instruments and Materials

Nuclear Magnetic Resonance

^{1}H NMR	300 MHz JOEL ECX-300
	500 MHz Joel As500
^{13}C NMR	300 MHz JOEL ECX-300
	500 MHz Joel As500
^{19}F NMR	300 MHz JOEL ECX-300
	500 MHz Joel As500

All spectra were recorded at 298 K unless otherwise specified. Delta NMR software v. 4.3.5 was used for data analysis. Chemical shifts are reported in ppm, assigning tetramethylsilane (Acros Organics, NMR grade, 99.9% purity), [δ(TMS) = 0.00 ppm] as ^{1}H and ^{13}C reference and trichlorofluoromethane [$\delta(CFCl_3)$ = 0.00 ppm] as ^{19}F reference.

Signal assignments were made based on homo- and heteronuclear 2D NMR experiments and on comparison with analogous compounds when applicable. Chemical shifts denoted with * were mutually exchangeable signals. The signal structure is indicated with the usual abbreviations for singlet (s), doublet (d), etc., and multiplets are quoted over the entire signal range. If a signal has an apparent singlet, doublet, or triplet structure it is quoted as s_{app}, d_{app}, or t_{app}, respectively.

Infrared Spectroscopy

AT-IR spectra were collected on a PerkinElmer SpectrumOne FT-IR Spectrometer with Spectrum software version 5.0.2.

Mass Spectrometry

GC-MS measurements were taken with an Agilent Technologies 6850 Network GC System with Agilent MSD Chemstation and GC-MS Data Analysis Software.

ESI-MS were recorded on a PerSeptive Biosystems: Mariner Biospectrometry Workstation model using Mariner Instrument Control Panel v. 4.0.0.0 software and Data Explorer v. 4.0.0.1 software for data analysis.

X-ray Crystallographic Analysis

X-ray diffraction data were collected using a Bruker SMART APEX II diffractometer equipped with an APEX II 4 K charge-coupled device (CCD) area detector (by use of the program APEX) and a sealed-tube X-ray source (graphite-monochromated Mo-Kα radiation, $\lambda = 0.71073$ Å). A complete sphere of data was collected to better than 0.8 Å resolution. Processing was carried out by using the program SAINT, which applied Lorentz and polarization corrections to three-dimensionally integrated diffraction spots. The program, SADABS, was used for the scaling of diffraction data, the application of decay

correction based on redundant reflections. All calculations were made using the SHELXTL Plus package for structure determination, refinement and molecular graphics. Unit cell dimensions and crystal lattice are confirmed using the XPREP 101 program. Unit cells, distance and angle measurements were found using Mercury 2.2 software. A solution was obtained using direct methods. Successive difference Fourier syntheses revealed all atoms. The final refinement was obtained by introducing a weighting factor and anisotropic thermal parameters for all non-hydrogen atoms.

Chemicals and Materials

All commercially purchased chemicals were used as received unless otherwise specified. For column chromatography, alumina (basic, neutral and acidic) was purchased from Aldrich and silica gel was purchased from Silicycle Chemical Division.

7.2. Procedures and Experimental Data

7.2.1. *para*-Disubstituted 2-Indanones

General Procedure for the Knoevenagel Condensation to Cinnamic Acid Derivatives

A mixture of the corresponding benzaldehyde (176 mmol), malonic acid (317 mmol), pyridine (80 mL), and piperidine (6 mL) was brought to reflux. After 4 h, the temperature was lowered to 80 °C and stirred overnight. The solution was poured into 150 mL half concentrated hydrochloric acid. The resulting precipitate was collected by suction filtration with a fritted filter and washed thoroughly with water to afford the clean product as a beige solid in quantitative yield.

(2*E*)-3-(2,5-difluorophenyl)-2-propenoic acid (38c):

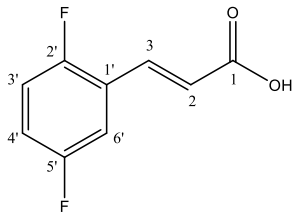

Yield: 99% $C_9H_6F_2O_2$ 184.14 g mol^{-1}

^{1}H NMR (300 MHz, $CDCl_3$): δ = 7.85 (d, 1H, H_3), 7.25 (m, 1H, $H_{6'}$), 7.1 (m, 2H, $H_{3',4'}$), 6.52 (d, 1H, H_2) ppm.

^{19}F NMR (283 MHz, $CDCl_3$): δ = -117.8 (m, 1F), -119.7 (m, 1F) ppm.

(2*E*)-3-(2,5-dimethoxyphenyl)-2-propenoic acid (38i):

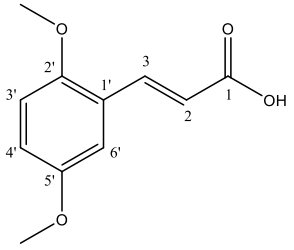

Yield: 98% $C_{11}H_{12}O_4$ 208.20 g mol^{-1}

^{1}H NMR (300 MHz, $CDCl_3$): δ = 8.08 (d, 1H, H_3), 7.06 (s, 1H, $H_{6'}$), 6.95 (d, 1H, $H_{3'}$), 6.85 (d, 1H, $H_{4'}$), 6.52 (d, 1H, H_2), 3.86 (s, 3H, H_{OMe}), 3.80 (s, 3H, H_{OMe}) ppm.

General Procedure for Nickel Boride Reduction of Cinnamic Acid Derivatives

To a green solution of the corresponding cinnamic acid (109 mmol) and nickel chloride hexahydrate (31.1 mmol) in 500 mL ethanol was added sodium borohydride (502 mmol) portion-wise over 1 h. After complete addition, the resulting black solution was stirred an additional 1 h at room temperature then was filtered over celite by suction filtration. The solvent was evaporated *in vacuo* to afford a grey solid that was dissolved in 5% aqueous hydrochloric acid and extracted with methylene chloride. The combined organic phase was dried over anhydrous $MgSO_4$. The solvent was evaporated *in vacuo* to afford the clean product as a beige solid.

2,5-difluoro-propionic acid (39c):

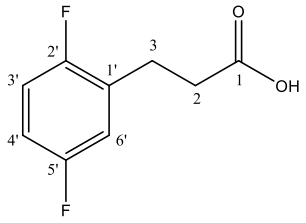

Yield: 85% $C_9H_8F_2O_2$ 185.15 g mol^{-1}

^{1}H NMR (300 MHz, $CDCl_3$): δ = 6.95 (m, 3H, $H_{3',4',6'}$), 2.95 (t, 2H, H_3), 2.70 (t, 2H, H_2) ppm.

^{19}F NMR (283 MHz, $CDCl_3$): δ = -119.1 (m, 1F), -124.3 (m, 1F) ppm.

2,5-dimethoxy-propionic acid (39i):

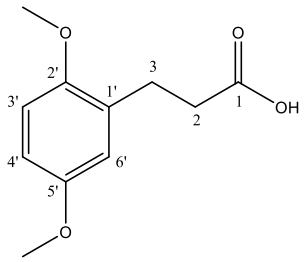

Yield: 85% $C_{11}H_{14}O_4$ 210.22 g mol^{-1}

^{1}H NMR (300 MHz, $CDCl_3$): δ = 6.80-6.68 (m, 3H, $H_{3',4',6'}$), 3.79 (s, 3H, H_{OMe}), 3.77 (s, 3H, H_{OMe}), 2.92 (t, 3H, H_3), 2.67 (t, 3H, H_2) ppm.

4,7-difluoro-1-indanone (40c):

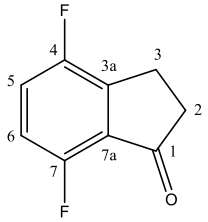

To a solution of 2,5-difluoro-propionic acid (4.00 g, 21.5 mmol) in 30 mL methylene chloride was added $SOCl_2$ (12 mL, 16.5 mmol). After stirring at room temperature overnight, the excess $SOCl_2$ was removed by distillation. To the crude material was added $AlCl_3$ (80.9 mmol) and the mixture was stirred vigorously at 130 °C. After 1 h, the reaction mixture was carefully quenched with ice water and extracted with methylene chloride. The combined organic phase was dried over anhydrous $MgSO_4$. The solvent was evaporated *in vacuo* to afford the product as a tan solid. The product can be purified to colorless crystalline material via sublimation at 70 °C under high vacuum.

Yield: 80% $C_9H_6F_2O$ 168.13 g mol^{-1}

^1H NMR (300 MHz, $CDCl_3$): δ = 7.22 (dt, 1H, H_6), 6.98 (dt, 1H, H_5), 3.15 (t, 2H, H_2), 2.77 (t, 2H, H_3) ppm.

^{19}F NMR (283 MHz, $CDCl_3$): δ = -121.1 (m, 1F), -125.1 (m, 1F) ppm.

GC-MS (EI 70 eV): *m/z* (%) = 169 (10), 168 (100), 167 (28), 141 (13), 140 (94), 139 (41), 138 (7), 125 (5), 121 (6), 120 (13), 119 (26), 114 (26), 113 (6), 112 (15), 99 (12), 93 (5), 87 (5), 81 (6), 75 (6), 74 (7), 63 (10), 62 (7).

4,7-difluoro-1-indanol (42c):

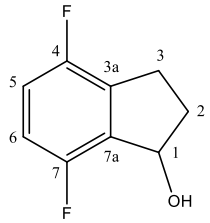

To a solution of 4,7-difluoro-1-indanone (2.00 g, 11.9 mmol) in 50 mL ethanol was added sodium borohydride (0.22 g, 6.08 mmol) portion-wise over 15 min. After stirring overnight at room temperature, the solution was carefully poured into 1 M hydrochloric acid and extracted with chloroform. The combined organic phase was dried over anhydrous

$MgSO_4$. The solvent was evaporated *in vacuo* to afford a light brown oil, which homogenizes over a 24 h period on the benchtop to afford the clean product.

Yield: 90% $C_9H_8F_2O$ 170.14 g mol^{-1}

^1H NMR (300 MHz, $CDCl_3$): δ = 7.18 (dd, 1H, H_6), 7.02 (dd, 1H, H_5), 5.20 (t, 1H, H_1), 3.00 (m, 1H, H_2)*, 2.78 (m, 1H, H_2)*, 2.55 (m, 1H, H_3)*, 2.00 (m, 1H, H_3)* ppm.

^{19}F NMR (283 MHz, $CDCl_3$): δ = -138.6 (m, 1F), -140.5 (m, 1F) ppm.

4,7-difluoro-indene (42c):

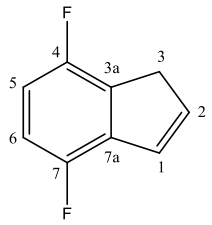

To a light brown solution of 4,7-difluoro-1-indanol (1.50 g, 8.83 mmol) in 50 mL benzene was added a catalytic amount of PTSA and the solution was heated to 100 °C, fitted with a dean stark trap and reflux condenser. After stirring 2 h, the combined solution from the reaction flask and the dean stark trap was washed with saturated sodium bicarbonate. The organic phase was dried over anhydrous $MgSO_4$. The solvent was evaporated *in vacuo* with caution not to pull below 100 mbar to afford the clean product as a brown oil.

Yield: 90% $C_9H_6F_2$ 152.13 g mol^{-1}

^1H NMR (300 MHz, $CDCl_3$): δ = 7.25 (dd, 1H, H_6), 7.13 (dd, 1H, H_5), 6.99 (d, 1H, H_1), 6.60 (d, 1H, H_2), 3.35 (s, 2H, H_3) ppm.

^{19}F NMR (283 MHz, $CDCl_3$): δ = -142.1 (m, 1F), -143.7 (m, 1F) ppm.

4,7-difluoro-2-indanone (10c):

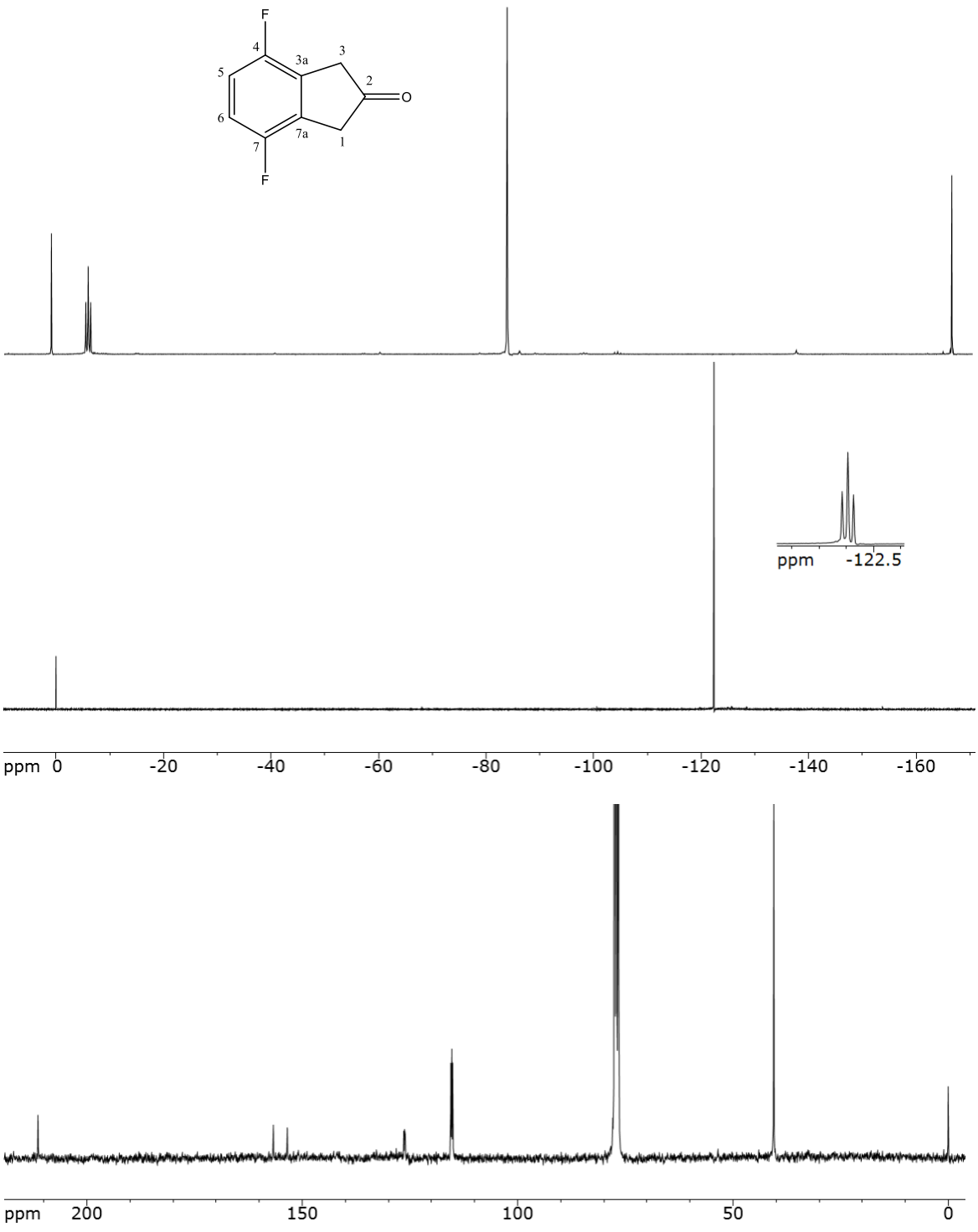

To a solution of indene (0.500 g, 3.29 mmol) in 12 mL methylene chloride was added *m*CPBA (0.623 g, 3.61 mmol). After stirring at room temperature for 3 h, the solution was stretched with methylene chloride and washed with sodium thiosulfate then saturated sodium bicarbonate. The organic phase was dried over anhydrous $MgSO_4$ and solvent was evaporated in vacuo. The crude yellow solid intermediate was dissolved in 30 mL benzene. A catalytic amount of PTSA was added and the solution was heated to 100 °C, fitted with a dean stark trap and reflux condenser. After stirring 2 h at 100 °C, the combined solution from the reaction flask and the dean stark trap was washed with saturated sodium bicarbonate. The organic phase was dried over anhydrous $MgSO_4$ and the solvent was evaporated *in vacuo* to afford clean product as a beige solid.

Yield: 80% $C_9H_6F_2O$ 168.13 g mol^{-1}

^{1}H NMR (300 MHz, $CDCl_3$): δ = 6.96 (t, 2H, $H_{5,6}$), 3.58 (s, 4H, $H_{1,3}$) ppm.

^{19}F NMR (283 MHz, $CDCl_3$): δ = -122.4 (t_{app}, 2F) ppm.

^{13}C NMR (75 MHz, $CDCl_3$): δ = 211.5 (C_2), 155.0 ($C_{4,7}$), 126.5 ($C_{3a,7a}$), 115.5 ($C_{5,6}$), 49.0 ($C_{1,3}$) ppm.

IR (AT-IR): ṽ = 3464, 3131, 3078, 3056, 2954, 2900, 2850, 1758, 1625, 1608, 1576, 1555, 1496, 1456, 1441, 1391, 1333, 1287, 1244, 1231, 1220, 1197, 1144, 1097, 1067, 964, 944, 862, 844, 801, 752, 743, 686 cm^{-1}.

GC-MS (EI 70 eV): *m/z* (%) = 168 [$M^{\cdot+}$] (26), 141 (8), 140 (-CO, 100), 139 (24), 120 (8), 119 (12), 114 (18), 99 (6).

4,7-dimethoxy-1-indanone (40i):

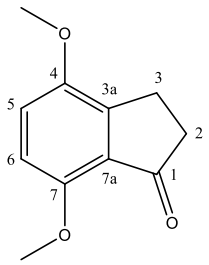

To hot, stirring polyphosphoric acid (~30 mL) in a 100 mL RBF was added 2,5-dimethoxy-propionic acid (2.00 g, 9.51 mmol). After stirring 2 h at 80 °C, the solution was carefully poured into cold water and extracted with diethyl ether. The combined organic phase was washed with saturated sodium bicarbonate and dried over anhydrous $MgSO_4$. The solvent was evaporated *in vacuo* to afford the clean product as a beige crystalline solid.

Yield: 80% $C_{11}H_{12}O_3$ 192.21 g mol^{-1}

^1H NMR (300 MHz, $CDCl_3$): δ = 6.99 (d, 1H, H_6), 6.72 (d, 1H, H_5), 3.90 (s, 3H, H_{OMe}), 3.87 (s, 3H, H_{OMe}), 2.99 (t, 2H, H_2), 2.68 (t, 2H, H_3) ppm.

GC-MS (EI 70 eV): *m/z* (%) = 193 (12), 192 (100), 191 (15), 177 (23), 173 (5), 164 (10), 163 (92), 162 (5), 159 (9), 149 (33), 135 (7), 134 (11), 133 (6), 131 (8), 121 (32), 119 (8), 106 (11), 105 (10), 103 (8), 91 (23), 90 (6), 89 (11), 79 (8), 78 (13), 77 (17), 76 (5), 65 (7), 63 (9), 51 (8).

4,7-dimethoxy-2-oxime-indan-1-one (46):

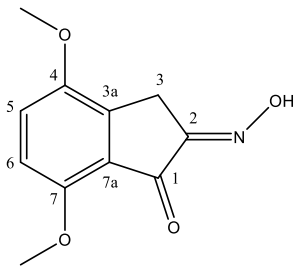

To a suspension of 4,7-dimethoxy-1-indanone (2.80 g, 14.6 mmol) in 18 mL 1,2-dimethoxyethane and 6 mL concentrated hydrochloric acid was added isoamyl nitrite (2.055 g, 17.5 mmol) dropwise. After stirring overnight at room temperature, water was added to facilitate product precipitation. The resulting precipitate was collected by suction filtration over a fritted filter, washed with water, and air-dried to afford clean product as a beige solid.

Yield: 90% $C_{11}H_{11}NO_4$ 221.19 g mol^{-1}

^1H NMR (300 MHz, $CDCl_3$): δ = 7.09 (d, 1H, H_6), 6.81 (d, 1H, H_5), 3.94 (s, 3H, H_{OMe}), 3.89 (s, 3H, H_{OMe}), 3.72 (s, 2H, H_3) ppm.

4,7-dimethoxy-indan-1,2-dione (47):

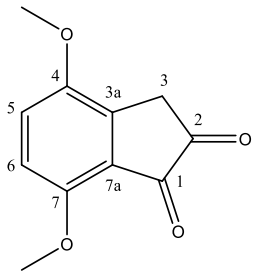

To 4,7-dimethoxy-2-oxime-indan-1-one (3.10 g, 14.0 mmol) was added 6.3 mL 37% formaldehyde and 11.4 mL concentrated hydrochloric acid. After stirring overnight at room temperature, water was added to facilitate product precipitation. The resulting precipitate was collected by suction filtration over a fritted filter, washed with water, and air-dried to afford clean product as a brown solid.

Yield: 95% $C_{11}H_{10}O_4$ 206.19 g mol^{-1}

^1H NMR (300 MHz, $CDCl_3$): δ = 7.19 (d, 1H, H_6), 6.88 (d, 1H, H_5), 3.96 (s, 3H, H_{OMe}), 3.89 (s, 3H, H_{OMe}), 3.48 (s, 2H, H_3) ppm.

4,7-dimethoxy-indan-1,2-diol (44i):

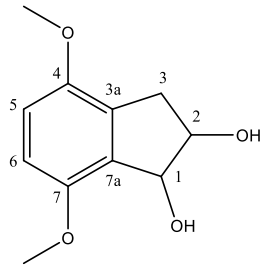

To a solution of 4,7-dimethoxy-indan-1,2-dione (2.00 g, 9.70 mmol) in 75 mL anhydrous THF at 0 °C was added a borane•dimethylsulfide complex (1.6 mL) dropwise. After stirring 2 d at room temperature, the reaction was cooled to 0 °C and 7 mL concentrated sulfuric acid was carefully added. After stirring an additional 2 h, the layers were separated with Brine and extracted with diethyl ether. The combined organic phase was dried over anhydrous $MgSO_4$ and the solvent evaporated *in vacuo* to afford clean product as a beige crystalline solid.

Yield: 80% $C_{11}H_{14}O_4$ 210.22 g mol^{-1}

4,7-dimethoxy-2-indanone (10i):

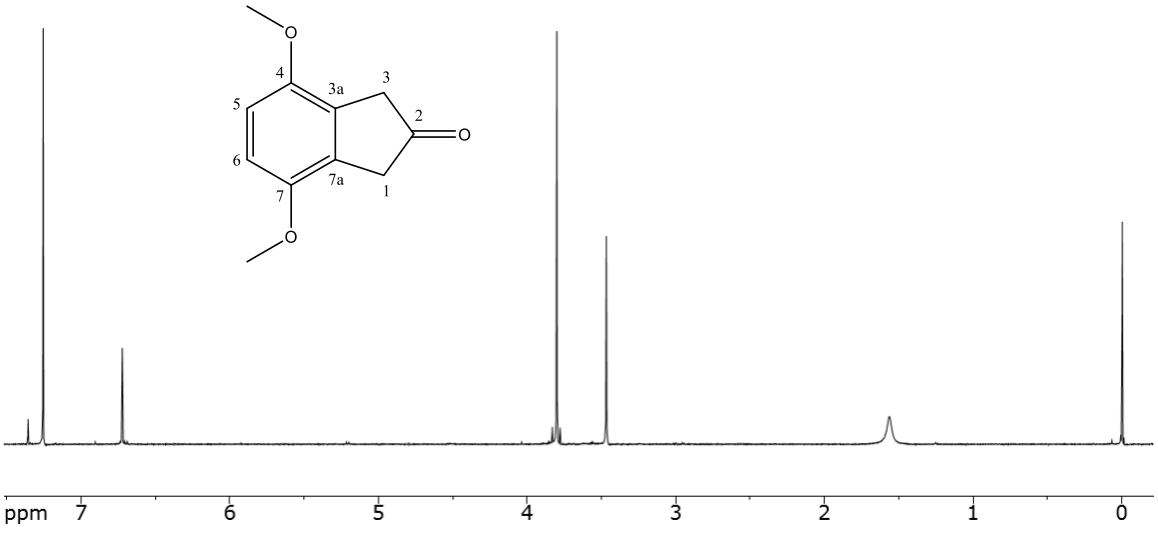

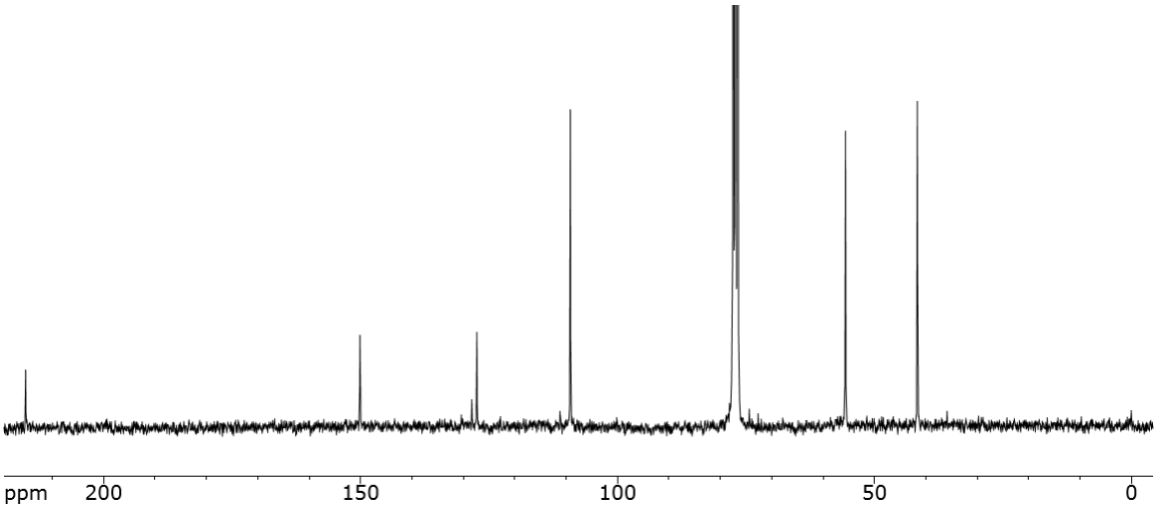

To a solution of 4,7-dimethoxy-indan-1,2-diol (0.978 g, 4.65 mmol) in 100 mL benzene was added a catalytic amount of PTSA and the solution was refluxed fitted with a dean stark trap and reflux condenser. After stirring 1 h, the combined solution from the reaction flask and the dean stark trap was washed with saturated sodium bicarbonate. The organic phase was dried over anhydrous $MgSO_4$. The solvent was evaporated *in vacuo* to afford the crude product as a brown solid that was triturated with diethyl ether to afford clean product as a beige solid.

Yield: 50% $C_{11}H_{12}O_3$ 192.21 g mol^{-1}

^1H NMR (300 MHz, $CDCl_3$): δ = 6.72 (s, 2H, $H_{5,6}$), 3.80 (s, 6H, H_{OMe}), 3.46 (s, 4H, $H_{1,3}$) ppm.

^{13}C NMR (75 MHz, $CDCl_3$): δ = 215.1 (C_2), 150.1 ($C_{3a,7a}$), 127.3 ($C_{4,7}$), 109.1 ($C_{5,6}$), 55.6 (C_{OMe}), 41.6 ($C_{1,3}$) ppm.

IR (AT-IR): $\tilde{\nu}$ = 3399, 2997, 2897, 1741, 1604, 1495, 1461, 1440, 1383, 1333, 1285, 1257, 1192, 1178, 1145, 1063, 1015, 917, 860, 802, 713, 681 cm^{-1}.

GC-MS (EI 70 eV): *m/z* (%) = 193 (12), 192 (100), 165 (9), 164 (84), 163 (14), 150 (9), 149 (90), 134 (11), 133 (8), 121 (26), 119 (11), 105 (6), 104 (6), 91 (33), 90 (5), 89 (12), 82 (8), 78 (14), 77 (25), 63 (11), 54 (5), 53 (6), 52 (6), 51 (12).

4,7-dimethyl-indene (42m):

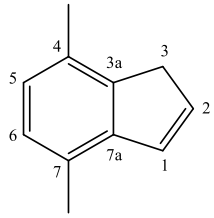

Sodium (12.5 g, 547 mmol) was reacted in 150 mL methanol and cooled to 0 °C. Freshly cracked and distilled cyclopentadiene (27.1 mL, 328 mmol) was added dropwise under N2. After stirring 30 minutes, hexan-2,5-dione (25.5 mL, 219 mmol) was added dropwise and the reaction was warmed to room temperature. After stirring overnight at room temperature, the reaction was diluted with water and extracted with diethyl ether. The combined organic phase was dried over anhydrous $MgSO_4$. The solvent was evaporated *in vacuo* to afford crude material as a brown oil that was purified by distillation to give clean product as a yellow liquid.

Yield: 85% $C_{11}H_{12}$ 144.20 g mol^{-1}

^1H NMR (300 MHz, $CDCl_3$): δ = 7.03-7.00 (m, 2H, $H_{6,1}$), 6.95 (d, 1H, H_5), 6.59 (d, 1H, H_2), 3.32 (s, 2H, H_3), 2.45 (s, 3H, H_{Me}), 2.35 (s, 3H, H_{Me}) ppm.

4,7-dimethyl-2-indanone (10m):

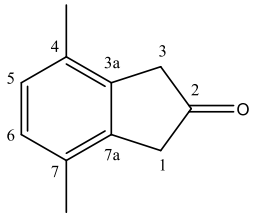

A solution of 140 mL formic acid (88% w/v) and 24 mL hydrogen peroxide (30% w/v) was heated to 35 °C, with the temperature held constant indene (20.0 g, 139 mmol) was added drop-wise over approximately 15 min. After stirring overnight at room temperature, the residual formic acid was removed under aspirator pressure at 55 °C (ensured temperature remained under 60 °C). The reaction flask was cooled to room temperature, the crude sticky solid was dissolved in 200 mL of 7% aqueous sulfuric acid and a steam distillation was carried out and the distillate was extracted with methylene chloride. The combined organic phase was dried over anhydrous $MgSO_4$ and solvent was evaporated *in vacuo* to afford clean product as a colorless crystalline solid.

Yield: 50% $C_{11}H_{12}O$ 160.20 g mol^{-1}

^1H NMR (300 MHz, $CDCl_3$): δ = 7.02 (s, 2H, $H_{5,6}$), 3.47 (s, 4H, $H_{1,3}$), 2.22 (s, 6H, H_{Me}) ppm.

GC-MS (EI 70 eV): *m/z* (%) = 161 (8), 160 (71), 133 (10), 132 (100), 131 (22), 118 (6), 117 (64), 116 (10), 115 (28), 91 (16), 77 (7), 65 (6), 64 (6), 63 (5), 51 (6).

α-bromo-acetophenone (50):

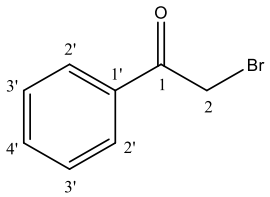

To a solution of acetophenone (10.05 g, 83.6 mmol) in 350 mL acetonitrile was added PTSA (23.891 g, 126 mmol) and the mixture was brought to reflux. NBS (14.888 g, 83.6 mmol) was added portion-wise over approximately 30 minutes. After refluxing 3 h, the reaction was cooled to room temperature and the solvent was evaporated in vacuo. The crude residue was taken up in 200 mL CH_2Cl_2 and washed with water. The organic phase

was dried over anhydrous $MgSO_4$ and the solvent evaporated *in vacuo* to afford the product as a tan solid that could be purified by recrystallization.

Yield: 90% C_8H_7BrO 199.03 g mol^{-1}

^1H NMR (300 MHz, $CDCl_3$): δ = 7.99 (d, 2H, $H_{2'}$), 7.61 (p, 2H, $H_{3'}$), 7.49 (p, 1H, $H_{4'}$), 4.47 (s, 2H, H_2) ppm.

dibenzoylethane (51):

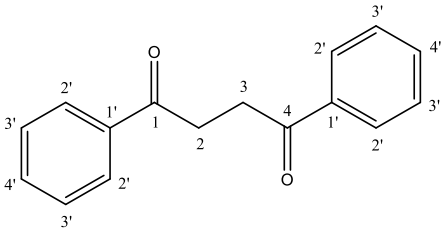

To a solution of a-bromoacetophenone (5.00 g, 25.1 mmol) in 50 mL anhydrous THF was added Zn dust (1.641 g, 25.1 mmol) then a catalytic amount of I_2. After stirring at 65 °C overnight the reaction was cooled to room temperature and insoluble material was filtered off over Celite. Water was added to the filtrate to facilitate precipitation and the crude material was collected by suction filtration. Recrystallization from chloroform:hexane (4:1) affords clean product as a beige solid.

Yield: 70% $C_{16}H_{14}O_2$ 238.27 g mol^{-1}

^1H NMR (300 MHz, $CDCl_3$): δ = 8.05 (d, 4H, $H_{2'}$), 7.58 (p, 4 H, $H_{3'}$), 7.45 (p, 2H, $H_{4'}$), 3.48 (s, 4H, $H_{2,3}$) ppm.

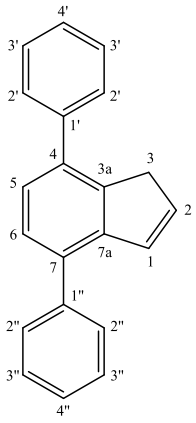

4,7-diphenyl-indene (42n):

To a solution of t-BuOK (0.471 g, 4.2 mmol) in 70 mL methanol was added cyclopentadiene (1.386 g, 21 mmol) under N_2. After stirring 30 min, dibenzoylethane (5.00 g, 21 mmol) was added all at once. After stirring at 40 °C 5 d, the reaction mixture was diluted with water and extracted with diethyl ether. The combined organic phase was dried over anhydrous $MgSO_4$ and the solvent evaporated *in vacuo* to afford the crude material as a brown solid. Purification by column chromatography on silica with pentane:ethyl acetate (5:1) to afford clean product as a colorless crystalline solid.

Yield: 45% $C_{21}H_{16}$ 268.34 g mol^{-1}

^1H NMR (300 MHz, $CDCl_3$): δ = 7.62-7.27 (m, 12H), 7.12 (m, 1H, H_1), 6.62 (m, 1H, H_2), 3.57 (t, 2H, H_3) ppm.

IR (AT-IR): $\tilde{\nu}$ = 3048, 3025, 2956, 2922, 2889, 2852, 1953, 1894, 1682, 1599, 1575, 1566, 1504, 1469, 1447, 1439, 1388, 1368, 1320, 1279, 1260, 1182, 1173, 1160, 1121, 1090, 1073, 1021, 1000, 971, 960, 932, 915, 906, 885, 846, 828, 819, 779, 756, 747, 694, 655 cm^{-1}.

GC-MS (EI 70 eV): *m/z* (%) = 269 (22), 268 (100), 267 (25), 266 (6), 265 (16), 263 (7), 253 (8), 252 (15), 239 (7), 191 (11), 190 (5), 189 (16), 134 (5), 133 (9), 132 (8), 126 (13), 119 (7).

4,7-diphenyl-2-indanone (10n):

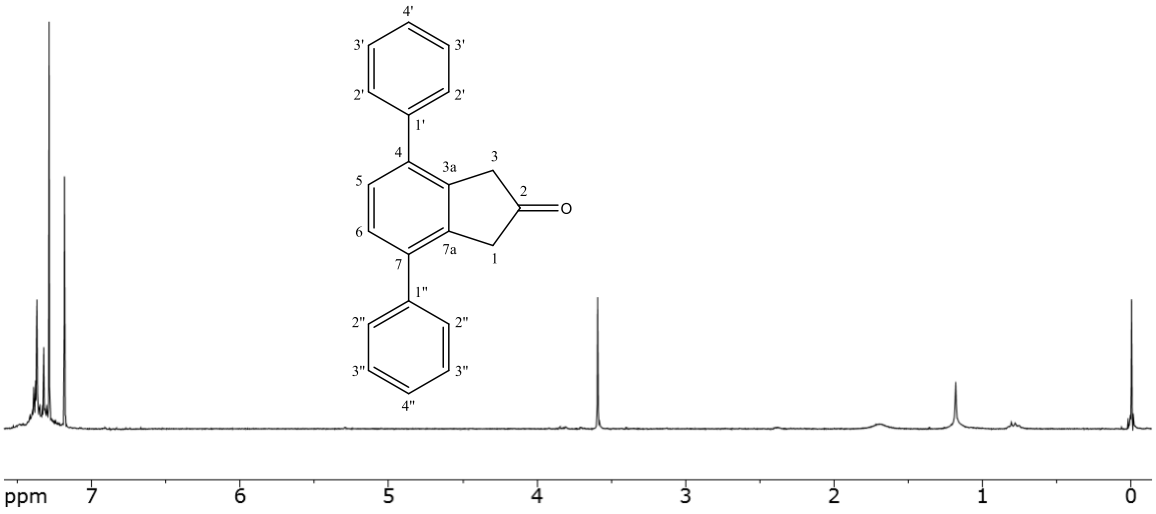

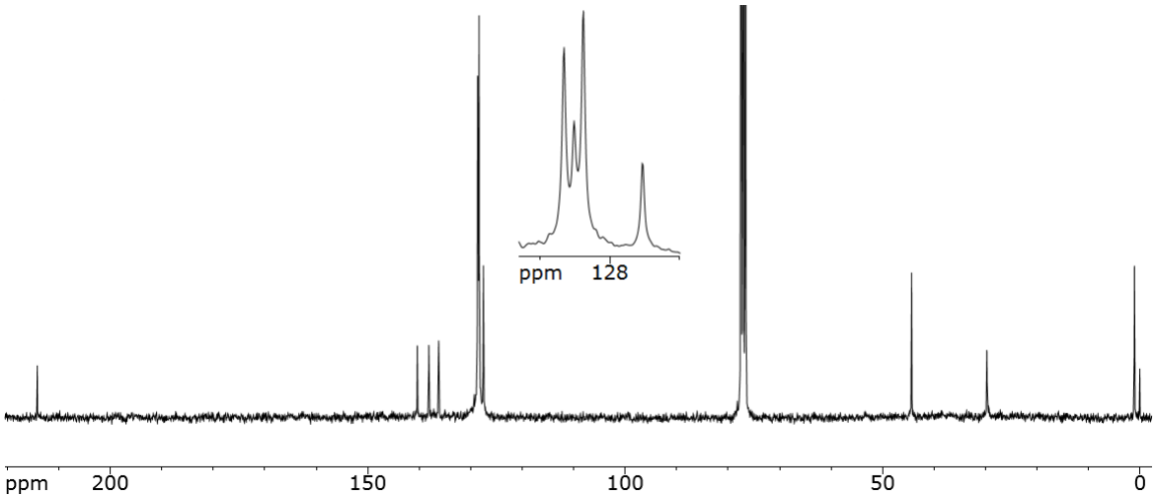

To a solution of indene (0.30 g, 1.12 mmol) in 8 mL methylene chloride was added *m*CPBA (0.212 g, 1.23 mmol). After stirring at room temperature for 3 h, the solution was stretched with methylene chloride and washed with sodium thiosulfate then saturated sodium bicarbonate. The organic phase was dried over anhydrous $MgSO_4$ and solvent was evaporated in vacuo. The crude yellow solid intermediate was dissolved in 30 mL benzene. A catalytic amount of PTSA was added and the solution was heated to 100 °C, fitted with a dean stark trap and reflux condenser. After stirring 2 h at 100 °C, the combined solution from the reaction flask and the dean stark trap was washed with saturated sodium bicarbonate. The organic phase was dried over anhydrous $MgSO_4$ and the solvent was evaporated *in vacuo* to afford clean product as a beige solid.

Yield: 80% $C_{21}H_{16}O$ 284.34 g mol^{-1}

^1H NMR (300 MHz, $CDCl_3$): δ = 7.50-7.34 (m, 12H), 3.68 (s, 4H, $H_{1,3}$) ppm.

^{13}C NMR (75 MHz, $CDCl_3$): δ = 214.2 (C_2), 140.4 ($C_{5,6}$), 138.1 ($C_{1,1'}$), 136.2 ($C_{4',4''}$), 128.7 ($C_{2',2''}$), 128.5 ($C_{4,7}$), 128.4 ($C_{3',3''}$), 127.5 ($C_{3a,7a}$), 44.4 ($C_{1,3}$) ppm.

IR (AT-IR): $\tilde{\nu}$ = 2942, 2922, 2889, 1743, 1601, 1589, 1473, 1459, 1380, 1258, 1194, 1023, 913, 800, 756, 734, 701 cm^{-1}.

GC-MS (EI 70 eV): *m/z* (%) = 285 (15), 284 (66), 257 (8), 256 (48), 255 (100), 254 (14), 253 (26), 252 (25), 250 (5), 241 (15), 240 (13), 239 (23), 226 (5), 215 (5), 165 (7), 128 (7), 127 (12), 126 (28), 125 (6), 120 (15), 114 (13), 113 (13), 101 (9).

7.2.2. Toward Tetrafluorothiophene S,S-Dioxide

2,2,3,3-tetrafluoro-1,4-di(tosyloxy)butane (53):[55]

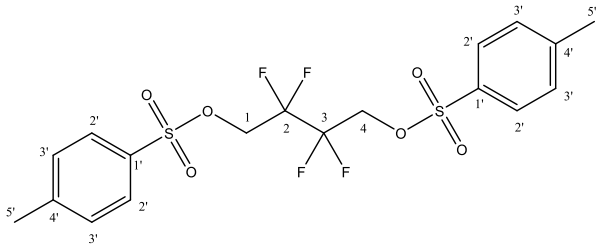

To a solution of 2,2,3,3-tetrafluorobutane-1,4-diol (12.5 g, 77.1 mmol) in 175 mL pyridine was added tosyl chloride (42.7 g, 224 mmol). After stirring 24 h at 55 ºC, the mixture was poured into an Erlenmeyer flask cooled in ice and 150 mL H_2O was added while swirling. The precipitate was collected by filtration over a fritted filter, washed with water, then taken up in CH_2Cl_2 and washed with two equal portions of 5% H_2SO_4. The organic phase was dried over anhydrous Na_2SO_4 and the solvent was evaporated *in vacuo* to afford the product as a tan solid.

Yield: 98% $C_{18}H_{18}F_4O_6S_2$ 470.45 g mol^{-1}

^1H NMR (300 MHz, $CDCl_3$): δ = 7.80 (d, 4H, $H_{2'}$), 7.42 (d, 4H, $H_{3'}$), 4.42-4.29 (m, 4H, $H_{1,4}$), 2.48 (s, 6H, $H_{5'}$) ppm.

^{19}F NMR (283 MHz, $CDCl_3$): δ = -120.8 (m, 4F) ppm.

3,3,4,4-tetrafluorothiolane (54):[55]

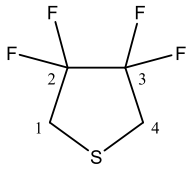

To a 500 mL Schlenk flask was added 2,2,3,3-tetrafluoro-1,4-di(tosyloxy)butane (25 g, 53.1 mmol) and 115 mL DMA. The mixture was degassed by performing three

freeze/pump/thaw cycles with Ar. Sodium sulfide (10.38 g, 133 mmol) was added under Ar and the mixture was heated to 70 ºC. After stirring 8 h, a liquid N2-cooled u-tube trap-to-trap vacuum transfer was carried out at 16 mbar for 20 min. The contents of the u-tube were pipetted into a pear-shaped flask and the thiolane layer was carefully removed. Concentrated H2SO4 was added to sequester any remaining water and the product was short-path distilled.

Yield: 55% $C_4H_4F_2S$ 122.13 g mol^{-1}

^1H NMR (300 MHz, $CDCl_3$): δ = 3.29-3.17 (m, 4H, $H_{1,4}$) ppm.

^{19}F NMR (283 MHz, $CDCl_3$): δ = -120.4 (m, 4F) ppm.

MS (EI, 70 eV): m/z (%) = 162 (5), 161 (6), 160 (100), 121 (9), 96 (94), 95 (13), 78 (5), 77 (18), 69 (6), 64 (16), 59 (5).

***cis*- and *trans*-2,3,4,4,5-hexafluorothiolane (55):**[55]

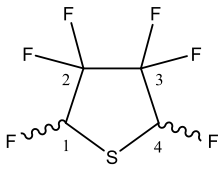

To a two-neck RBF was added 3,3,4,4-tetrafluorothiolane (4.58 g, 37.5 mmol) and 50 mL sulfolane. The flask was fitted with a solid addition funnel and placed in a cool water bath. Selectfluor (11.23 g, 31.7 mmol) was added slowly via solid addition funnel with vigorous stirring. After complete addition stirring was continued for 25 min, then another addition of Selectfluor (17.99 g, 50.8 mmol) was added all at once and the mixture was heated to 65 °C. After stirring 4 h, a liquid N_2-cooled u-tube trap-to-trap vacuum transfer was carried out under high vacuum while gradually raising the temperature to 120 °C and maintaining

that temperature for 10 min. The contents of the u-tube were transferred by pipet and short-path distilled without water in the condenser.

Yield: 50% $C_4H_2F_6S$ 196.12 g mol^{-1}

^1H NMR (300 MHz, $CDCl_3$): δ = 6.25-5.95 (dm, 4H, $H_{1,4}$ – both isomers) ppm.

^{19}F NMR (283 MHz, $CDCl_3$): *cis* δ = -120.2, -123.0 (ABq, 4F), -163.6 (d, 2F); *trans* δ = -121.3 (d, 2F), -134.1 (d, 2F), -161.1 (d, 2F) ppm.

tetrafluorothiophene (56):[55]

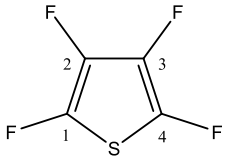

To a solution of hexafluorothiolane (5.04 g, 25.7 mmol) in 55 mL DMSO, in a room temperature water bath, was added powdered KOH (10.6 g, 189 mmol). After stirring 2.5 h at room temperature, a liquid N2-cooled u-tube trap-to-trap vacuum transfer was carried out at 45 °C while the pressure was gradually reduced to 10 mbar and maintaining that pressure for 20 min. The product was collected from the u-tube by pipet.

Yield: 75% C_4F_4S 156.10 g mol^{-1}

^{19}F NMR (283 MHz, $CDCl_3$): δ = -155.7 (t, 2F), -164.5 (t, 2F) ppm.

MS (EI, 70 eV): m/z (%) = 157.9 (5), 156.9 (5), 155.9 (100), 124.9 (12), 105.9 (12), 94 (7), 93 (78), 87 (65), 75 (5), 74 (8), 63 (29).

***cis*- and *trans*-2,5-dibromo-2,3,4,5-tetrafluorothiol-3-ene (57):**[55]

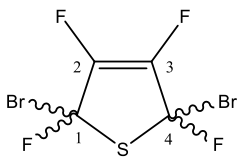

To an immersion well flask was added tetrafluorothiophene (0.40 g, 2.56 mmol), bromine (0.455 g, 2.85 mmol), and 10 mL CCl4. The solution was irradiated with a 5.5 W UV lamp. After 3 h, the solution was transferred to an RBF and the solvent was evaporated in vacuo.

Yield: 90% $C_4Br_2F_4S$ 315.90 g mol^{-1}

^{19}F NMR (283 MHz, $CDCl_3$): cis δ = -63.8 (m, 2F), -140.1 (m, 2F); trans δ = -75.6 (m, 2F), -140.5 (m, 2F) ppm.

7.2.3. Isoindenone Generation and "Mixed" Dimerization

General Procedure for the Silylation of 2-indanone Derivatives

To a solution of the corresponding 2-indanone (1.51 mmol) and TBDMSCl (1.66 mmol) in 4 mL benzene was added DBU (1.66 mmol) dropwise. After stirring 30 min at room temperature, the mixture was diluted with cold Et_2O and washed with cold H_2O (3X). The organic phase was dried over anhydrous Na_2SO_4 and the solvent was evaporated *in vacuo* to afford the crude product as an oil in quantitative yield.

2-(*tert*-butyldimethylsiloxy)-indene (28a):

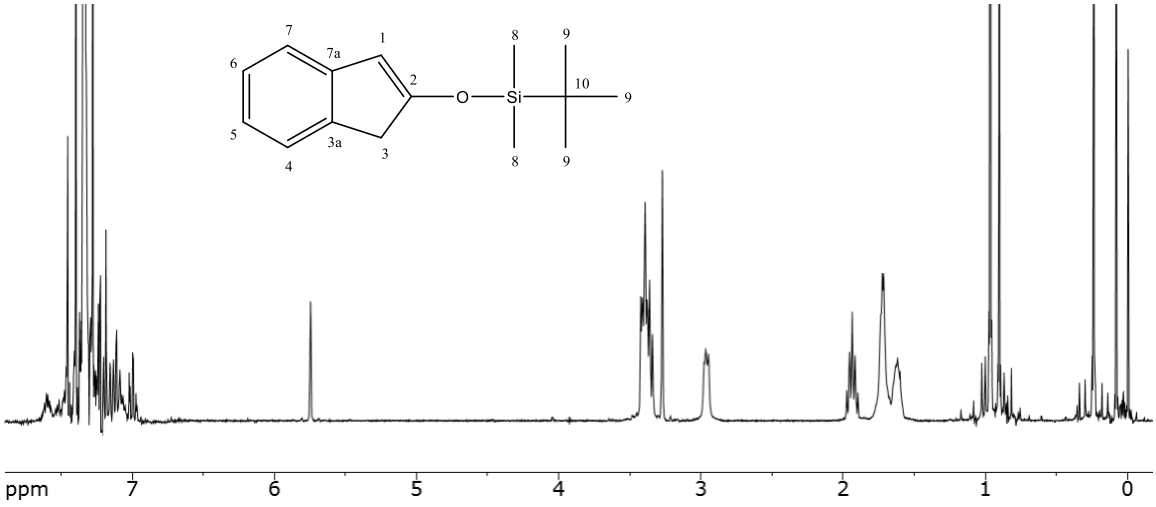

Yield: 98% $C_{15}H_{22}OSi$ 246.41 g mol^{-1}

^{1}H-NMR (300 MHz, $CDCl_3$): δ = 7.31 (d, 1H, H_7), 7.15 (d, 1H, H_4), 7.05-6.85 (m, 2H, $H_{5,6}$), 5.75 (s, 1H, H_1), 3.28 (s, 2H, H_3), 0.98 (s, 9H, H_9), 0.25 (s, 6H, H_8) ppm.

MS (EI, 70 eV): *m/z* (%) = 248.2 (7), 247.2 (26), 246.2 (100), 191.1 (6), 190.1 (30), 189.1 (76), 161.1 (6), 145.1 (8), 132.1 (10), 131.1 (7), 128.1 (5), 116.1 (22), 103.1 (9), 77.1 (6), 73.1 (47), 59.1 (7).

2-(*tert*-butyldimethylsiloxy)-5,6-difluoro-indene (28d):

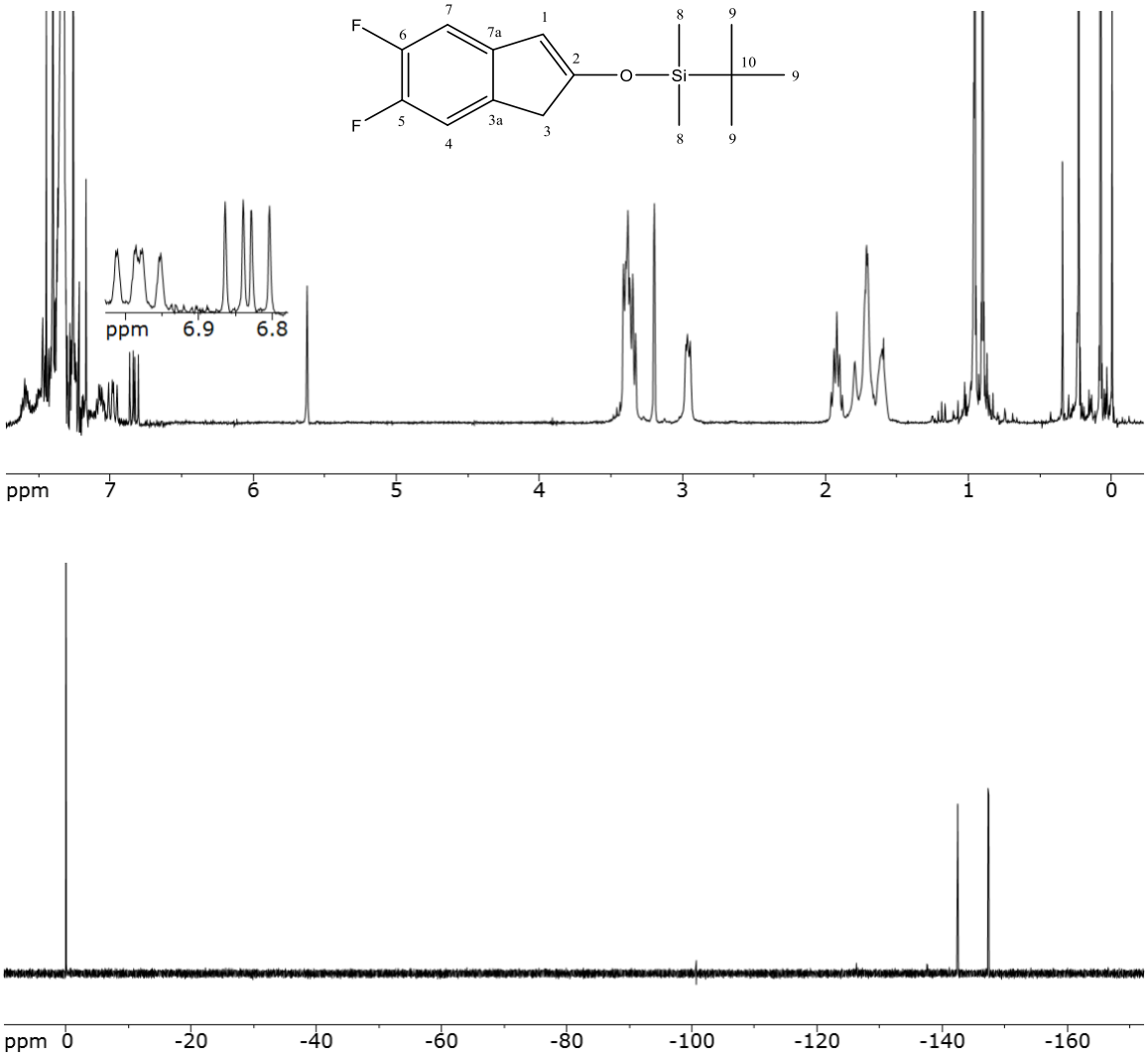

Yield: 98% $C_{15}H_{20}F_2OSi$ 282.39 g mol^{-1}

^{1}H-NMR (300 MHz, $CDCl_3$): δ = 7.00 (dd, 1H, H_7), 6.83 (dd, 1H, H_4), 5.62 (s, 1H, H_1), 3.20 (s, 2H, H_3), 0.98 (s, 9H, H_9), 0.25 (s, 6H, H_8) ppm.

^{19}F-NMR (283 MHz, $CDCl_3$): δ = -142.4 (m, 1F), -147.4 (m, 1F) ppm.

MS (EI, 70 eV): *m/z* (%) = 283.1, 282.1 ($M^{\cdot+}$, 100), 226.1 (21), 225.1 (38), 151 (70), 129 (18), 101 (24), 75 (17), 73.1 (82).

2-(*tert*-butyldimethylsiloxy)-4,7-difluoro-indene (28c):

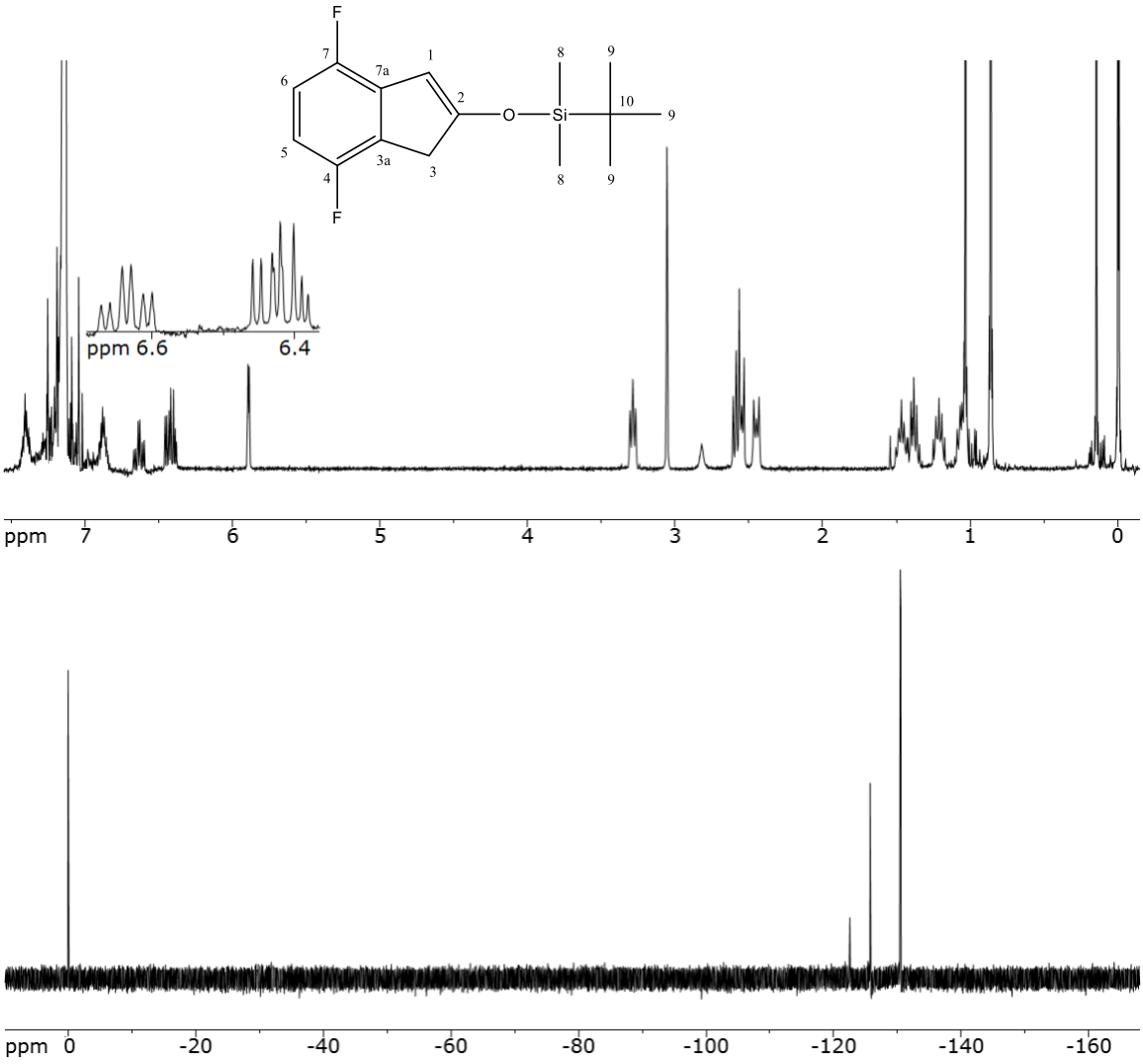

Yield: 98% $C_{15}H_{20}F_2OSi$ 282.39 g mol^{-1}

^{1}H-NMR (300 MHz, $CDCl_3$): δ = 6.64 (td, 1H, H_6), 6.42 (td, 1H, H_5), 5.91 (s, 1H, H_1), 3.08 (s, 2H, H_3), 0.99 (s, 9H, H_9), 0.24 (s, 6H, H_8) ppm.

^{19}F-NMR (283 MHz, $CDCl_3$): δ = -125.8 (m, 1F), -130.5 (m, 1F) ppm.

MS (EI, 70 ev): *m/z* (%) = 283.1, 282.1 ($M^{\cdot+}$, 62), 226 (20), 225 (27), 197 (24), 183 (13), 168 (7), 152 (8), 139 (6), 132 (8), 115 (15), 101 (12), 81 (8), 77 (33), 75 (27), 74 (11), 73 (100), 57.1 (7).

2-(*tert*-butyldimethylsiloxy)-4,7-dimethyl-indene (28m):

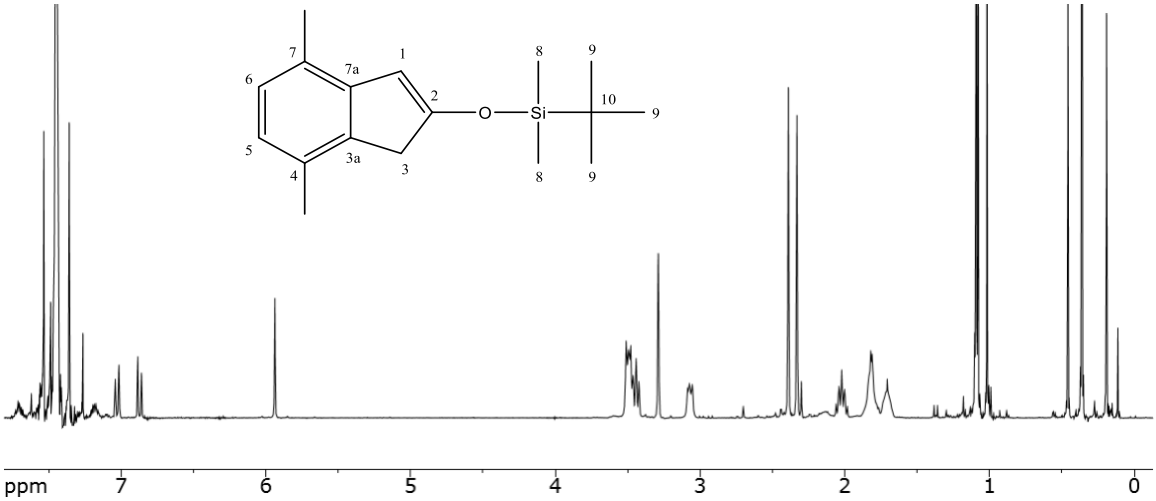

Yield: 98% $C_{17}H_{26}OSi$ 274.45 g mol^{-1}

^{1}H-NMR (300 MHz, $CDCl_3$): δ = 7.02 (d, 1H, H_6), 6.88 (d, 1H, H_5), 5.94 (s, 1H, H_1), 3.30 (s, 2H, H_3), 1.01 (s, 9H, H_9), 0.30 (s, 6H, H_8) ppm.

MS (EI, 70 eV): *m/z* (%) = 276.2 (5), 275.2 (21), 274.2 (89), 218.1 (7), 217.1 (5), 160.1 (5), 145.1 (5), 144.1 (18), 143.1 (100), 141.1 (5), 129.1 (5), 128.1 (15), 115.1 (6), 75 (13), 73.1 (29).

2-(tert-butyldimethylsiloxy)-5,6-dimethoxy-indene (28j):

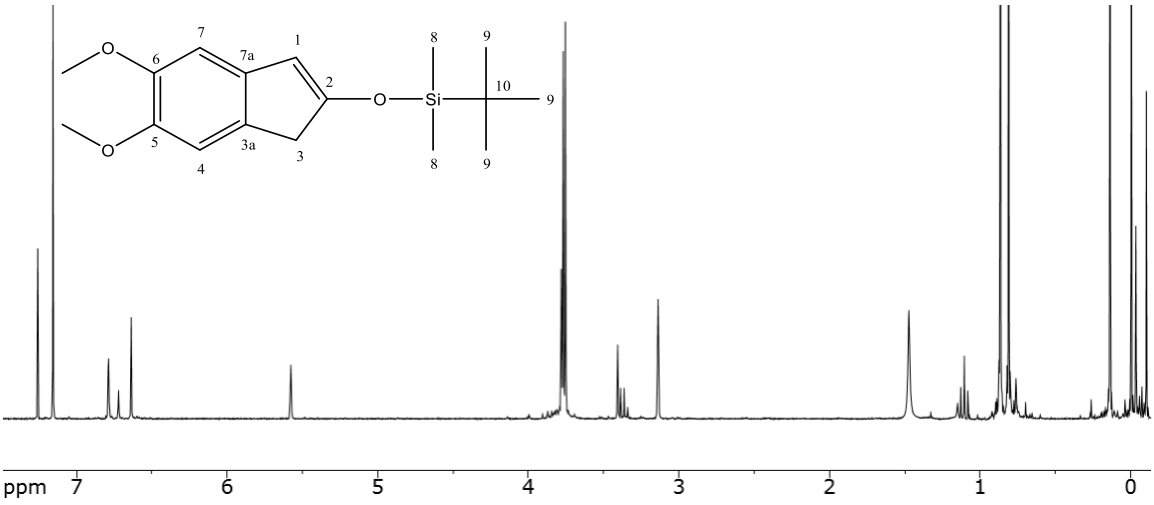

Yield: 98% $C_{17}H_{26}O_3Si$ 306.45 g mol^{-1}

^{1}H-NMR (300 MHz, $CDCl_3$): δ = 6.89 (s, 1H, H_7), 6.74 (s, 1H, H_4), 5.68 (s, 1H, H_1), 3.87 (s, 3H, H_{OMe}), 3.85 (s, 3H, H_{OMe}), 3.24 (s, 2H, H_3), 0.96 (s, 9H, H_9), 0.91 (s, 6H, H_8) ppm.

2-(*tert*-butyldimethylsiloxy)-4,7-dimethoxy-indene (28i):

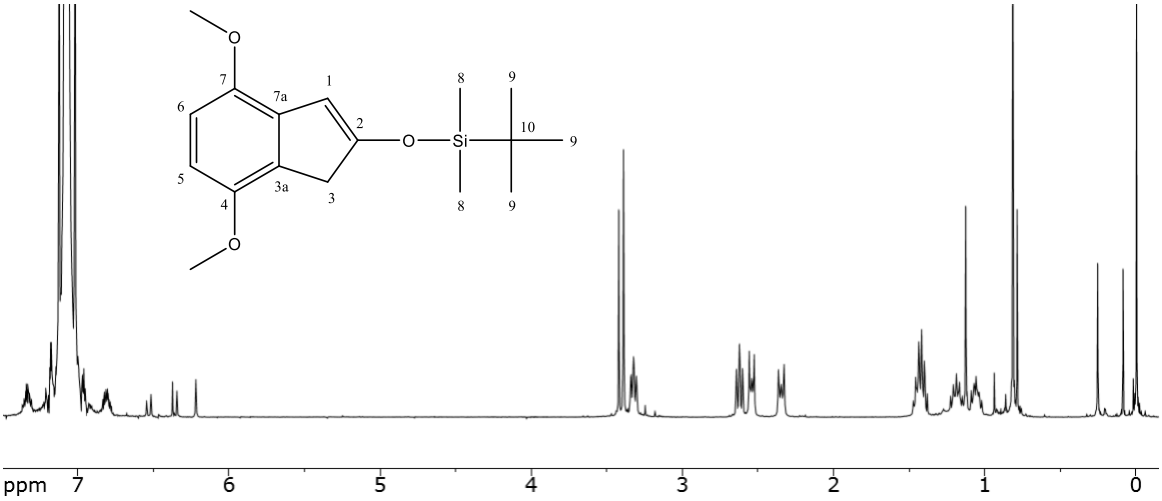

Yield: 98% $C_{17}H_{26}O_3Si$ 306.45 g mol^{-1}

^{1}H-NMR (300 MHz, $CDCl_3$): δ = 6.72 (d, 1H, H_6), 6.56 (d, 1H, H_5), 5.91 (s, 1H, H_1), 3.86 (s, 3H, H_{OMe}), 3.84 (s, 3H, H_{OMe}), 3.32 (s, 2H, H_3), 0.99 (s, 9H, H_9), 0.28 (s, 6H, H_8) ppm.

General Procedure for the Bromination of Silyl Enol Ether Derivatives

To a solution of the corresponding silyl enol ether (1.51 mmol) in 5 mL CCl_4 was added NBS (1.66 mmol) and a catalytic amount of AIBN. The mixture was brought to reflux, and conversion was monitored by NMR. The reaction mixture was filtered over a fine frit and thoroughly washed with CCl_4. The solvent was evaporated *in vacuo* to afford the crude product as an oil in quantitative yield.

3-bromo-2-(*tert*-butyldimethylsiloxy)-indene (27a):

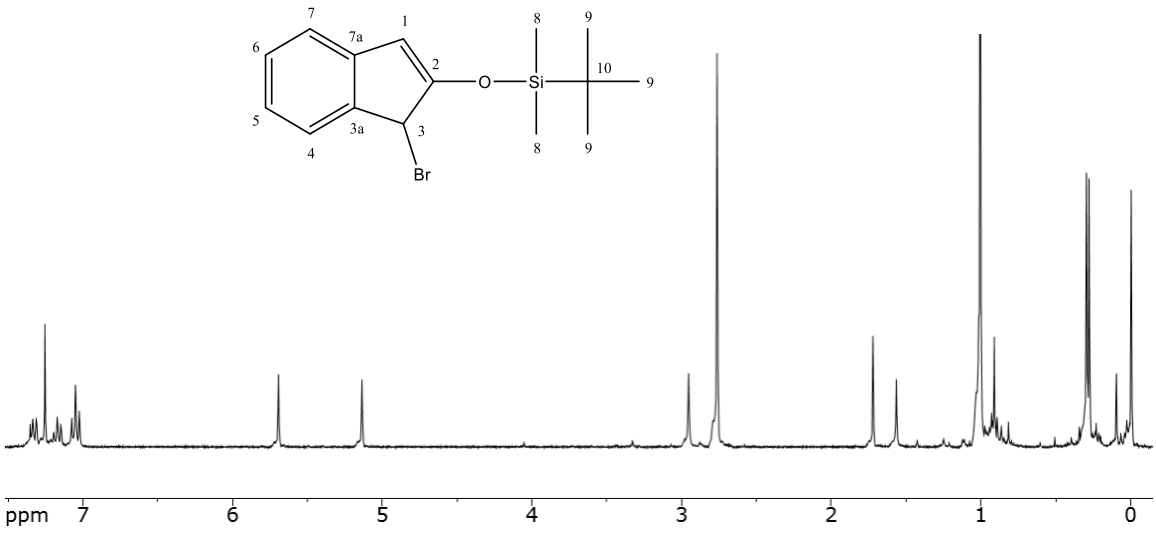

Yield: 98% $C_{15}H_{21}BrOSi$ 325.29 g mol^{-1}

^{1}H-NMR (300 MHz, $CDCl_3$): δ = 7.32 (t, 1H, H_7), 7.18 (d, 2H, $H_{5,6}$), 7.04 (t, 1H, H_4), 5.70 (s, 1H, H_1), 5.12 (s, 1H, H_3), 1.01 (s, 9H, H_9), 0.29 (s, 6H, H_8) ppm.

MS (EI, 70 eV): *m/z* (%) = 327.1 (6), 326.1 (30), 325.1 (6), 324.1 (29), 271 (8), 270 (40), 269 (71), 268 (40), 267 (65), 246.1 (16), 190.1 (10), 189.1 (45), 161.1 (6), 160.1 (16), 159.1 (10), 146 (7), 145 (48), 143 (13), 140.9 (26), 138.9 (37), 136.9 (13), 132 (5), 131 (15), 130 (50), 129.1 (57), 128.1 (20), 127.1 (6), 119 (6), 116.1 (13), 115.1 (100), 114.1 (7), 105 (5), 103 (6), 102.1 (28), 75 (11), 74.1 (5), 73.1 (51), 59 (8), 57.1 (36).

3-bromo-2-(*tert*-butyldimethylsiloxy)-5,6-difluoro-indene (27d):

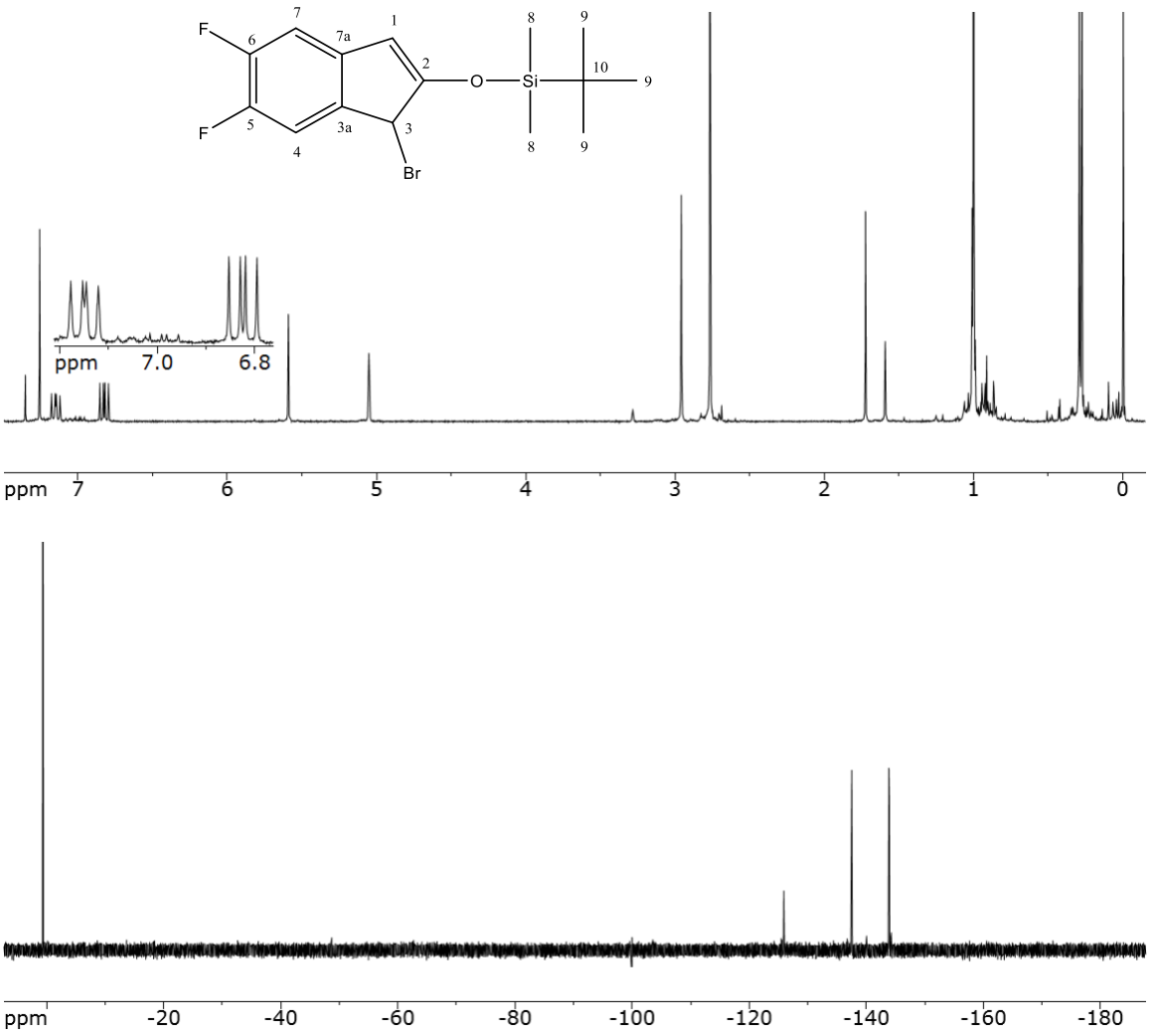

Yield: 98% $C_{15}H_{19}BrF_2OSi$ 345.28 g mol^{-1}

^{1}H-NMR (300 MHz, $CDCl_3$): δ = 7.15 (dd, 1H, H_7), 6.82 (dd, 1H, H_4), 5.59 (s, 1H, H_1), 5.06 (s, 1H, H_3), 1.00 (s, 9H, H_9), 0.28 (s, 6H, H_8) ppm.

^{19}F-NMR (283 MHz, $CDCl_3$): δ = -138.2 (m, 1F), -144.5 (M, 1F) ppm.

MS (EI, 70 eV): *m/z* (%) = 362.0 (35), 360 (34), 306 (30), 305 (84), 304 (30), 225 (26), 196 (16) 181 (42), 167 (15) 166 (67), 165 (44) 164 (19), 151 (41), 145 (23), 140.9 (22), 138.9 (54), 138 (37), 136.9 (33), 132 (17), 129 (16), 101 (18) 73.1 (100), 57.1 (71).

3-bromo-2-(*tert*-butyldimethylsiloxy)-4,7-difluoro-indene (27c):

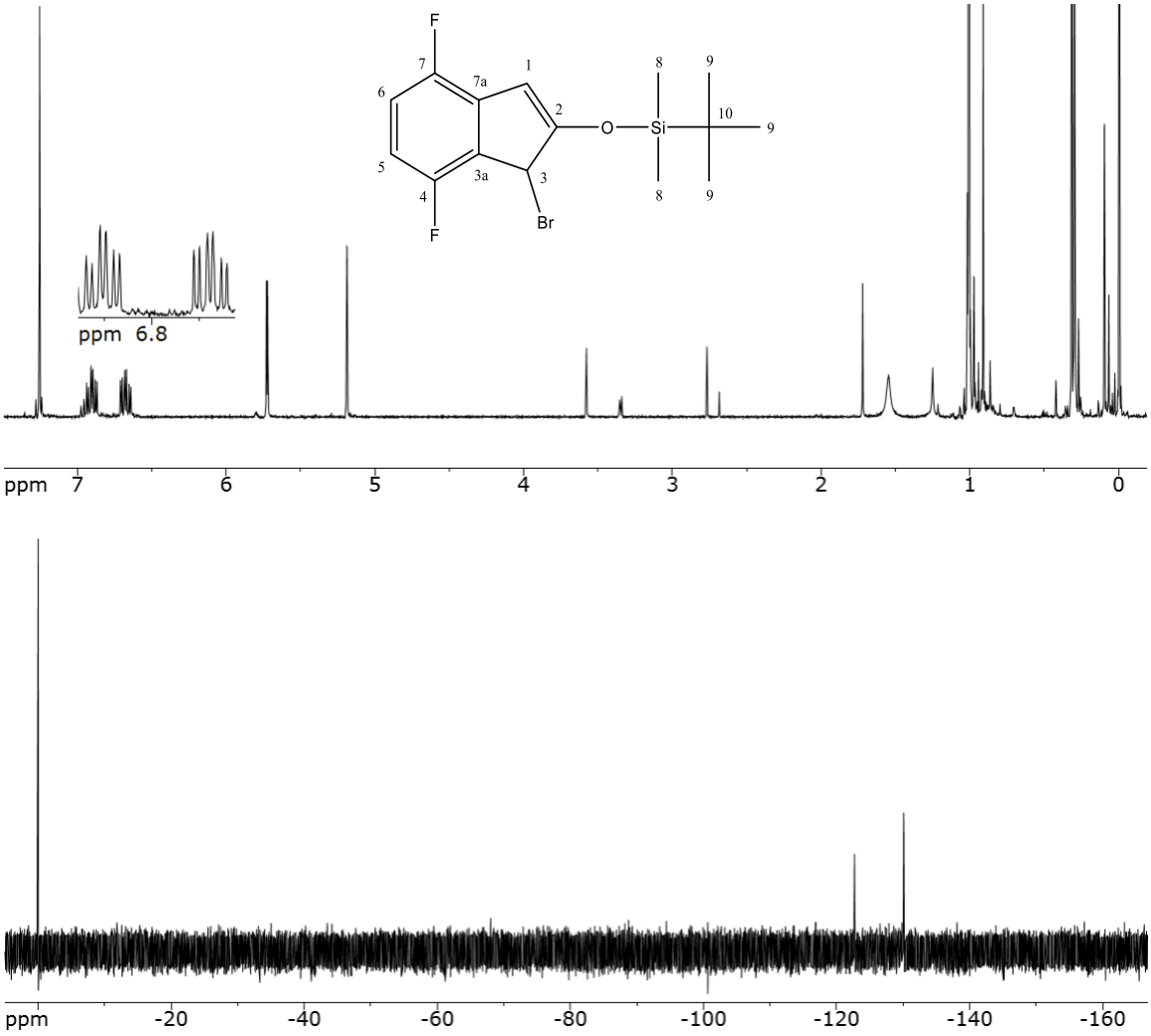

Yield: 98% $C_{15}H_{19}BrF_2OSi$ 345.28 g mol^{-1}

^{1}H-NMR (300 MHz, $CDCl_3$): δ = 6.82 (td, 1H, H_6), 6.58 (td, 1H, H_5), 5.64 (s, 1H, H_1), 5.09 (s, 1H, H_3), 1.01 (s, 9H, H_9), 0.23 (s, 6H, H_8) ppm.

^{19}F-NMR (283 MHz, $CDCl_3$): δ = -122.7 (m, 1F), -130.1 (m, 1F) ppm.

MS (EI, 70 eV): *m/z* (%) = 362 (14), 360 ($M^{\cdot+}$, 15), 305.9 (25), 305 (62), 304 (25), 302.9 (59), 283.1 (7), 282.1 (30), 227 (9), 226 (12), 225 (35), 224 (6), 209 (9), 204.9 (5), 197 (25), 196 (7), 183 (13), 181 (10), 167 (9), 166 (29), 165 (24), 164 (12), 151 (17), 150 (10),

149 (6), 147 (13), 146 (26), 145 (23), 140.9 (13), 139.9 (34), 138 (21), 136.9 (19), 134 (7), 133 (18), 132 (6), 129 (6), 128.1 (7), 127 (7), 119 (6), 116.1 (6), 115 (45), 114 (10), 112 (9), 101 (10), 99 (8), 89 (5), 81 (14), 79 (10), 77 (31), 75 (17), 74 (14), 73 (100), 59 (14), 58 (9), 57.1 (84).

3-bromo-2-(*tert*-butyldimethylsiloxy)-4,7-dimethyl-indene (27m):

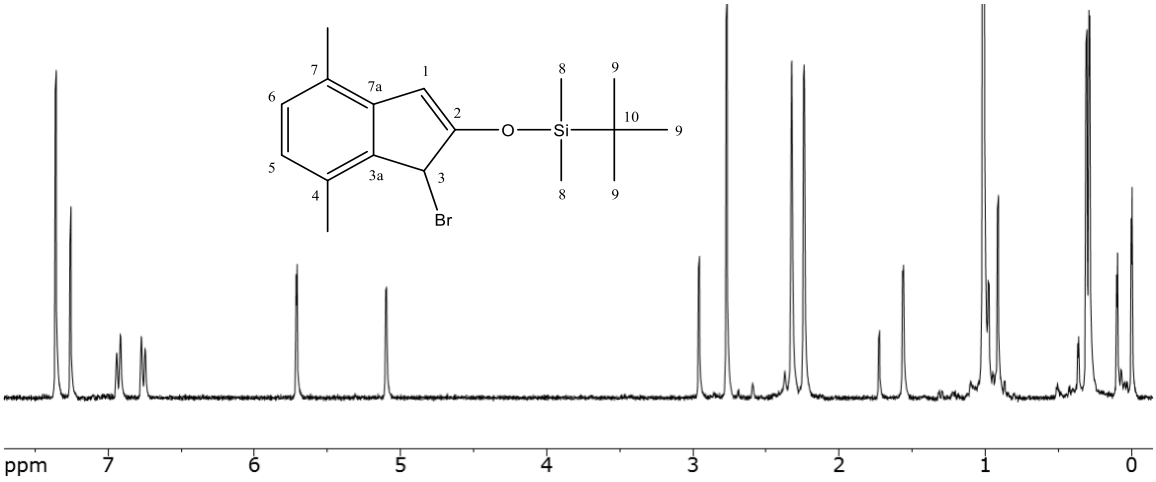

Yield: 98% $C_{17}H_{25}BrOSi$ 353.35 g mol^{-1}

^{1}H-NMR (300 MHz, $CDCl_3$): δ = 6.92 (d, 1H, H_6), 6.75 (d, 1H, H_5), 5.71 (s, 1H, H_1), 5.09 (s, 1H, H_3), 1.02 (s, 9H, H_9), 0.29 (s, 6H, H_8) ppm.

MS (EI, 70 eV): *m/z* (%) = 355.1 (5), 354.1 (24), 353.1 (6), 352.1 (23), 298 (15), 297 (36), 296 (15), 295 (34), 274.2 (9), 217.1 (13), 173.1 (19), 159.1 (7), 158.1 (26), 157.1 (20), 144.1 (13), 143.1 (100), 142.1 (9), 141 (13), 138.9 (8), 130.1 (10), 129.1 (5), 128.1 (10), 115.1 (8), 75 (9), 73.1 (20), 57.1 (9).

3-bromo-2-(*tert*-butyldimethylsiloxy)-5,6-dimethoxy-indene (27j):

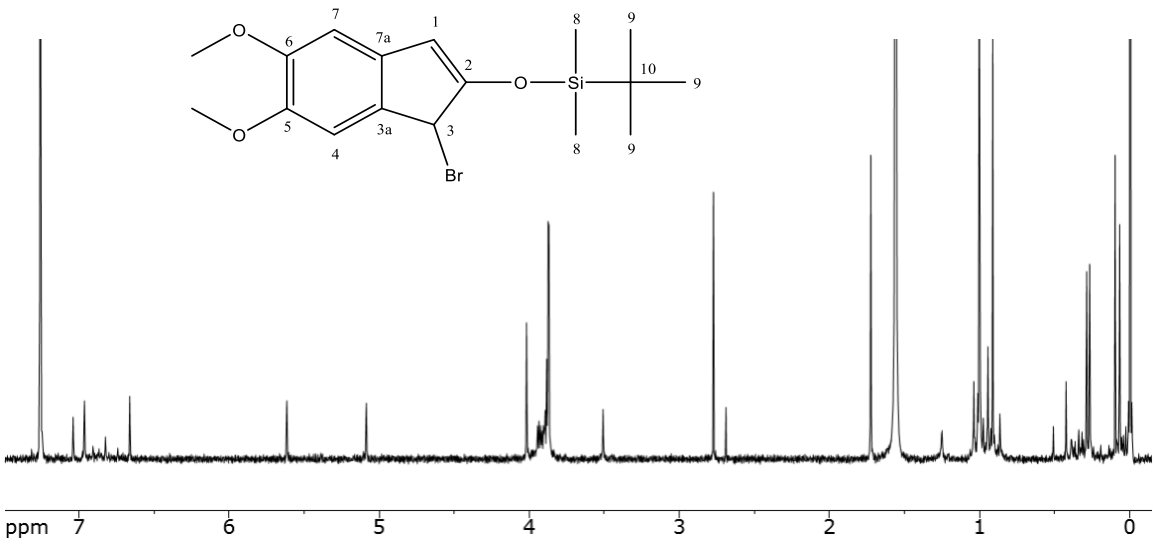

Yield: 98% $C_{17}H_{25}BrO_3Si$ 385.35 g mol^{-1}

^{1}H-NMR (300 MHz, $CDCl_3$): δ = 6.95 (s, 1H, H_4), 6.66 (s, 1H, H_7), 5.61 (s, 1H, H_1), 5.08 (s, 1H, H_3), 3.87 (s, 3H, H_{OMe}), 3.86 (s, 3H, H_{OMe}), 1.00 (s, 9H, H_9), 0.91 (s, 6H, H_8) ppm.

3-bromo-2-(*tert*-butyldimethylsiloxy)-4,7-dimethoxy-indene (27i):

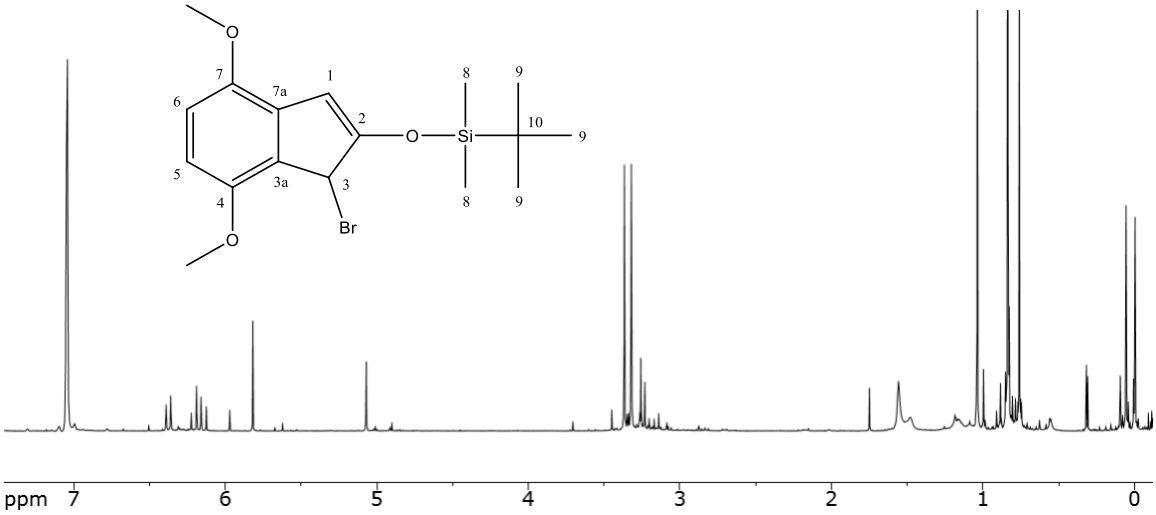

Yield: 98% $C_{17}H_{25}BrO_3Si$ 385.35 g mol^{-1}

^{1}H-NMR (300 MHz, $CDCl_3$): δ = 6.90 (d, 1H, H_6), 6.81 (d, 1H, H_5), 5.68 (s, 1H, H_1), 5.16 (s, 1H, H_3), 0.96 (s, 9H, H_9), 0.28 (s, 6H, H_8) ppm.

Isoindenone Generation and Subsequent Dimerization via Fluoride Induced Cleavage of Bromo Silyl Enol Ethers

To a vigorously stirred suspension of CsF (3.32 mmol) in 250 mL degassed CH_3CN at reflux was slowly added a solution of the combined corresponding bromo silyl enol ethers (3.02 mmol) in 20 mL CH_3CN via syringe pump. After complete addition, the mixture was stirred at reflux for an additional 1 h. The solvent was evaporated *in vacuo* and the crude was suspended in H_2O and extracted with methylene chloride. The combined organic phase was dried over anhydrous $MgSO_4$ and the solvent was evaporated *in vacuo* to afford the crude product as a brown sticky solid.

4,7,12,15-tetrafluoropentacyclo[8.6.1.1^{2,9}.0^{3,8}.0^{11,16}]octadeca-3,5,7,11,13,15-hexaene-17,18-dione (14c):

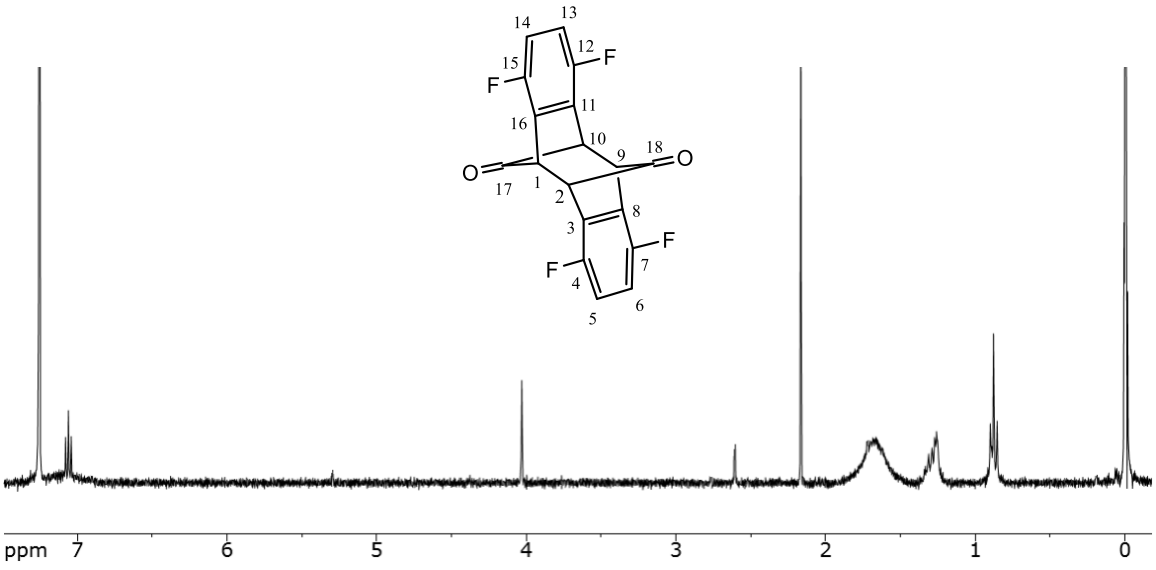

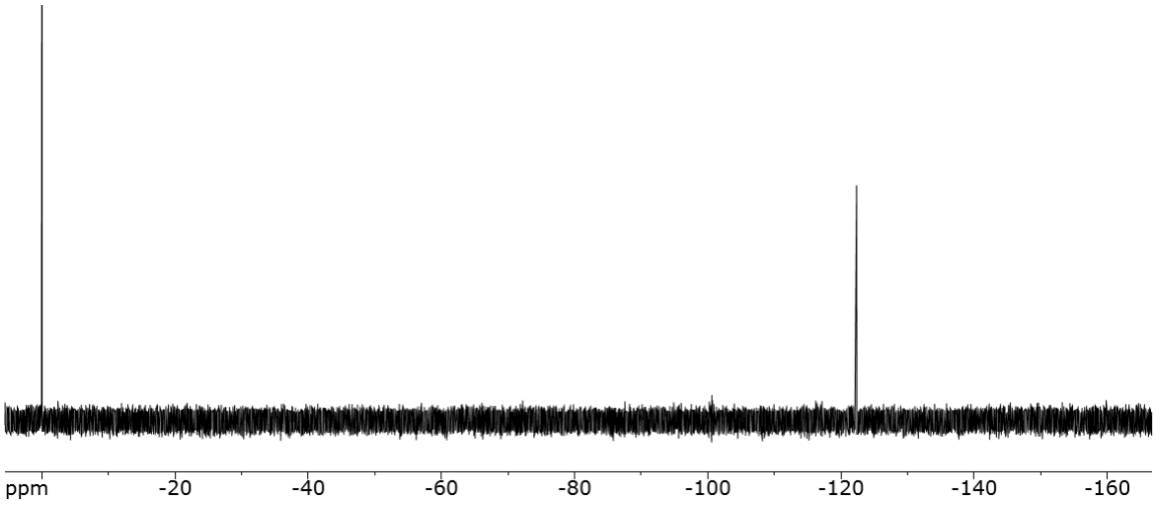

Yield: 45% $C_{18}H_8F_4O_2$ 332.24 g mol^{-1}

^{1}H-NMR (300 MHz, $CDCl_3$): δ = 7.03 (t, 4H, $H_{4,7,12,15}$), 4.02 (s, 4H, $H_{1,2,9,10}$) ppm.

^{19}F-NMR (283 MHz, $CDCl_3$): δ = -122.3 (t_{app}, 4F) ppm.

MS (EI, 70 eV): *m/z* (%) = 332 (5), 312 (5), 305 (8), 304 (42), 303 (13), 277 (19), 276 (100), 275 (86), 274 (45), 258 (6), 257 (38), 256 (43), 255 (7), 254 (10), 250 (8), 243 (5), 236 (6), 225 (5), 152 (6), 138 (27), 137 (23), 128 (27), 127 (6), 125 (9), 118 (7), 112 (7), 87 (5), 81 (6), 74 (5), 57 (5).

5,6-difluoropentacyclo[8.6.1.1^{2,9}.0^{3,8}.0^{11,16}]octadeca-3,5,7,11,13,15-hexaene-17,18-dione (14t):

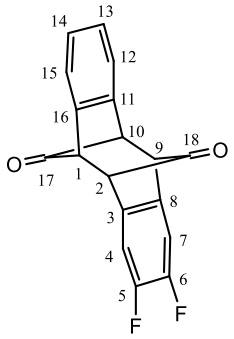

Yield: 30% $C_{18}H_{10}F_2O_2$ 296.26 g mol^{-1}

^{1}H-NMR (300 MHz, $CDCl_3$): δ = 7.49-7.45 (m, 2H, $H_{4,7}$), 7.37-7.32 (m, 4H, $H_{12,13,14,15}$), 3.72 (s_{app}, 2H, $H_{2,9}$), 3.70 (s_{app}, 2H, $H_{1,10}$) ppm.

^{19}F-NMR (283 MHz, $CDCl_3$): δ = -135.7 (t_{app}, 2F) ppm.

MS (EI, 70 eV): *m/z* (%) = 297 ($M^{\cdot+}$, 5), 296 (16), 281 (9), 268.9 (7), 268 (31, -CO), 267 (31), 251 (7), 241 (17), 240.1 (97, -CO), 239.1 (100), 238.1 (63), 236.9 (6), 236 (8), 221 (19), 220 (17), 219 (7), 218 (8), 208 (7), 207 (27), 137.9 (6), 119.1 (33), 110 (15), 109 (6), 106.9 (9), 106 (6), 102 (10), 96.2 (5), 94.2 (11), 76 (6), 73.9 (5), 63 (5).

4,7-dimethylpentacyclo[8.6.1.1^{2,9}.0^{3,8}.0^{11,16}]octadeca-3,5,7,11,13,15-hexaene-17,18-dione (14o):

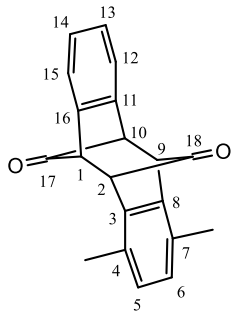

Yield: 35% $C_{20}H_{16}O_2$ 288.32 g mol^{-1}

^{1}H-NMR (300 MHz, $CDCl_3$): δ = 7.48-7.43 (m, 2H, $H_{12,15}$), 7.35-7.31 (m, 2H, $H_{13,14}$), 7.03 (s, 2H, $H_{5,6}$), 3.79 (s_{app}, 2H, $H_{2,9}$), 3.75 (s, 6H, H_{Me}), 3.71 (s_{app}, 2H, $H_{1,10}$) ppm.

MS (EI, 70 eV): *m/z* (%) = 289.1 ($M^{\cdot+}$, 10), 288.1 (44), 260.1 (17, -CO), 259.1 (10), 246.1 (7), 245.1 (32), 233.1 (20), 232.1 (100, -CO), 231.1 (5), 218.1 (18), 217.1 (95), 216.1 (26), 215.1 (46), 203.1 (13), 202.1 (50), 189 (9), 130 (10), 128 (8), 116 (9), 115 (15), 114.1 (6), 107.7 (21), 101.9 (8), 101 (22), 94.5 (9), 89 (5), 63 (5).

4,7-dimethoxypentacyclo[8.6.1.1^{2,9}.0^{3,8}.0^{11,16}]octadeca-3,5,7,11,13,15-hexaene-17,18-dione (14p):

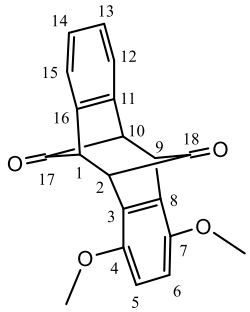

Yield: 60% $C_{20}H_{16}O_4$ 320.32 g mol^{-1}

^{1}H-NMR (300 MHz, $CDCl_3$): δ = 7.45-7.38 (m, 2H, $H_{12,15}$), 7.35-7.29 (m, 2H, $H_{13,14}$), 6.75 (s, 2H, $H_{5,6}$), 3.93 (s_{app}, 2H, $H_{2,9}$), 3.75 (s, 6H, H_{OMe}), 3.65 (s_{app}, 2H, $H_{1,10}$) ppm.

MS (EI, 70 eV): *m/z* (%) = 321.1 ($M^{\cdot+}$, 9), 320.1 (41), 292.1 (23, -CO), 277.1 (25), 265.1 (20), 264.1 (100, -CO), 263.1 (7), 262.1 (9), 261.1 (15), 250.1 (10), 249.1 (57), 234.1 (20), 233.1 (45), 221.1 (11), 219.1 (6), 218.1 (14), 206.1 (10), 205.1 (11), 202.1 (6), 190.1 (14), 189.1 (24), 178.1 (18), 177.1 (8), 176.1 (13), 175 (7), 152.1 (17), 151.1 (10), 150.1 (5), 132.1 (9), 124.5 (6), 117 (6), 103 (6), 102.1 (5), 94.5 (7), 89 (10), 88 (6), 76 (14), 63 (5).

4,7-dimethoxy-12,15-dimethylpentacyclo[8.6.1.1^{2,9}.0^{3,8}.0^{11,16}]octadeca-3,5,7,11,13,15-hexaene-17,18-dione (14q):

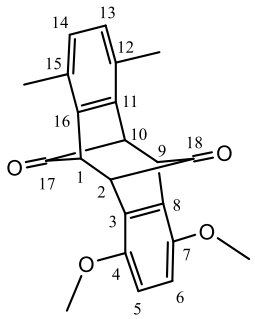

Yield: 45% $C_{22}H_{20}O_4$ 348.38 g mol^{-1}

^{1}H-NMR (300 MHz, $CDCl_3$): δ = 7.01 (s, 2H, $H_{13,14}$), 6.76 (s, 2H, $H_{5,6}$), 3.90 (s_{app}, 2H, $H_{2,9}$), 3.82 (s, 6H, H_{OMe}), 3.74 (s_{app}, 2H, $H_{1,10}$), 2.48 (s, 6H, H_{Me}) ppm.

MS (EI, 70 eV): *m/z* (%) = 349.1 ($M^{\cdot+}$, 13), 348.1 (42), 320.1 (16, -CO), 306.1 (5), 305.1 (16), 293.1 (23), 292.1 (100, -CO), 291.1 (5), 290.1 (6), 289.1 (11), 278.1 (13), 277.1 (65), 262.1 (19), 261.1 (26), 249.1 (5), 247.1 (11), 246 (9), 219.1 (10), 203.1 (6), 202 (9), 191 (7), 190.1 (13), 189 (12), 175 (10), 165 (7),152.1 (5), 146.1 (10), 145 (8), 138.7 (6), 130.1 (9), 128 (6), 117 (6), 115 (7), 101 (7), 94.7 (7), 89 (8), 76 (5).

7.2.4. Toward Dibenzo[b,e]fulvalenes

General Procedure for McMurry Reaction of 2-Indanone Derivatives

To THF (20 mL) at 0 °C was added titanium tetrachloride (6.65 mmol) dropwise to afford a canary yellow solution. Under argon was added Zn dust (16.1 mmol) portionwise. After stirring 30 min at 0 °C, pyridine (0.64 mL) was added. A solution of 2-indanone (6.24 mmol) in THF (2 mL) was added dropwise and stirred at 90 °C overnight. The reaction was cooled to room temperature then carefully quenched with 10% potassium carbonate, filtered over Celite, and extracted with diethyl ether. The combined organic phase was washed with 5% HCl, dried over anhydrous $MgSO_4$ and the solvent was evaporated *in vacuo* to afford the crude product as a sticky solid.

General Procedure for Targeted Pinacol Coupling of 2-Indanone Derivatives

To a Schlenk flask is added mercuric chloride (0.615 mmol), magnesium powder (23.0 mmol), and THF (12 mL) and the mixture was allowed to stir at room temperature. After 15 min, the supernatant was removed and the resulting amalgam was washed three times with THF. To a suspension of the amalgam in THF (20 mL) at -10 °C was added titanium tetrachloride (6.59 mmol) dropwise. A solution of 2-indanone (7.57 mmol) in THF (20 mL) was added dropwise and stirred at room temperature. After stirring 20.5 h, the reaction was quenched with 10 % potassium carbonate and allowed to stir 30 min. The mixture was diluted with diethyl ether, filtered over Celite, and extracted with diethyl ether. The combined organic phase was washed with Brine, dried over anhydrous $MgSO_4$ and the solvent evaporated *in vacuo* to afford the crude product as a sticky solid.

1H,1'H,2H,2'H,3H,3'H-[2,2'-biindene]-2,2'-diol (71a):

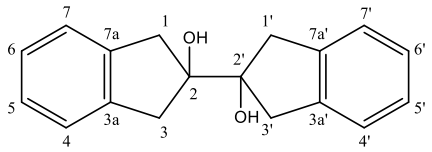

Yield: 70% $C_{18}H_{18}O_2$ 266.32 g mol^{-1}

^{1}H-NMR (300 MHz, $CDCl_3$): δ = 7.52 (m, 8H), 3.38 (d, 4H, $H_{1,3'}$), 3.04 (d, 4H, $H_{1',3}$) ppm.

MS (EI, 70 eV): *m/z* (%) = 266 (5), 248 (7), 230 (5), 143 (17), 134 (26), 133 (60), 132 (100), 131 (10), 116 (22), 115 (22), 106 (9), 105 (32), 104 (23), 103 (16), 79 (8), 78 (9), 77 (13).

4,4',7,7'-tetramethyl-1H,1'H,2H,2'H,3H,3'H-[2,2'-biindene]-2,2'-diol (71b):

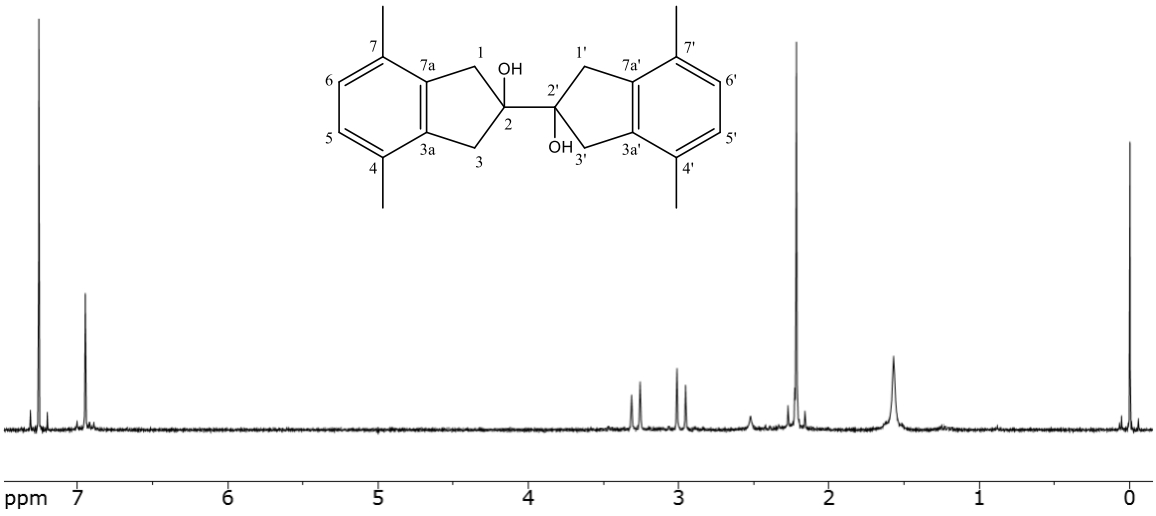

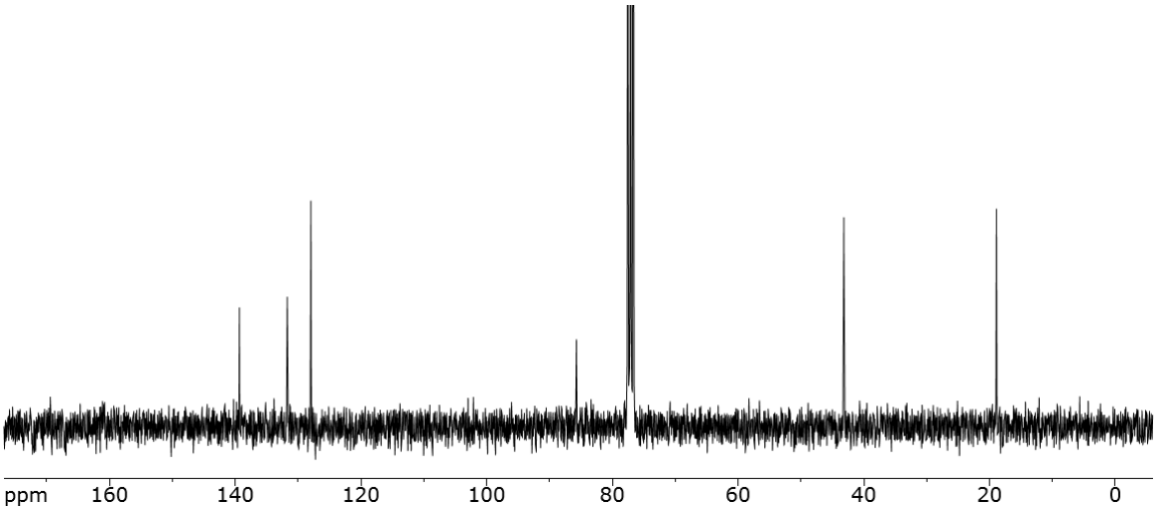

Yield: 80% $C_{22}H_{26}O_2$ 322.42 g mol^{-1}

^{1}H-NMR (300 MHz, $CDCl_3$): δ = 6.95 (s, 4H, $H_{5,5',6,6'}$), 3.28 (d, 4H, $H_{1,3'}$), 2.98 (d, 4H, $H_{1',3}$), 2.21 (s, 12H, H_{Me}) ppm.

^{13}C NMR (75 MHz, $CDCl_3$): δ = 139.3 ($C_{4,7}$), 131.7 ($C_{3a,7a}$), 127.9 ($C_{5,6}$), 85.7 ($C_{2,2'}$), 43.1 ($C_{1,1',3,3'}$), 18.9 (C_{Me}) ppm.

IR (AT-IR): ṽ = 3528, 3443, 3037, 3013, 2918, 2864, 1702, 1607, 1537, 1496, 1449, 1377, 1300,1276, 1266, 1253, 1221, 1208, 1191, 1153, 1043, 1021, 958, 949, 908, 841, 814, 729, 699, 677, 643, 617 cm^{-1}.

MS (EI, 70 eV): *m/z* (%) = 322 (6), 304 (11), 286 (9), 172 (5), 171 (38), 162 (34), 161 (50), 160 (100), 147 (5), 146 (13), 145 (17), 144 (23), 143 (12), 134 (7), 133 (27), 132 (30), 131 (16), 129 (11), 128 (13), 127 (6), 119 (19), 117 (23), 116 (6), 115 (20), 105 (5), 91 (12), 77 (5).

4,4',7,7'-tetramethoxy-1H,1'H,2H,2'H,3H,3'H-[2,2'-biindene]-2,2'-diol (71c):

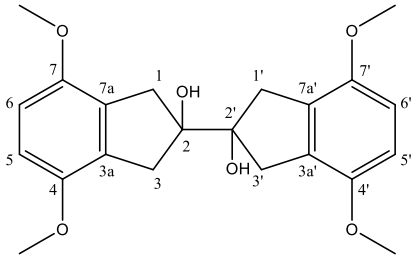

Yield: 55% $C_{22}H_{26}O_6$ 386.42 g mol^{-1}

^{1}H-NMR (300 MHz, $CDCl_3$): δ = 6.63 (s, 4H, $H_{5,5',6,6'}$), 3.75 (s, 12H, H_{OMe}), 3.28 (d, 4H, $H_{1,3'}$), 2.99 (d, 4H, $H_{1',3}$) ppm.

MS (EI, 70 eV): *m/z* (%) = 387 (22), 386 (94), 368 (10), 217 (5), 203 (30), 195 (7), 194 (53), 193 (68), 192 (100), 179 (9), 178 (14), 177 (31), 176 (28), 175 (6), 166 (23), 165 (27), 164 (24), 163 (21), 162 (24), 161 (14), 151 (20), 150 (5), 149 (19), 147 (9), 135 (8), 134 (8), 133 (10), 121 (12), 119 (6), 118 (5), 107 (6), 105 (7), 103 (5), 91 (16), 79 (5), 78 (5), 77 (12).

1H,1'H,3H,3'H-2,2'-biindenylidene (70a):

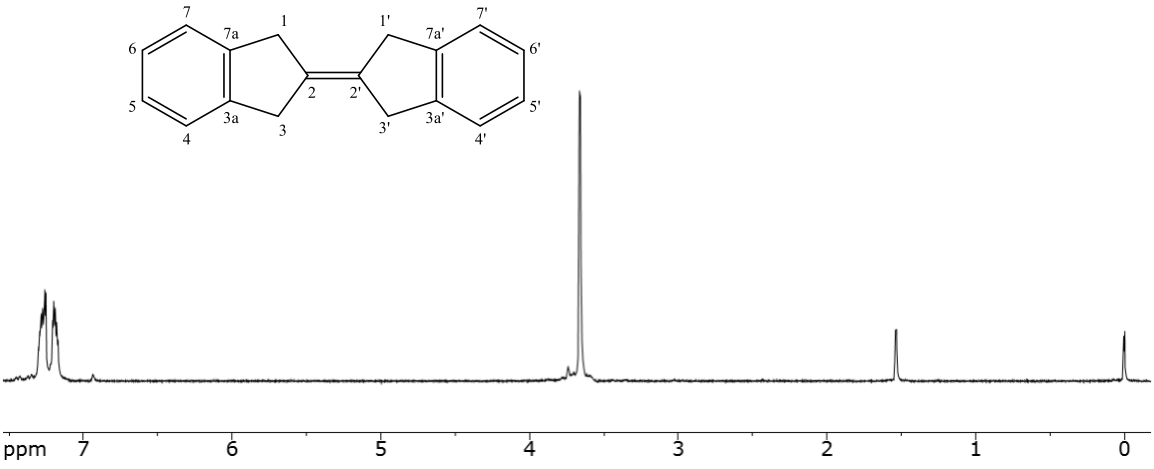

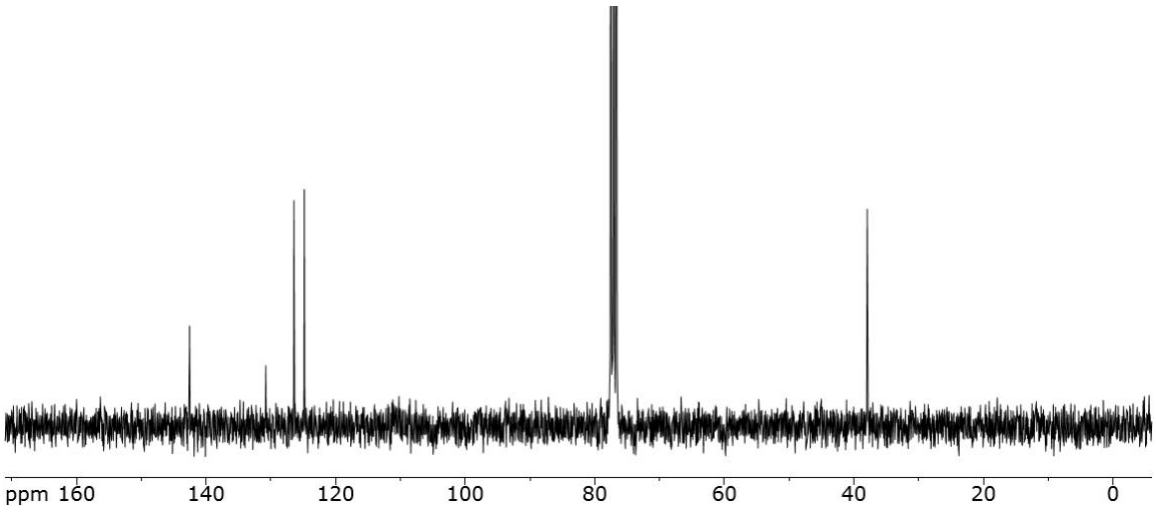

Yield: 25% $C_{18}H_{16}$ 232.30 g mol^{-1}

^{1}H-NMR (300 MHz, $CDCl_3$): δ = 7.35-7.10 (m, 8H, H), 3.66 (s, 8H, $H_{1,1',3,3'}$) ppm.

^{13}C NMR (75 MHz, $CDCl_3$): δ = 142.5 ($C_{4,7}$), 130.7 ($C_{2,2'}$), 126.4 ($C_{5,6}$), 124.8 ($C_{3a,7a}$), 37.9 ($C_{1,1',3,3'}$) ppm.

IR (AT-IR): ṽ = 3073, 3039, 3019, 2870, 2813, 1583, 1483, 1458, 1434, 1413, 1389, 1353, 1316, 1301, 1263, 1207, 1150, 1124, 1085, 1024, 960, 941, 913, 854, 836, 822, 735, 717, 695 cm^{-1}.

MS (EI, 70 eV): *m/z* (%) = 233 (14), 232 (73), 231 (10), 229 (5), 228 (8), 226 (7), 218 (5), 217 (27), 216 (13), 215 (26), 203 (5), 202 (14), 141 (6), 128 (5), 117 (25), 116 (100), 115 (49), 114 (5), 104 (20), 101 (6), 89 (5).

4,4',7,7'-tetramethyl-1H,1'H,3H,3'H-2,2'-biindenylidene (70b):

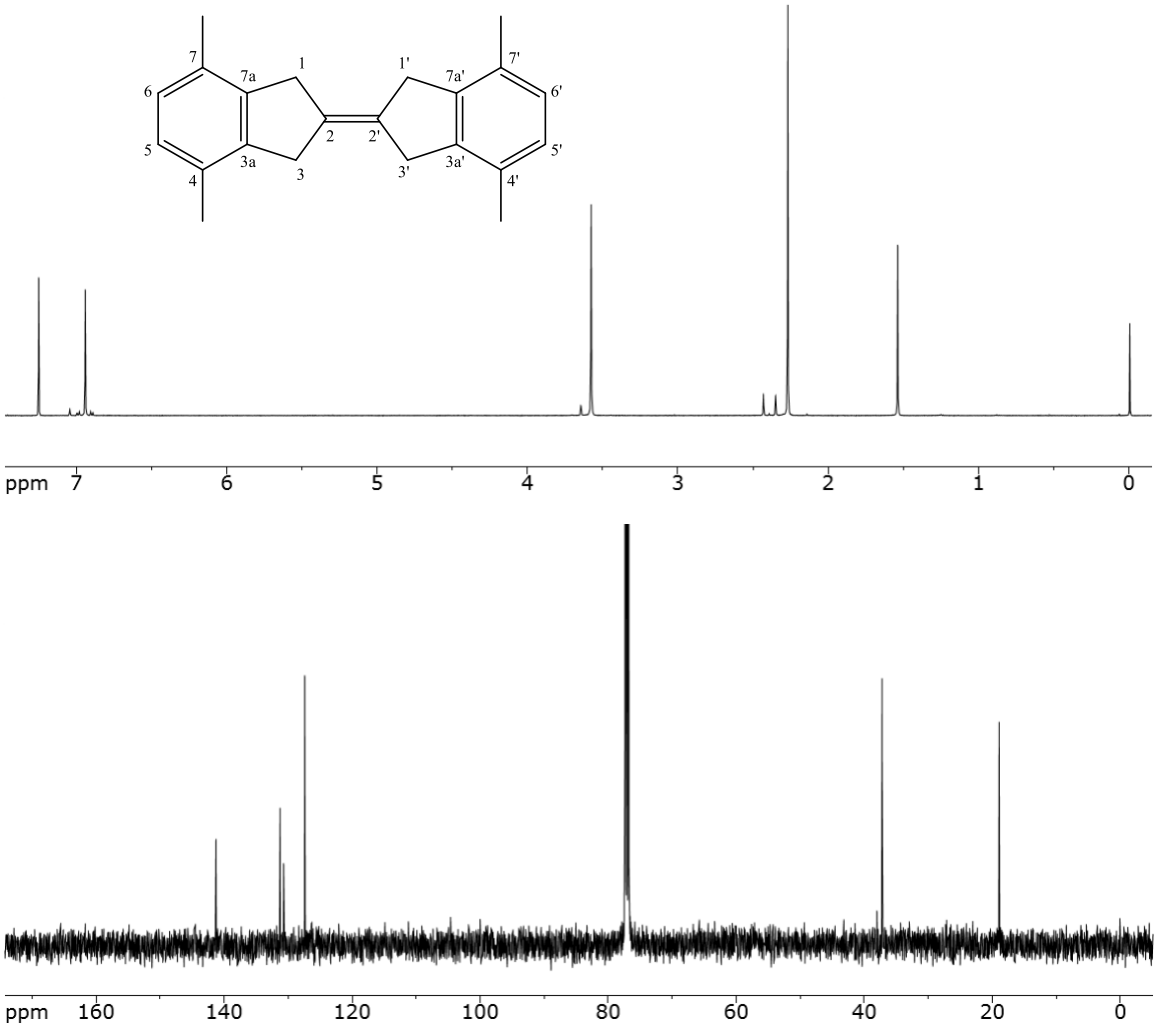

Yield: 10% $C_{22}H_{24}$ 288.41 g mol^{-1}

^{1}H-NMR (300 MHz, $CDCl_3$): δ = 6.94 (s, 4H, $H_{5,5',6,6'}$), 3.57 (s, 8H, $H_{1,1',3,3'}$), 2.27 (s, 12H, H_{Me}) ppm.

^{13}C NMR (75 MHz, $CDCl_3$): δ = 141.2 (4C, $C_{4,7}$), 131.2 (4C, $C_{5,6}$), 130.6 ($C_{2,2'}$), 127.4 ($C_{3a,7a}$), 37.2 (4C, $C_{1,1',3,3'}$), 18.9 (C_{Me}) ppm.

IR (AT-IR): ṽ = 3039, 3011, 2959, 2913, 2879, 2857, 2804, 2729, 1874, 1607, 1593, 1531, 1497, 1455, 1437, 1404, 1376, 1320, 1268, 1251, 1159, 1050, 1034, 937, 829, 803, 730, 703 cm^{-1}.

MS (EI, 70 eV): *m/z* (%) = 289 (10), 288 (43), 273 (6), 243 (5), 145 (29), 144 (100), 143 (12), 132 (5), 130 (7), 129 (32), 128 (19), 127 (6), 115 (6).

4,4',7,7'-tetramethoxy-1H,1'H,3H,3'H-2,2'-biindenylidene (70c):

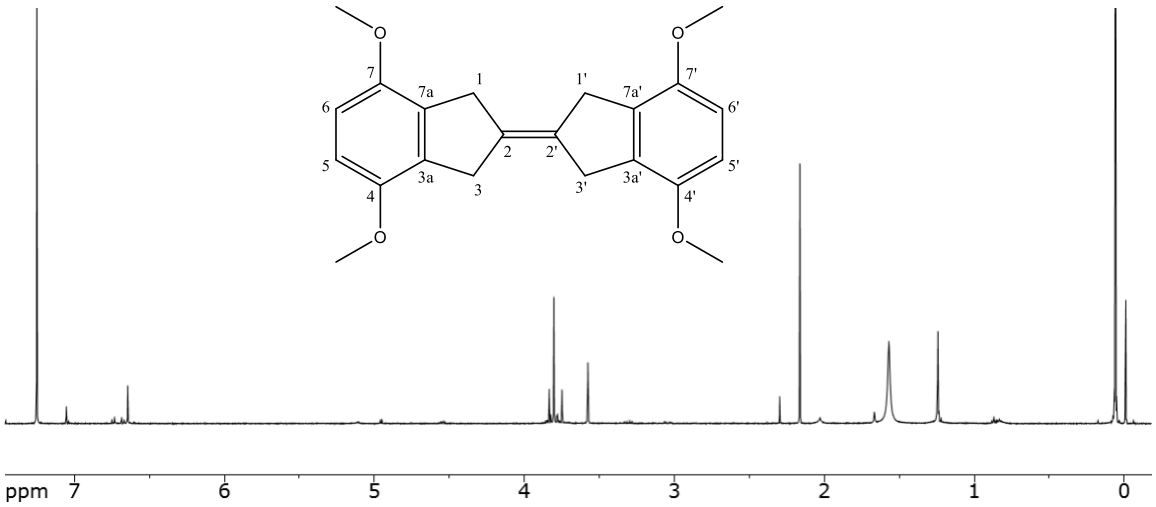

Yield: 15% $C_{22}H_{24}O_4$ 352.41 g mol^{-1}

^{1}H-NMR (300 MHz, $CDCl_3$): δ = 6.64 (s, 4H, $H_{5,5',6,6'}$), 3.80 (s, 12H, H_{OMe}), 3.57 (s, 8H, $H_{1,1',3,3'}$) ppm.

IR (AT-IR): ṽ = 3003, 2960, 2918, 2849, 2833, 1608, 1495, 1457, 1438, 1385, 1360, 1346, 1331, 1313, 1296, 1254, 1239, 1185, 1141, 1086, 1060, 1030, 1014, 978, 967, 881, 833, 789, 784, 709 cm^{-1}.

MS (EI, 70 eV): *m/z* (%) = 353 (16), 352 (78), 351 (5), 350 (10), 321 (12), 281 (17), 209 (5), 208 (7), 207 (36), 203 (5), 193 (6), 192 (8), 191 (6), 189 (6), 178 (6), 177 (32), 176 (100), 175 (18), 165 (6), 164(, 9), 163 (6), 162 (7), 161 (32), 149 (9), 147 (7), 146 (5), 145 (9), 133 (14), 132 (6), 131 (5), 121 (5), 118 (5), 115 (7), 91 (6), 89 (5), 73 (5).

General Procedure for PTSA Catalyzed Elimination of Pinacol Derivatives

To a solution of pinacol (2.48 mmol) in 55 mL benzene was added a catalytic amount of PTSA, the solution was heated to 100 °C, fitted with a dean stark trap and reflux condenser. The reaction was stirred vigorously and progress was monitored by ^{1}H NMR, the combined solution from the reaction flask and the dean stark trap was washed with saturated sodium bicarbonate. The organic phase was dried over anhydrous $MgSO_4$. The solvent was evaporated *in vacuo* to afford the crude product as a tan solid. Trituration with acetone afforded the clean product as a beige crystalline solid.

4,4',7,7'-tetramethyl-1H,1'H-2,2'-biindene (15b):

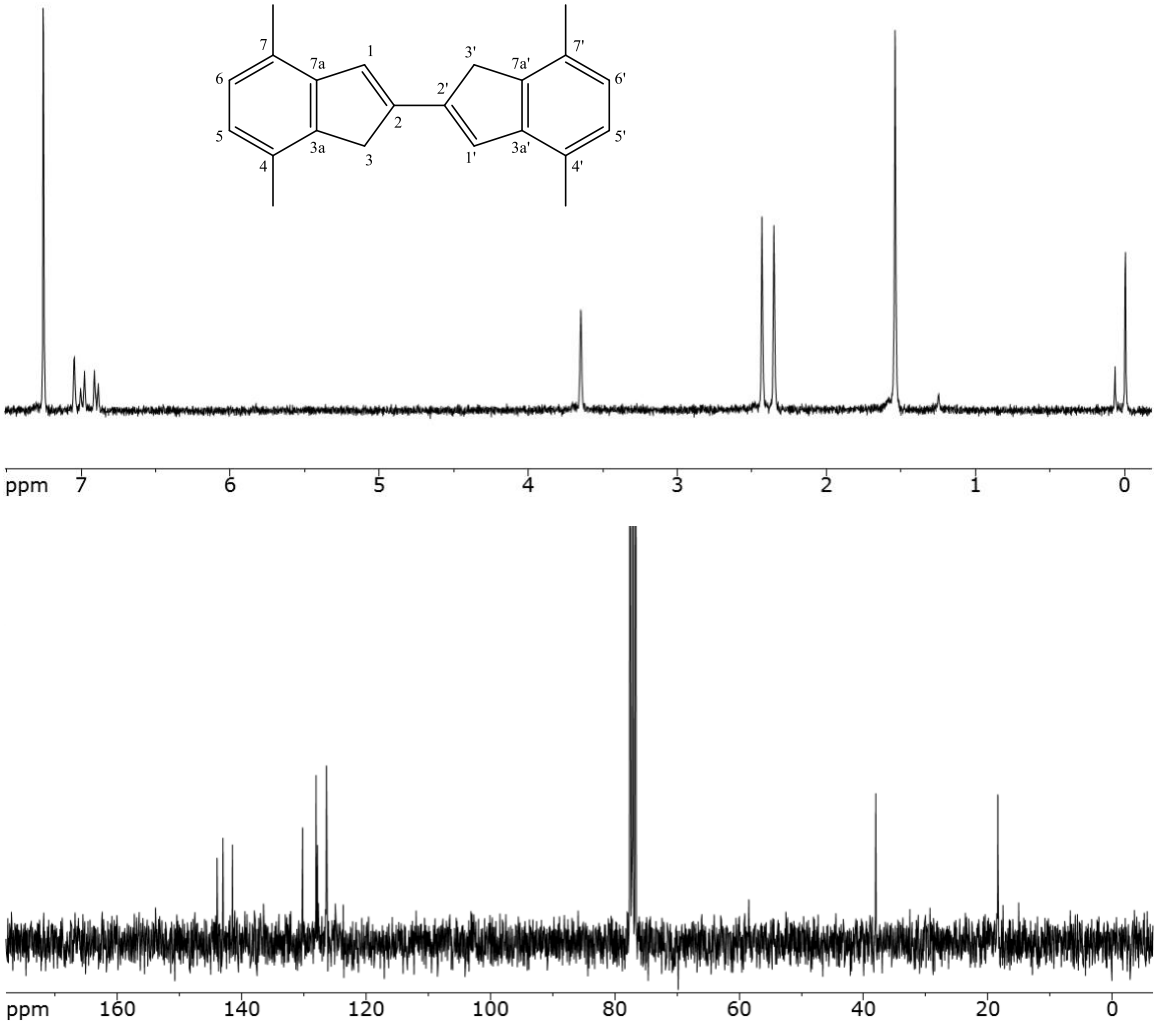

Yield: 50% $C_{22}H_{22}$ 286.39 g mol^{-1}

^{1}H-NMR (300 MHz, $CDCl_3$): δ = 7.05 (s, 2H, $H_{1,1'}$), 6.99 (d, 2H, $H_{6,6'}$), 6.90 (d, 2H, $H_{5,5'}$), 3.65 (s, 4H, $H_{3,3'}$), 2.43 (s, 6H, H_{Me}), 2.35 (s, 6H, H_{Me}) ppm.

^{13}C NMR (75 MHz, $CDCl_3$): δ = 143.9 (2C, $C_{x,x}$), 143.0 (2C, $C_{x,x}$), 141.4 (2C, $C_{x,x}$), 130.2 (2C, $C_{x,x}$), 128.0 (2C, $C_{x,x}$), 127.8 (2C, $C_{x,x}$), 126.4 (2C, $C_{x,x}$), 126.3 (2C, $C_{x,x}$), 38.0 (2C, $C_{x,x}$), 18.5 (2C, $C_{x,x}$), 18.4 (2C, $C_{x,x}$) ppm.

IR (AT-IR): $\tilde{\nu}$ = 3043, 3010, 2969, 2913, 2857, 1693, 1591, 1530, 1486, 1437, 1373, 1262, 1250, 1032, 978, 914, 830, 802, 732, 612 cm^{-1}.

MS (EI, 70 eV): *m/z* (%) = 287 (25), 286 (100), 271 (14), 256 (13), 255 (7), 253 (5), 252 (5), 241 (5), 240 (6), 239 (11), 144 (11), 143 (91), 142 (6), 141 (5), 128 (25), 127 (8), 126 (8), 120 (7).

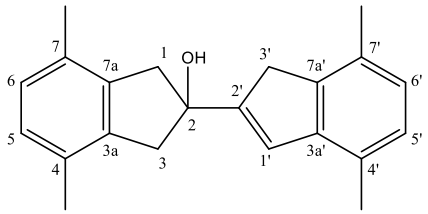

4,4',7,7'-tetramethyl-2,3-dihydro-1H,1'H-[2,2'-biinden]-2-ol:

Yield: 25% $C_{22}H_{24}O$ 304.41 g mol^{-1}

^{1}H-NMR (300 MHz, $CDCl_3$): Product was characterized by GC-MS as proton NMR showed significant amounts of impurities.

MS (EI, 70 eV): *m/z* (%) = 305 (6), 304 (25), 172 (12), 171 (100), 161 (6), 144 (20), 133 (5), 129 (8), 128 (9), 117 (7), 115 (8), 91 (5).

4,4',7,7'-tetramethoxy-1H,1'H-2,2'-biindene (15c):

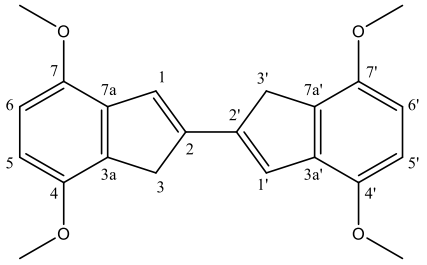

Yield: 25% $C_{22}H_{22}O_4$ 350.39 g mol^{-1}

^{1}H-NMR (300 MHz, $CDCl_3$): δ = 7.05 (s, 2H, $H_{1,1'}$), 6.74 (d, 2H, $H_{6,6'}$), 6.66 (d, 2H, $H_{5,5'}$), 3.83 (s, 6H, H_{OMe}), 3.75 (s, 6H, H_{OMe}), 3.58 (s, 4H, $H_{3,3'}$) ppm; signal assignment was extracted from NMR of the crude material.

General Procedure for Bromohydrin Derivatives

To a solution of the corresponding indene (6.93 mmol) in 10 mL DMSO and 0.33 mL H_2O cooled to 0 °C was added NBS (13.8 mmol) all at once. After stirring at 0 °C 10 min, the reaction was warmed to room temperature and stirred an additional 30 min. To the reaction was added 20 mL saturated sodium bicarbonate to facilitate precipitation and the clean product was collected by suction filtration as a yellow solid.

Note: For the fluorinated derivative the product did not precipitate upon the addition of sodium bicarbonate. The mixture was acidified with 1 M HCl and extracted with methylene chloride. The combined organic phase was washed thoroughly with water and dried over anhydrous MgSO4. The solvent was evaporated *in vacuo* to afford clean product as a brown oil.

2-bromo-4,7-dimethyl-2,3-dihydro-1H-inden-1-ol (74m):

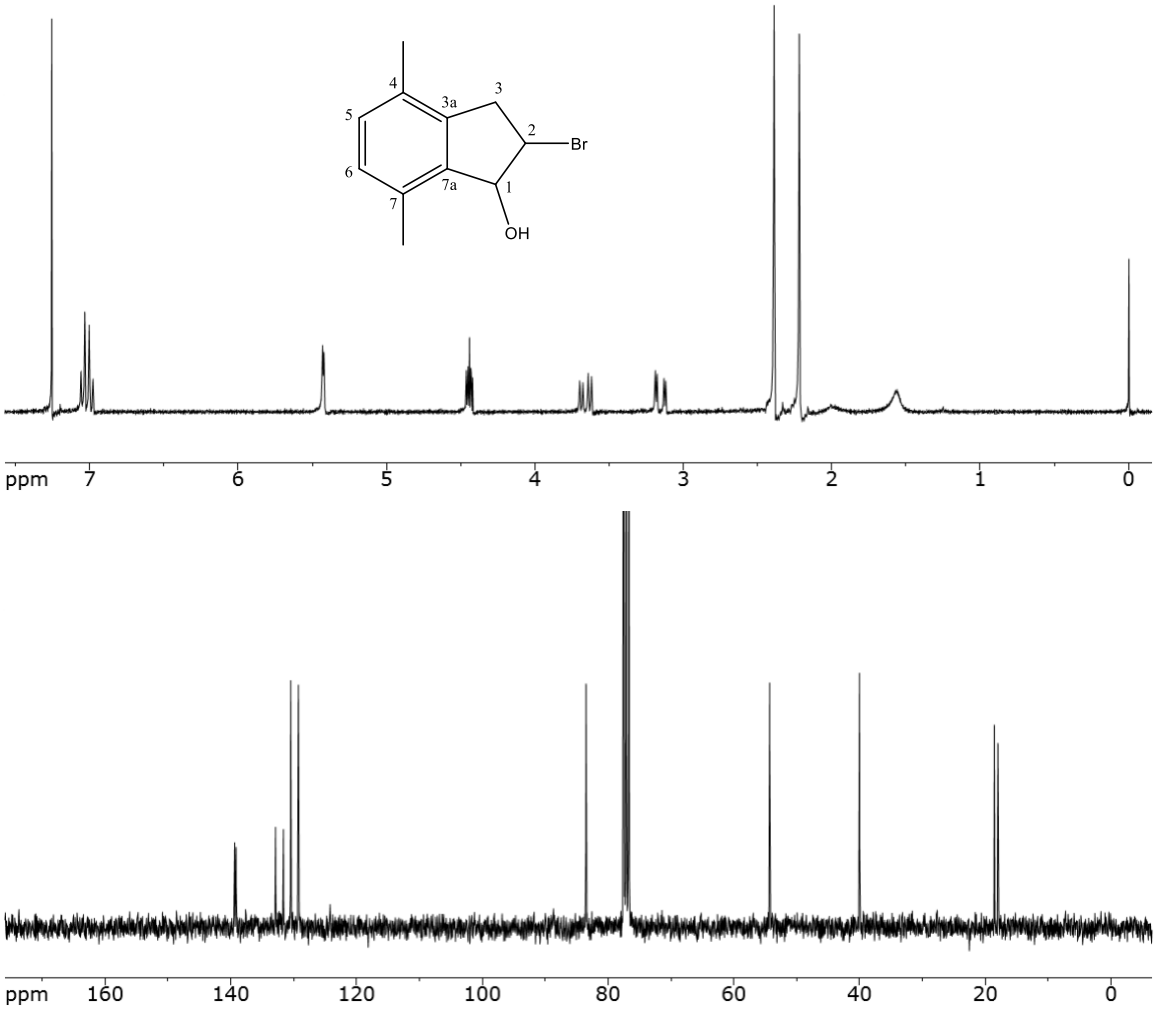

Yield: 87% $C_{11}H_{13}BrO$ 241.11 g mol^{-1}

^{1}H-NMR (300 MHz, $CDCl_3$): δ = 7.15 (d, 1H, H_6), 6.99 (d, 1H, H_5), 5.42 (d, 1H, H_1), 4.44 (m, 1H, H_2), 3.65 (dd, 1H, H_3)*, 3.16 (dd, 1H, H_3)*, 2.39 (s, 3H, H_{Me}), 2.25 (s, 3H, H_{Me}) ppm.

^{13}C NMR (75 MHz, $CDCl_3$): δ = 139.3 (1C), 139.1 (1C), 132.8 (1C), 131.6 (1C), 130.4 (1C), 129.2 (1C), 83.5 (1C), 54.3 (1C), 40.0 (1C), 18.5 (1C), 17.9 (1C) ppm.

MS (EI, 70 eV): *m/z* (%) = 243 (5), 242 (29), 241 (6), 240 (30), 162 (11), 161 (100), 160 (26), 159 (8), 146 (13), 145 (30), 144 (24), 143 (85), 141 (6), 131 (12), 129 (21), 128 (30), 127 (10), 119 (6), 117 (9), 116 (10), 115 (32), 105 (8), 103 (6), 91 (16), 79 (8), 77 (10), 65 (5), 63 (6), 55 (47), 51 (7).

2-bromo-4,7-difluoro-2,3-dihydro-1H-inden-1-ol (74c):

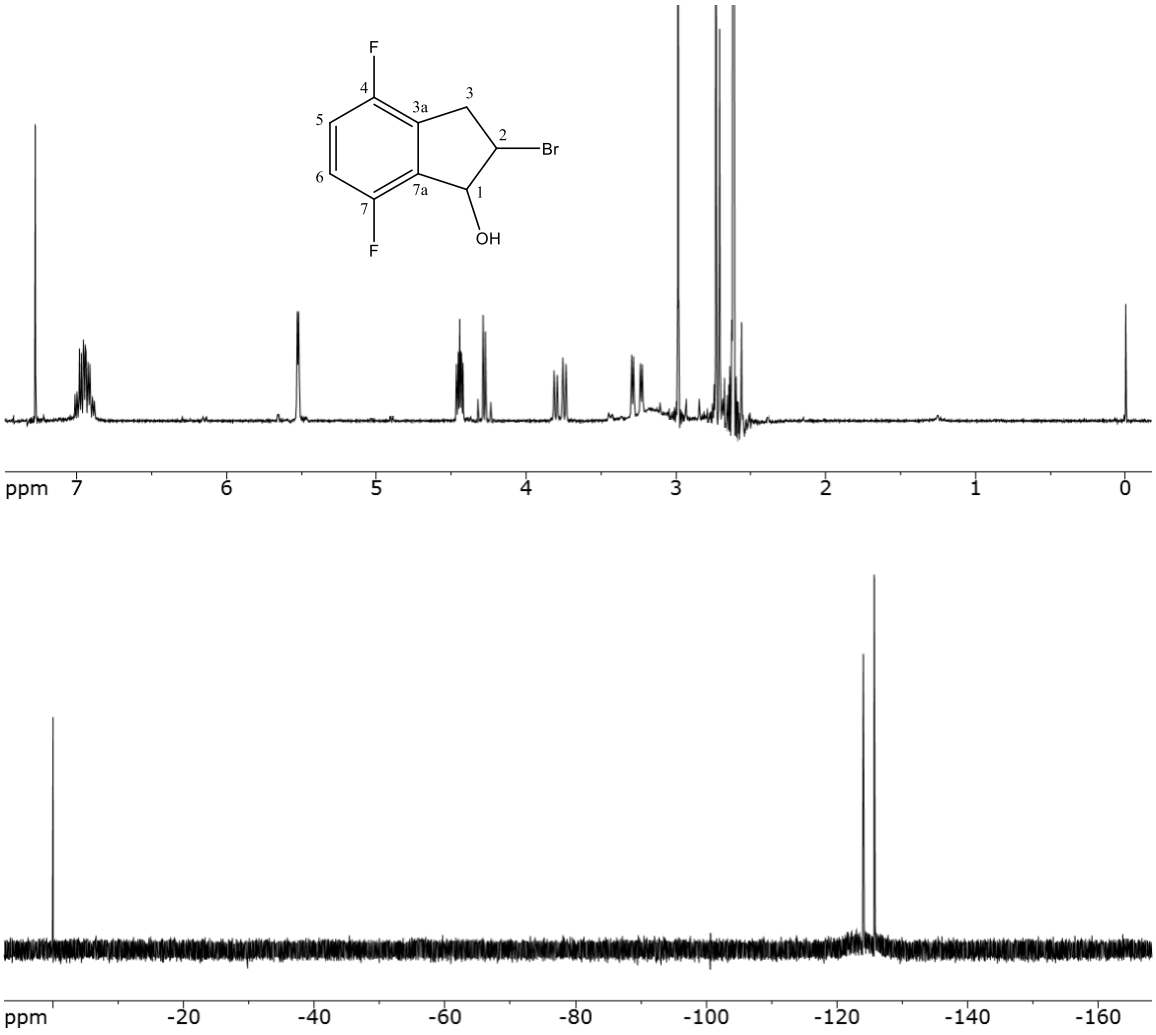

Yield: 60% $C_9H_7BrF_2O$ 249.04 g mol^{-1}

^{1}H-NMR (300 MHz, $CDCl_3$): δ = 7.05-6.88 (m, 2H, $H_{6,5}$), 5.52 (d, 1H, H_1), 4.48-4.42 (m, 1H, H_2), 4.79 (dd, 1H, H_3)*, 3.28 (dd, 1H, H_3)* ppm.

^{19}F-NMR (283 MHz, $CDCl_3$): δ = -124.0 (m, 1F), -125.8 (m, 1F) ppm.

MS (EI, 70 eV): *m/z* (%) = 250 (16), 248 (16), 170 (9), 169 (100), 168 (15), 152 (13), 151 (42), 149 (10), 141 (6), 139 (5), 121 (13), 120 (6), 119 (11), 101 (14), 99 (6).

General Procedure for Elimination to 2-Bromo-Indene Derivatives

To a solution of the corresponding bromohydrin (6.01 mmol) in 20 mL benzene was added a catalytic amount of PTSA and the mixture was heated to 100 °C, fitted with a dean stark trap and reflux condenser. After stirring overnight, the combined solution from the reaction flask and the deak stark trap was washed with saturated sodium bicarbonate. The organic phase was dried over anhydrous MgSO4 and the solvent evaporated *in vacuo* to afford the clean product as a tan crystalline solid.

Note: For the fluorinated derivative the crude product was a brown oil that was purified by column chromatography on silica with hexane:ethyl acetate (20:1) to afford clean product.

2-bromo-4,7-dimethyl-1H-indene (75m):

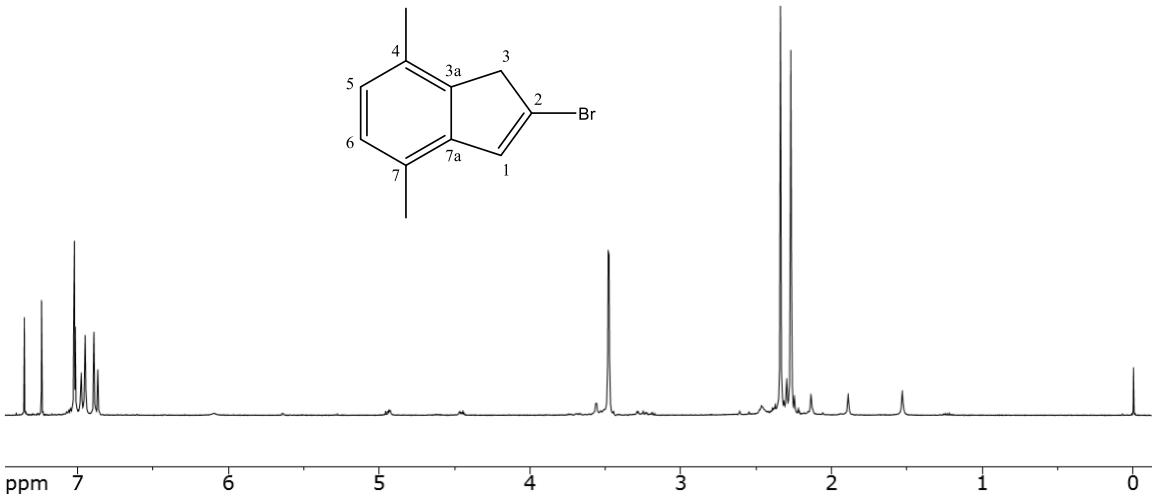

Yield: 75% $C_{11}H_{11}Br$ 223.09 g mol^{-1}

^{1}H-NMR (300 MHz, $CDCl_3$): δ = 7.01 (s, 1H, H_1), 6.99 (d, 1H, H_6), 6.89 (d, 1H, H_5), 3.49 (s, 2H, H_3), 2.37 (s, 3H, H_{Me}), 2.27 (s, 3H, H_{Me}) ppm.

IR (AT-IR): ṽ = 3050, 3016, 2976, 2944, 2917, 2886, 2859, 2728, 1875, 1762, 1713, 1609, 1592, 1557, 1490, 1447, 1324, 1299, 1271, 1261, 1247, 1159, 1126, 1070, 1031, 1006, 940, 911, 837, 801, 731, 696, 678, 655 cm^{-1}.

MS (EI, 70 eV): *m/z* (%) = 224 (19), 222 (20), 144 (11), 143 (100), 142 (6), 141 (12), 128 (39), 127 (8), 115 (14).

2-bromo-4,7-difluoro-1H-indene (75c):

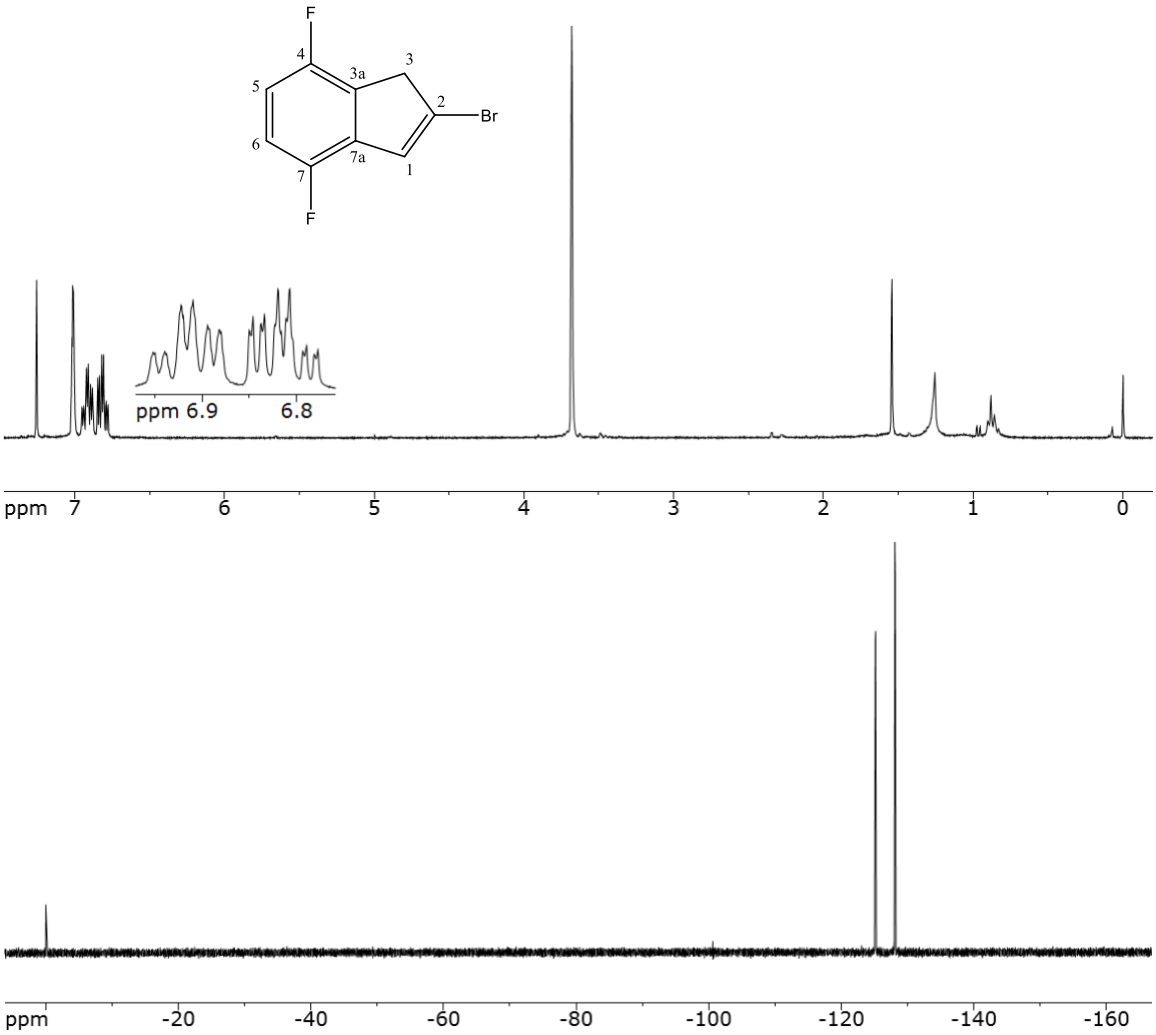

Yield: 15% $C_9H_5BrF_2$ 231.03 g mol^{-1}

^{1}H-NMR (300 MHz, $CDCl_3$): δ = 7.01 (s, 1H, H_1), 6.92 (dt, 1H, H_6), 6.82 (dt, 1H, H_5), 3.69 (s, 2H, H_3) ppm.

^{19}F-NMR (283 MHz, $CDCl_3$): δ = -125.1 (m, 1F), -128.1 (m, 1F) ppm.

MS (EI, 70 eV): *m/z* (%) = 232 (11), 230 (11), 152 (10), 151 (100), 150 (6), 76 (5).

General Procedure for the Dehalogenative Coupling of 2-Bromo-Indene Derivatives

A mixture of Zn dust (4.48 mmol), anhydrous $NiCl_2$ (1.79 mmol), and KI (8.96 mmol) in 9 mL 1-methyl-2-pyrrolidinone was heated to 60-65 °C. After stirring 1 h, the corresponding 2-bromo-indene (4.48 mmol) was added in one portion. After stirring for 3 d, the reaction mixture was cooled to room temperature and 1 mL of 6 M HCl was slowly added while stirring. After gas evolution ceased, the mixture was diluted with water and extracted with methylene chloride. The combined organic layer was filtered over Celite, with thorough washing of the Celite with methylene chloride. The filtrate was concentrated *in vacuo* and methanol was added to the crude material to facilitate product precipitation to afford clean product as a crystalline solid.

General Procedure for the Oxidative Homocoupling of 1-Indanone Derivatives

To a suspension of sodium hydride (16.2 mmol) in 29 mL THF was added a solution of the corresponding 1-indanone (14.9 mmol in 48 mL THF). After stirring at room temperature for 1 h, the mixture was cooled to -78 °C and anhydrous copper (II) chloride (16.5 mmol) was added all at once. After stirring at -78 °C for 5 h, the dry ice was allowed to evaporate and the reaction was brought to room temperature. After stirring at room temperature

overnight, the reaction was quenched with water (24 mL) and the volatiles were evaporated *in vacuo*. The residue was taken up in diethyl ether, dried over anhydrous $MgSO_4$ and filtered over a silica pad. The solvent was evaporated *in vacuo* to afford the crude product in 40% yield as a light green, turbid oil.

7.2.5. Toward Fluorinated Dendralene Derivatives

α-bromo-β,β-difluoro-styrene (11b):

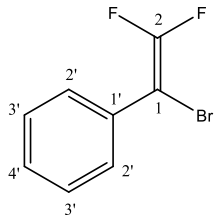

To an ampule flask was added phenylboronic acid (61 mg, 0.50 mmol), CsF (152 mg, 1.0 mmol), $Pd_2dba_3 \cdot CHCl_3$ (2.6 mg, 2.5 µmol), and dppm (1.9 mg, 4.9 µmol) and the mixture was purged with N_2. Degassed mixed solvent (2.5 mL 1,4-dioxane/water = 2:1) and 1,1-dibromo-2,2-difluoroethylene (48 µL, 0.50 mmol) were added. After stirring 3 h at 60 °C, the mixture was quenched with saturated aqueous NH_4Cl and extracted with diethyl ether. The combined organic phase was washed with saturated Brine and dried over anhydrous Na_2SO_4. The solvent was evaporated *in vacuo* and the resulting yellow solid was purified by column chromatography on silica gel with pentane to afford a colorless oil.

Yield: 85% $C_8H_5BrF_2$ 219.02 g mol^{-1}

Alternative Method: To a solution of (1,2-dibromo-2,2-difluoroethyl)benzene (2.36 mmol) in 5 mL THF was added DBU (2.59 mmol). After stirring at room temperature 1 h, the reaction mixture was quenched with water and extracted with methylene chloride. The combined organic phase was washed with saturated Brine and dried over anhydrous Na_2SO_4. The solvent was evaporated *in vacuo* to afford clean product as a turbid oil.

^{1}H-NMR (300 MHz, $CDCl_3$): δ = 7.50 (dd, 2H, $H_{2'}$), 7.42-7.29 (m, 3H, $H_{3',4'}$) ppm.

^{19}F-NMR (283 MHz, $CDCl_3$): δ = -78.9 (d, 1F), -85.1 (d, 1F) ppm.

MS (EI, 70 eV): *m/z* (%) = 220.9 (5), 219.9 (56), 218.9 (5), 217.9 (59), 140 (10), 139 (100), 138 (13), 120 (11), 119 (74), 99 (18), 89 (11), 88 (7), 87 (8), 69 (9), 63 (15), 62 (10), 61 (5), 51.1 (5).

β,β-difluorostyrene (90):

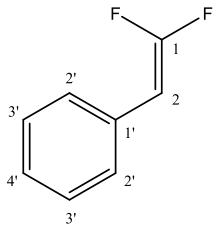

To an ampule flask containing a solution of benzaldehyde (0.25 g, 2.36 mmol) in 24 mL 8% DMF/CH3CN was added PPh3 (1.854 g, 7.07 mmol), LiI (0.631 g, 4.72 mmol), and TMSCF3 (0.837 g, 5.89 mmol). After stirring 22 h at 120 °C, the reaction was cooled to room temperature, quenched with H2O, and extracted with diethyl ether. The combined organic phase was dried over anhydrous MgSO4. The solvent was removed in vacuo into a clean receiving flask as the clean product is pulled over with the diethyl ether, effectively separating it from organic byproducts.

Yield: no yield obtained $C_8H_6F_2$ 140.12 g mol^{-1}

^{1}H NMR (300 MHz, $CDCl_3$): 7.70-7.20 (m, 5H, $H_{2',3',4'}$), 4.72 (s, 1H, H_2) ppm.

^{19}F NMR (283 MHz, $CDCl_3$): -83.0 (dd, 1F), -84.8 (dd, 1F) ppm.

MS (EI, 70 eV): m/z (%) = 141 (9), 140 (100), 139 (16), 120 (11), 119 (8), 114 (14), 101 (5), 90 (6), 89 (11), 63 (8), 51 (5).

(1,2-dibromo-2,2-difluoroethyl)benzene (91):

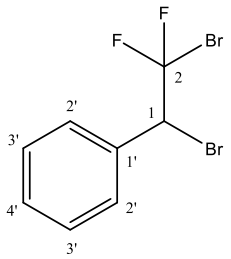

To a room temperature solution of β,β-difluorostyrene (1.980 g, 14.1 mmol) in diethyl ether was added bromine (2.484 g, 15.5 mmol) dropwise. After stirring 1 h, the solvent was evaporated in vacuo to afford the crude product as a sticky orange solid.

Yield: 95% $C_8H_5Br_2F_2$ 298.92 g mol^{-1}

^1H NMR (300 MHz, $CDCl_3$): 7.72-7.23 (m, 5H, $H_{2',3',4'}$) ppm.

^{19}F NMR (283 MHz, $CDCl_3$): -45.1 (dd, 1F), -54.3 (dd, 1F) ppm.

MS (EI, 70 eV): m/z (%) = 300 (5), 221 (43), 219 (45), 171 (7), 169 (7), 141 (8), 140 (100), 139 (8), 120 (5), 119 (5), 114 (5), 89 (7), 70 (6), 63 (6).

1,1-difluoro-2,2-diiodo-ethylene (12b):

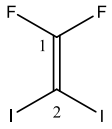

To a solution of CF_3CH_2I (4.198 g, 20 mmol) in 20 mL anhydrous THF cooled to -100 °C was added a freshly prepared LDA solution dropwise. After stirring 30 min at -100 °C a solution of I_2 (5.33 g, 21 mmol in 10 mL THF) was added. After stirring 1 h at -100 °C, the reaction was warmed to room temperature, quenched with saturated ammonium chloride, and extracted with diethyl ether. The combined organic phase was washed with

Brine and dried over anhydrous Na_2SO_4. The solvent was evaporated *in vacuo*, with caution not to pull below 175 mbar, to afford crude product as a dark brown oil.

Yield: 80% $C_2F_2I_2$ 316.02 g mol^{-1}

^{19}F NMR (283 MHz, $CDCl_3$): -163.9 (s, 2F) ppm.

MS (EI, 70 eV): *m/z* (%) = 316.9 (5), 315.9 (100), 265.8 (5), 253.8 (8), 188.9 (52), 169.9 (8), 157.9 (7), 138.9 (16), 126.9 (42).

7.3. X-Ray Crystallographic Reports

4,7-difluoro-1-indanone (40c):

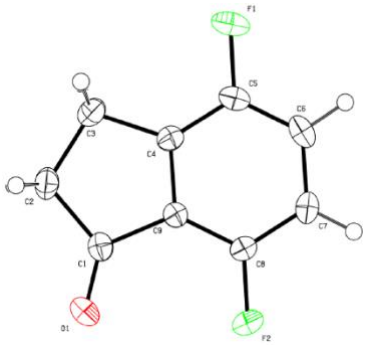

Empirical formula	$C_9H_6OF_2$	
Formula weight	168.14 g/mol	
Temperature, K	153(2)	
Wavelength, Å	0.71073	
Crystal system	monoclinic	
Space group	$P2_1/c$	
Unit cell dimensions	a = 8.2803(14) Å	α = 90
	b = 13.131(2) Å	β = 114.614(2)
	c = 7.2264(12) Å	γ = 90
Unit cell volume, Å	714.3(2)	
Z	4	
Density (calculated), g cm^{-1}	1.563	
Absorption coefficient, mm^{-1}	0.136	
F(000)	344	
Limiting indices (h, k, l_{max})	10, 16, 9	

4,7-dimethoxy-1-indanone (40i):

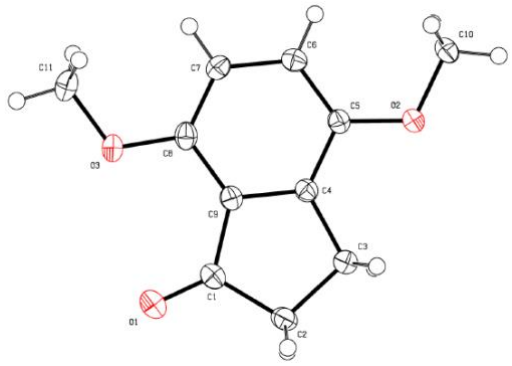

Empirical formula	$C_{11}H_{12}O$	
Formula weight	192.21 g/mol	
Temperature, K	100	
Wavelength, Å	1.54184	
Crystal system	monoclinic	
Space group	$P2_1/c$	
Unit cell dimensions	a = 9.0417(3) Å	α = 90
	b = 15.4434(4) Å	β = 112.265(4)
	c = 7.1845(2) Å	γ = 90
Unit cell volume, Å	928.41(5)	
Z	4	
Density (calculated), g cm^{-1}	1.375	
Absorption coefficient, mm^{-1}	0.822	
F(000)	408.0	
Limiting indices (h, k, l_{max})	11, 19, 9	
Bond precision, Å	0.0024	

4,7-dimethoxy-2-indanone (10i):

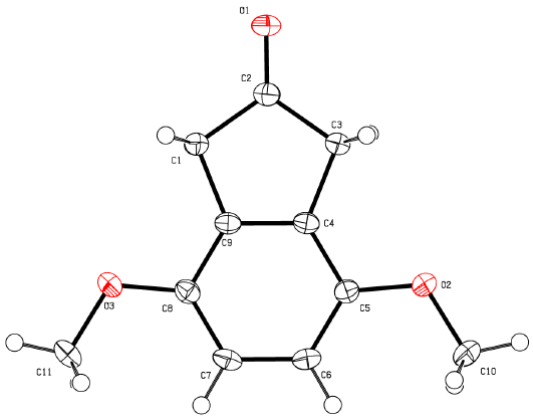

Empirical formula	$C_{11}H_{12}O$	
Formula weight	192.21 g mol^{-1}	
Temperature, K	100	
Wavelength, Å	1.54184	
Crystal system		
Space group	$P2_1/c$	
Unit cell dimensions	a = 6.7663(1) Å	α = 90
	b = 8.3188(2) Å	β = 93.783(2)
	c = 16.8444(3) Å	γ = 90
Unit cell volume, Å	946.06(3)	
Z	4	
Density (calculated), g cm^{-1}	1.349	
Absorption coefficient, mm^{-1}	0.807	
F(000)	408.0	
Limiting indices (h, k, l_{max})	8, 10, 20	
Bond precision, Å	0.0015	

4,7-diphenyl-indene (42n):

Empirical formula	$C_{21}H_{16}$	
Formula weight	268.34 g mol^{-1}	
Temperature, K	116.00(18)	
Wavelength, Å		
Crystal system	monoclinic	
Space group	$P2_1/c$	
Unit cell dimensions	a = 7.33530(10) Å	$\alpha = 90$
	b = 15.0001(2) Å	$\beta = 91.0820(10)$
	c = 12.7987(2) Å	$\gamma = 90$
Unit cell volume, Å	1407.99(3)	
Z	4	
Density (calculated), g cm^{-1}	1.266	
Absorption coefficient, mm^{-1}	0.539	
F(000)	568.0	
Limiting indices (h, k, l_{max})	9, 19, 16	

4,4',7,7'-tetramethyl-1H,1'H,3H,3'H-2,2'-biindenylidene (70b):

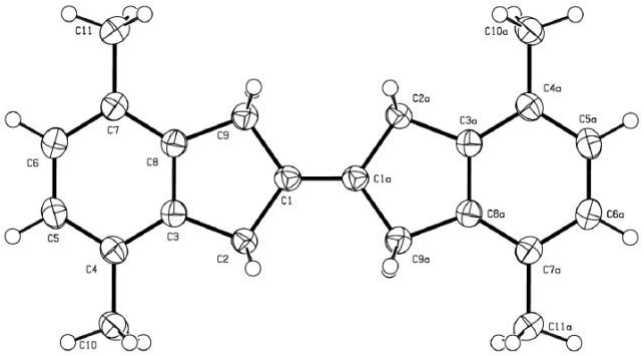

Empirical formula	$C_{11}H_{12}$	
Formula weight	144.21 g mol^{-1}	
Temperature, K	115	
Wavelength, Å	1.54184	
Crystal system	monoclinic	
Space group	I2/a	
Unit cell dimensions	a = 7.9881(1) Å	α = 90
	b = 8.5463(2) Å	β = 97.065(1)
	c = 23.8746(3) Å	γ = 90
Unit cell volume, Å	1617.51(5)	
Z	8	
Density (calculated), g cm^{-1}	1.184	
Absorption coefficient, mm^{-1}	0.493	
F(000)	624.0	
Limiting indices (h, k, l_{max})	10, 10, 30	
Bond precision, Å	0.0016	

4,4',7,7'-tetramethyl-1H,1'H,2H,2'H,3H,3'H-[2,2'-biindene]-2,2'-diol (71b):

Empirical formula	$C_{22}H_{26}O_2$	
Formula weight	322.43	
Temperature, K	116.5(5)	
Wavelength, Å	1.54184	
Crystal system	triclinic	
Space group	P1	
Unit cell dimensions	a = 8.5424(2) Å	α = 72.977(2)
	b = 9.2882(2) Å	β = 75.149(2)
	c = 11.9534(2) Å	γ = 87.029(2)
Unit cell volume, Å	876.30(4)	
Z	2	
Density (calculated), g cm^{-1}	1.222	
Absorption coefficient, mm^{-1}	0.594	
F(000)	348.0	
Limiting indices (h, k, l_{max})	10, 11, 15	

REFERENCES

1. Phelan, N. F.; Orchin, M. "Cross Conjugation" *J. Chem. Educ.* **1968**, 45, 633-637.

2. Hopf, H. "Dendralenes: The Breakthrough." *Angew. Chem. Int. Ed.* **2001**, 40, 705-707.

3. Wilke, G. "Contributions to Organo-Nickel Chemistry." *Angew. Chem. Int. Ed. Engl.* **1988**, 28, 185-206.

4. Kaftory, M.; Botoshansky, M.; Hyoda, S.; Watanabe, T.; Toda, F. "Effects of Overcrowding in [n]Radialenes on the Synthesis of bis[4]Radialenes." *J. Org. Chem.* **1999**, 64, 2287-2292.

5. Hopfner, T.; Jones, P. G.; Ahrens, B.; Dix, I.; Ernst, L.; Hopf, H. "[6]Radialenes Revisited." *Eur. J. Org. Chem.* **2003**, 2596-2611.

6. Sugimoto, T.; Misaki, Y.; Kajita, T.; Yoshida, Z.; Kai, Y.; Kasai, N. "Hexakis(1,3-dithiol-2-ylidene)cydohexane With Two Different Conformations of the Six-Membered Ring." *J. Am. Chem. Soc.* **1987**, 109, 4106-4107.

7. Shinozaki, S.; Hamura, T.; Ibusuki, Y.; Fujii, K.; Uekusa, H.; Suzuki, K. "Hexaradialenes by Successive Ring Opening of Tris(alkoxy-tricyclobutabenzenes): Synthesis and Characterization." *Angew. Chem. Int. Ed.* **2010**, 49, 3026-3029.

8. Van der Wiel, B. C.; Williams, R. M.; Van Walree, C. A. "Photoinduced Charge Separation in a Donor-Acceptor Functionalized 2,3-Diphenylbutadiene: Charge Transport Over a Doubly Bifurcated Spacer." *Org. Biomol. Chem.* **2004**, 2, 3432.

9. Banert, K; Toth, C. "Synthesis and Reactions of Vinyl Isoselenocyanates." *Angew. Chem. Int. Ed. Engl.* **1995**, 34, 1627-1629.

10. Banert, K.; Groth, S.; Huckstadt, H.; Lehmann, J.; Schlott, J.; Vrobel, K. "Rearrangement Reactions; 12: Synthesis and Reactions of Isothiocyanate Substituted Allenes." *Synthesis* **2002**, 1423-1433.

11. Tsuge, O.; Hatta, T.; Yoshitomi, H.; Kurosaka, K.; Fujiwara, T.; Maeda, H.; Kakehi, A. "Diene-Transmissive Diels-Alder Reaction of 2-vinyl-1-oxabutadiene System." *Heterocycles* **1995**, 41, 225-228.

12. Tsuge, O.; Hatta, T.; Fujiwara, T.; Yokohari, T.; Tsuge, A.; Moriguchi, T. "Diene-Transmissive Hetero Diels-Alder Reaction of 1,5-diphenyl-1,4-pentadien-3-one." *Heterocycles* **1999**, 50, 661-666.

13. Hopf, H.; Maas, G. “Preparation and Properties, Reactions, and Applications of Radialenes.” *Angew. Chem. Int. Ed. Engl.* **1992**, 31, 931-954.

14. Takahashi, K.; Tarutani, S. “Novel Electron Acceptors For Organic Conductors: 1,2-bis(p-benzoquino)-3-[2-(dicyanomethylene)-2,5-thienoquino]cyclopropane Derivatives.” *J. Chem. Soc. Chem. Commun.* **1994**, 519-520.

15. Takahashi, K.; Tarutani, S. “New Acceptors For Highly Conducting Charge-Transfer Complexes and Radical-Anion Salts: 1,2-bis(p-benzoquino)-3-(dicyanomethyleneheteroquino)cyclopropane (BQDCNH-CP) Derivatives.” *Synth. Met.* **1995**, 70, 1165-1166.

16. Takahashi, K.; Tarutani, S. “Novel Molecular Metals Composed of a [3]Radialene Type Acceptor: 1,2-bis(p-benzoquino)-3-[2-(dicyanomethylene)-2,5-selenoquino] cyclopropane Derivative.” *Mol. Cryst. Liq. Cryst.* **1997**, 296, 145-147.

17. Domalski, E. S. “Selected Values of Heats of Combustion and Heats of Formation of Organic Compounds Containing the Elements Carbon, Hydrogen, Nitrogen, Oxygen, Phosphorus, and Sulfur.” *J. Phys. Chem. Ref. Data* **1972**, 1, 221-278.

18. Schlosser, M. “Parametrization of Substituents: Effects of Fluorine and Other Heteroatoms on OH, NH and CH Acidities.” *Angew. Chem. Int. Ed.* **1998**, 37, 1496-1513.

19. Behrman, E. J. “Borodin.” *J. Chem. Edu.* **2006**, 83, 1138-1139.

20. Percy, J. M. “Building Block Approaches to Aliphatic Organofluorine Compounds.” *Topics in Current Chemistry*. Vol. 193 **1997**, Springer Verlag Berlin Heidelberg.

21. Wiberg, K. B.; Rablen, P. R. “Origin of the Stability of Carbon Tetrafluoride: Negative Hyperconjugation Reexamined.” *J. Am. Chem. Soc.* **1993**, 115, 614-625.

22. Wiberg, K. B. “Bent Bonds in Organic Compounds.” *Acc. Chem. Res.* **1996**, 29, 229-234.

23. Dolibier Jr, W. R. “Fluorine Chemistry at the Millennium.” *J. Fluor. Chem.* **2005**, 126, 157-163.

24. Tyczkowsky, E. A.; Bigelow, L. A. “The Action of Elementary Fluorine upon Organic Compounds. XIX. A New Jet Fluorination Reactor.” *J. Am. Chem. Soc.* **1955**, 77, 3007-3008.

25. Furuya, T.; Klein, J. E. M. N.; Ritter, T. “Carbon–Fluorine Bond Formation for the Synthesis of Aryl Fluorides.” *Synthesis* **2010**, 11, 1804-1821.

26. Sankar Lal, G.; Pez, G. P.; Syvret, R. G. “Electrophilic NF Fluorinating Agents.” *Chem. Rev.* **1996**, 96, 1737-1755.

27. Tius, M. A. “Xenon Difluoride in Synthesis.” *Tetrahedron* **1995**, 51, 6605-6634.

28. Jones, D. W.; Ryder, T. C. L. M. “Generation and Inter- and Intra-molecular Trapping of Isoindenones (Inden-2-ones).” *Chem. Commun.* **1997**, 0, 1169-1170.

29. Bradshaw, D. P.; Jones, D. W.; Nongrum, F. M. “Stability of Alkoxy Substituted Inden-2-ones and 6,7-Dimethoxy-1,4-diphenyl-2,3-napthoquinone.” *J. Chem. Soc. Perkin Trans. 1*, **1991**, 1, 19-23.

30. Fuchs, B.; Pasternak, M.; Scharf, G. “The Dimer of 2,3-Dimethyl-3,4-(*o,o’*-biphenylene)cyclopentadienone: Thermal and Photochemical Transformations.” *Chem. Commun.* **1976**, 2, 53-54.

31. Jones, D. W.; Pomfret, A.; Wife, R. L. “Stabilised 2,3-Naphthoquinodimethanes via Transient 1,3-Diphenylbenz[f]inden-2-one.” *Chem. Commun.* **1980**, 10, 463-464.

32. Poater, J.; Solà, M.; Alkorta, I.; Elguero, J. “Aromaticity and Magnetic Properties of 1- and 2-Indenones and Their Aza Derivatives.” *Eur. J. Org. Chem.* **2014**, 5370-5377.

33. Holland, J. M.; Jones, D.W. “*o*-Quinonoid Compounds. Part IV. 1,3-Diphenylinden-2-one.” *J. Chem. Soc.* **1971**, 608-612.

34. Holland, J. M.; Jones, D. W. “Derivatives of Isoindenone.” *Chem. Commun.* **1969**, 11, 587-588.

35. Fuchs, B.; Pasternak, M. “Photochemical Studies. XXI. Dimers of 3,4-(o,o'-biphenylene)cyclopentadienones: Thermal and Photochemical Behavior.” *Tetrahedron.* **1981**, 37, 2501-2507.

36. Blatt, K.; Hoffman, R. W. “Reactivity of 1,3-Dihalogenoisoindenones.” *Liebigs Ann. Chem.* **1972**, 760, 114-126.

37. Etzkorn, M.; Smeltz-Zapata, S. D.; Meyers, T. B.; Yu, X.; Gerken, M. “From the *anti*-Tricyclo[4.2.1.12,5]deca-3,7-diene Framework to 4,5,6,7-Tetrachloro-isoindenone Derivatives.” *Tetrahedron Lett.* **2010**, 51, 6075-6077.

38. Franklin, J. L. M.S. Thesis, UNC Charlotte, **2017**.

39. Knoevenagel, E. “Condensation von Malonsäure mit aromatischen Aldehyden durch Ammoniak und Amine.” *Berichte der Deutschen Chemischen Gesellschaft* **1898**, 31(3), 2596-2619.

40. Novak, J.; Salemink, C. A. “Cannabis. Part 25. Synthesis of Cannabispirenone-B and its 5,7-Difluoro Analog.” **1982**, 10, 2403-2405.

41. Piccolrovazzi, N.; Pino, P.; Consiglio, G.; Sironi, A.; Moret, M. “Electronic Effects in Homogeneous Indenylzirconium Ziegler-Natta Catalysts.” *Organometallics* **1990**, 9(12), 3098-3105.

42. Patents: US 0148347 A1 and US 0099333 A.

43. Horan, J. E.; Schiessler, R.W. "2-Indanone." *Org. Synth.* **2003**, 41, 53.

44. McCormick, K. D.; Dong, L.; Boyce, C. W.; De, L. R. M.; Fevrier, S.; Wu, J.; Zheng, J.; Yu, Y.; Chao, J.; and Won, W. S. “Biaryl spiroaminooxazoline analogues as alpha2c adrenergic receptor modulators.” WO2010042473 **2010**.

45. Baxter, E. W.; Nortey, S. O.; Reitz, A. B.; Pulito, V. L.; Middleton, S. A. “Preparation of Dihydroindolyl Methanones as α1a/1d Adrenoreceptor Modulators for the Treatment of Benign Prostatic Hypertrophy and Lower Urinary Tract Symptoms.” *U.S. Pat. Appl. Publ.* **2006**, US 20060183902 A1 20060817.

46. Nakajima, Y.; Watanabe, H.; Adachi, M.; Tagawa, M.; Futagawa, M.; Furusato, T.; Ohya, H.; Nishioka, M. “Preparation of Cyclooctadienetetracarboxylic Acid Dianhydride and Dibenzocyclooctadiene Derivatives as Antithrombotics and Agrochemical Fungicides.” *PCT Int. Appl.* **1995**, WO 9521149 A1 19950810.

47. Hutchison, G. I.; Marshall, P. A.; Prager, R. H.; Tippett, J. M.; Ward, A. D. "Central nervous system active compounds. IV. Synthesis of 3-aminobenzylphthalides." *Aust. J. Chem.* **1980**, 33(12), 2699-2715.

48. Ho, T. L.; Hsieh, S. Y. “Regioselective Synthesis of Ellipticine.” *Helv. Chim. Acta* **2006**, 89(1), 111-116.

49. Leino, R.; Luttikhedde, H. J. G.; Lehtonen, A.; Sillanpaa, R.; Penninkangas, A.; Stranden, J.; Mattinen, J.; Nasman, J. H. “Bis[2-(tert-butyldimethylsiloxy)-4,7-dimethylindenyl]zirconium Dichloride: Synthesis, Torsional Isomerism and Olefin Polymerization Catalysis.” *J. Organomet. Chem.* **1998**, 558(1-2), 171-179.

50. Mavrynsky, D.; Rahkila, J.; Bandarra, D.; Martins, S.; Meireles, M.; Calhorda, M. J.; Kovacs, I. J.; Zupko, I.; Hanninen, M. M.; Leino, R. “Cytotoxicities of Polysubstituted Chlorodicarbonyl(cyclopentadienyl) and (Indenyl)ruthenium Complexes.” *Organometallics.* **2013**, 32(10), 3012-3017.

51. Erker, G.; Psiorz, C.; Frohlich, R.; Grehl, M.; Kruger, C.; Noe, R.; Nolte, M. "Preparation and Catalytic Application of a Novel Very Rigid Group 4 Ansa-Metallocene System." *Tetrahedron* **1995**, 51(15), 4347-4358.

52. Lee, J. C.; Bae, Y. H.; Chang, S. K. "Efficient α-Halogenation of Carbonyl Compounds by *N*-Bromosuccinimide and *N*-Chlorosuccinimide." *Bull. Korean Chem. Soc.* **2003**, 24, 407-408.

53. Ceylan, M.; Gurdere, M. B.; Budak, Y.; Kazaz, C.; Secen, H. "One-Step Preparation of Symmetrical 1,4-Diketones from α-Halo Ketones in the Presence of Zn-I2 as a Condensation Agent." *Synthesis* **2004**, 11, 1750-1754.

54. Coe, J. W.; Vetelino, M. G.; Kemp, D. S. "Indenes via Fulvene Intermediates." *Tetrahedron Lett.* **1994**, 35, 6627-6630.

55. Lemal, D. M.; Akashi, M.; Lou, Y.; Kumar, V. "Tetrafluorothiophene S,S-Dioxide: A Perfluorinated Building Block." *J. Org. Chem.* **2013**, 78, 12330-12337.

56. Burdon, J.; Campbell, J. G.; Parsons, I. W.; Tatlow, J. C. "Highly Fluorinated Heterocycles. V. Preparation and Reactions of Tetrafluorothiophene and Some Polyfluorothiophenes." *J. Chem. Soc.* **1971**, 2, 352-355.

57. Escher, A.; Rutsch, W.; Neuenschwander, M. "Nonafulvalen: Synthese Durch Oxidative Kupplung von Cyclononatetraenid und Valenzisomerisierung." *Helv. Chim. Acta.* **1986**, 69, 1644.

58. Anastassiou, A. G.; Setliff, F. L.; Griffin, G. W. "A *sym*-Dibenzfulvalene[1a]." *J. Org. Chem.* **1966**, 31, 2705-2708.

59. Kerber, R. C.; Waldbaum, B. "Synthesis and Structure of Novel Group 6 Complexes of Dibenzofulvalenes." *Organometallics.* **1995**, 14, 4742-4754.

60. Waldbaum, B. R.; Kerber, R. C. "Novel Organoiron Compounds Resulting From the Attempted Syntheses of Dibenzofulvalene Complexes." *Inorganica Chim. Acta.* **1999**, 291, 109-126.

61. Tilset, M.; Vollhardt, K. P. C.; Boese, R. "Chemistry of Dinuclear Fulvalene Complexes: Dihydrides, Zwitterions, and Ring-Slippage Complexes Derived From $FvM_2(CO)_6$ (M = Mo, W)." *Organometallics.* **1994**, 13, 3146-3169.

62. Delville, M. H.; Lacoste, M.; Astruc, D. "Salt-Induced, Ligand-Controlled, Intra- vs Intermolecular Electron Transfer in a Fulvalene-Bridged Organoiron Diradical." *J. Am. Chem. Soc.* **1992**, 114, 8310-8311.

63. Desbois, M. H.; Astruc, D.; Guillin, J.; Mariot, J. P.; Varret, F. "Organometallic "Electron Reservoirs". 23. 36-40 Electron Complexes (C_6R_6FeCp-$CpFeC_6R_6$) (R = H, Me; n = 0-2) and the First Delocalized Mixed Valence Complexes Containing Iron(I)." *J. Am. Chem. Soc.* **1985**, 107, 5280-5282.

64. Crabtree. The Organometallic Chemistry of the Transition Metals, Wiley, **1988**, 104-105.

65. Kerber, R. C.; Waldbaum, B. R. "Structure and Reactivity of (Dibenzo[b,e]fulvalene)$Mo_2(CO)_6$." *J. Organomet. Chem.* **1996**, 513, 277-280.

66. Tews, D.; Gaede, P. E. "Organorhodium Compounds With Novel Bridged Dibenzo[b,e]fulvalene Ligands." *Organometallics.* **2001**, 20, 3869-3875.

67. McMurry, J. E.; Fleming, M. P.; Kees, K. L.; Krepski, L. R. "Titanium-Induced Reductive Coupling of Carbonyls to Olefins." *J. Org. Chem.* **1978**, 43, 3255-3266.

68. Corey, E. J.; Danheiser, R. L.; Chandrasekaran, S. "New Reagents for the Intermolecular and Intramolecular Pinacolic Coupling of Ketones and Aldehydes." *J. Org. Chem.* **1976**, 41(2), 260-265.

69. Ephritikhine, M. "A New Look at the McMurry Reaction." *Chem. Commun.* **1998**, 2549-2554.

70. Jessup, D. W.; Paschal, J. W.; Rabideau, P. W. "Metal Reduction of Fluorinated Aromatic Compounds." *J. Org. Chem.* **1977**, 42, 2620-2621.

71. Schroth, W.; Schmidt, K. "2,2'-Diindenyl." *Z. Chem*. **1963**, 3, 309.

72. Corey, E. J.; Danheiser, R. L.; Chandrasekaran, S. "New Reagents for the Intermolecular and Intramolecular Pinacolic Coupling of Ketones and Aldehydes." *J. Org. Chem.* **1976**, 41(2), 260-265.

73. Corey, E. J.; Hopkins, P. B. "A Mild Procedure for the Conversion of 1,2-Diols to Olefins." *Tetrahedron Lett.* **1982**, 23, 1979-1982.

74. Schumann, H.; Karasiak, D. F.; Muhle, S. H.; Halterman, R. L.; Kaminsky, W.; Weingarten, U. "Synthesis and Characterization of 1- and 2-(ω-alken-1-yl)indenes, Their Lithium Salts and Dichlorozirconium(IV) Complexes." *J. Organomet. Chem.* **1999**, 579, 356-372.

75. Lindley, W. A.' MacDowell, D. W. H. "Keto-Enol Tautomerism in the Thiophene Analogues of Naphthacen-5-one." *J. Org. Chem.* **1982**, 47, 705-709.

76. Takagi, K.; Mimura, H.; Inokawa, S. “The In Situ-Generated Nickel(0)-catalyzed Homo-coupling of Alkenyl Halides With Zinc Powder. A Specific Outcome in Stereochemistry.” *Bull. Chem. Soc. Jpn.* **1984**, 57, 3517-3522.

77. Zhang, X.; Thimmaiah, M.; Fang, S. “Simple and Efficient Synthesis of 4,7-Dimethoxy-1(*H*)-indene.” *Synth. Commun.* **2007**, 37, 1873-1877.

78. Yildizhan, S.; Hopf, H.; Jones, P. G. “Attempts to Prepare an All-Carbon Indigoid System.” *Beilstein J. Org. Chem.* **2015**, 11, 363-372.

79. Pearson, A. J.; Schoffers, E. “Tricarbonyltris(pyridine)molybdenum: A Convenient Reagent for the Preparation of (π-Allyl)molybdenum Complexes.” *Organometallics* **1997**, 16, 5365-5367.

80. Davis, R.; Kane-Maguire, L. A. P. “Molybdenum Compounds with n2-n8 Carbons Ligands.” *Comprehensive Organometallic Chemistry* **1982**, 3, 1212-1215.

81. Payne, A. D.; Bojase, G. Paddon-Row, M. N.; Sherburn, M. S. “Practical Synthesis of the Dendralene Family Reveals Alternation in Behavior.” *Angew. Chem. Int. Ed.* **2009**, 48, 4836-4839.

82. Blomquist, A. T.; Verdol, J. A. “2-Vinyl-1,3-Butadiene.” *J. Am. Chem. Soc.* **1955**, 77, 81-83.

83. Bailey, W. J.; Nielsen, N. A. “Pyrolysis of Esters. XXIII. 2,3-Divinyl-1,3-Butadiene.” *J. Org. Chem.* **1962**, 27, 3088-3091.

84. Fielder, S.; Rowan, D. D.; Sherburn, M. S. “First Synthesis of the Dendralene Family of Fundamental Hydrocarbons.” *Angew. Chem. Int. Ed.* **2000**, 39, 4331-4333.

85. Saglam, M. F.; Fallon, T.; Paddon-Row, M. N.; Sherburn, M. S. “Discovery and Computational Rationalization of Diminishing Alternation in [*n*]Dendralenes.” *J. Am. Chem. Soc.* **2016**, 138, 1022-1032.

86. Mackay, E. G.; Sherburn, M. S. “Demystifying the Dendralenes.” *Pure Appl. Chem.* **2013**, 85(6), 1227-1239.

87. Hopf, H.; Sherburn, M. S. “Dendralenes Branch Out: Cross-conjugated Oligoenes Allow the Rapid Generation of Molecular Complexity.” *Angew. Chem. Int. Ed.* **2012**, 51, 2298-2338.

88. Sherburn, M. S. “Preparation and Synthetic Value of π-Bond-Rich Branched Hydrocarbons.” *Acc. Chem. Res.* **2015**, 48, 1961-1970.

89. Bojase, G.; Nguyen, T. V.; Payne, A. D.; Willis, A. C.; Sherburn, M. S. "Synthesis and Properties of the Ivyanes: The Parent 1,1-Oligocyclopropanes." *Chem. Sci.* **2011**, 2, 229-232.

90. Bach, R. D.; Dmitrenko, O. "The Effect of Carbonyl Substitution on the Strain Energy of Small Ring Compounds and Their Six-Member Ring Reference Compounds." *J. Am. Chem. Soc.* **2006**, 128, 4598-4611.

91. Eaton, P.; Nodari, N.; Neri, C.; Cassar, L.; Monti, F.; Alberici, F. "Fuel Composition with a High Energy Content." *Eur. Pat.* **1990**, 036 4051.

92. Fujita, T.; Suzuki, N.; Ichitsuka, T.; Ichikawa, J. "Facile Synthesis of Unsymmetrical 1,1-diaryl-2,2-difluoroethenes via Stepwise Coupling of 1,1-dibromo-2,2-difluoroethenes." *J. Fluor. Chem.* **2013**, 155, 97-101.

93. Krishnamoorthy, S.; Kothandaraman, J.; Saldana, J.; Prakash, G. K. S. "Direct Difluoromethylenation of Carbonyl Compounds by Using TMSCF3: The Right Conditions." *Eur. J. Org. Chem.* **2016**, 4965-4969.

94. Suzuki, N.; Fujita, T.; Ichikawa, J. "Method for the Synthesis of Dibenzo[g,p]Chrysenes: Domino Friedel-Crafts-Type Cyclization of difluoroethenes Bearing Two Biaryl Groups." *Org. Lett.* **2015**, 17, 4984-4987.

95. Ehm, C.; Akkerman, F. A.; Lentz, D. "Fluorinated Butatrienes." *J. Fluor. Chem.* **2010**, 131, 1173-1181.

96. Anilkumar, R.; Burton, D. J. "The First Preparation of the α-iodo-β,β-difluorovinylzinc Reagent (CF_2=CIZnCl) and a High-Yield One-Pot Synthesis of α-iodo-β,β-difluorostyrenes." *J. Fluor. Chem.* **2005**, 126, 457-463.

97. Fujita, T.; Ichitsuka, T.; Fuchibe, K.; Ichikawa, J. "Facile Synthesis of β,β-Difluorostyrenes via the Negishi Coupling of Thermally Stable 2,2-Difluorovinyl Zinc-TMEDA Complex." *Chem. Lett.* **2011**, 40, 986-988.

98. Rieke, R. D.; Sell, M. S.; Klein, W. R.; Chen, T.; Brown, J. D.; Hanson, M. V. In *Active Metals*; Furstner, A., Ed.; VCH: New York, **1996**, Chapter 1.

99. Dai, W.; Xiao, J.; Jin, G.; Wu, J.; Cao, S. "Palladium- and Nickel-Catalyzed Kumada Cross-Coupling Reactions of *gem*-Difluoroalkenes and Monofluoroalkenes with Grignard Reagents." *J. Org. Chem.* **2014**, 79, 10537-10546.

100. Piou, T.; Rovis, T. "Rh(III)-Catalyzed Cyclopropanation Initiated by C-H Activation: Ligand Development Enables a Diastereoselective [2 + 1] Annulation of N-Enoxyphthalimides and Alkenes." *J. Am. Chem. Soc.* **2014**, 136-11292-11295.

101. Cochran, J. C.; Phillips, H. K.; Tom, S.; Hurd, A. R.; Bronk, B. S. “Phenyl-Substituted Vinylstannanes: Synthesis and Reactivity in Electrophilic Substitution Reactions.” *Organometallics* **1994**, 13, 947-953.